# Modulation of protein functions by homo- and heterophilic protein interactions as studied with P2X receptors and glutamate transporters

Dissertation
zur Erlangung des Doktorgrades
der Naturwissenschaften

vorgelegt beim Fachbereich
Chemische und Pharmazeutische Wissenschaften
der Johann Wolfgang Goethe-Universität
in Frankfurt am Main

von
Sandra Gendreau
aus Ivry/seine (Frankreich)

Frankfurt 2004

Vom Fachbereich Chemische und Pharmazeutische Wissenschaften der Johann Wolfgang Goethe-Universität als Dissertation angenommen.

Dekan: Prof. Schwalbe

Gutachter: Prof. Lambrecht, Prof. Schmalzing, Prof. Steinhilber, Prof. Fendler

Datum der Disputation: 15. Oktober 2004

*On fait la science avec des faits, comme on fait une maison avec des pierres, mais une accumulation de faits n'est pas plus une science qu'un tas de pierres n'est une maison.*

*Henri Poincaré (1854-1912)*

Je dédie cette thèse à mon grand-père et à mes parents.
Vos encouragements et votre affection ont été essentiels à l'accomplissement de ce travail. Merci.

Diese Doktorarbeit widme ich meinem Großvater und meinen Eltern.
Die Unterstützung und Zuneigung meiner Familie war unentbehrlich für die Bewältigung dieser Aufgabe. Danke.

# Table of contents

# I/ Introduction

## I-1. Synthesis of membrane proteins: The secretory pathway

### 1.1 Membrane protein synthesis, folding and assembly

All proteins are synthesized in the cytosol by the ribosomes, but some selected proteins are captured by the endoplasmic reticulum (ER) as they are being synthesized. These proteins are of two types: membrane proteins, which are only partly translocated across the ER membrane and become embedded in it, and water-soluble proteins, which are fully translocated across the ER membrane and are released into the ER lumen. All of these proteins, regardless of their subsequent fate, are directed to the ER by the same kind of signal sequence and are translocated across it by similar mechanisms (Alberts et al., 1994).

Once their synthesis is complete, newly introduced polypeptides in the membrane and lumen of the ER must be folded, sorted, and transported. Secretory and membrane proteins undergo five principal modifications during their transit to the cell surface: (1) formation of disulfide bonds; (2) proper folding of the polypeptide; (3) addition and modification of carbohydrates; (4) specific proteolytic cleavages, and (5) formation of multichain proteins (assembly). Each modification takes place in a specific organelle through which these proteins pass. The first two and the fifth of these reactions take place exclusively in the ER, and addition of some carbohydrates and some proteolytic cleavages also occur in this organelle. The modifications that occur in the ER are essential for the protein to reach its proper cellular location. Only properly folded and assembled proteins are transported from the ER to the Golgi complex and to the cell surface. Unfolded, misfolded, or partly folded and assembled proteins are selectively retained in the ER, or are retrieved to the ER from the *cis*-Golgi reticulum. Misfolded proteins and unassembled subunits of multiple-polypeptide complexes are either degraded within the ER or translocated

back into the cytosol, where they are deglycosylated, ubiquitylated, and degraded in proteasomes.

Many important secretory and membrane proteins form oligomers, they are built of two or more polypeptides. Several prerequisite must be met in order for subunits to oligomerize. The associating subunits must co-exist spatially and temporally, recognize each other, and provide sufficient stabilization energy to form a stable structure (Deutsch, 2002). The formation of oligomeric proteins occurs in the ER membrane. Fig. 1 illustrates the series of events contributing to the biogenesis of oligomeric membrane proteins and the temporal organization of these events.

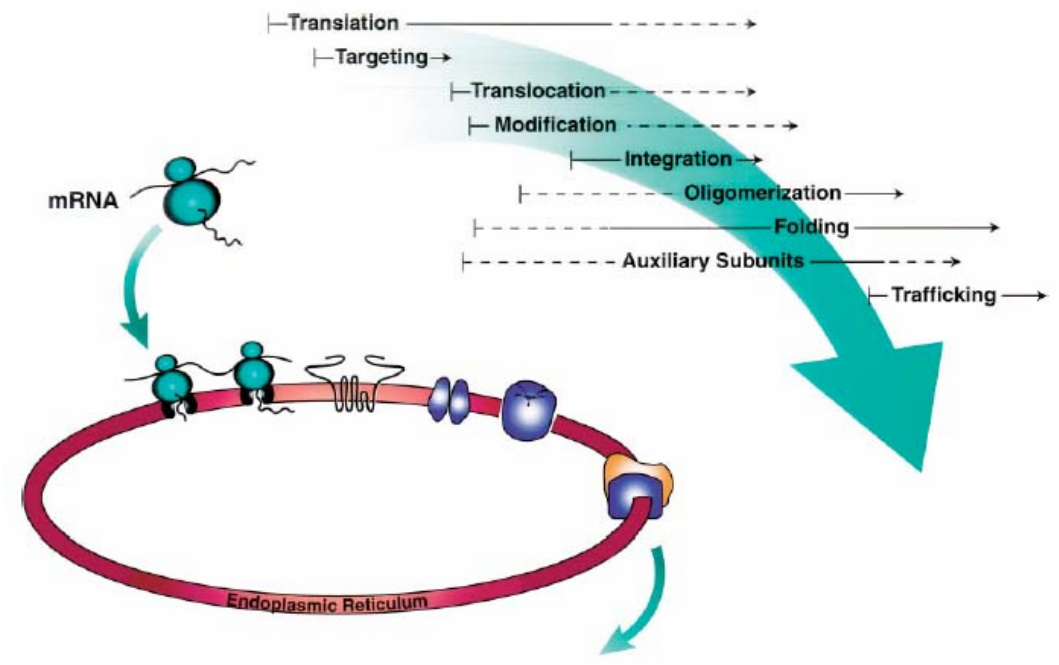


**Fig. 1: Channel biogenesis in the endoplasmic reticulum (Deutsch, 2002).**

## 1.2 N-linked glycosylation

*N*-linked glycans in glycoproteins are attached to the amide nitrogens of asparagine side chains. Glycosylated asparagine residue are almost invariably found in the sequences *Asn-X-Ser* or *Asn-X-Thr*, where X can be any amino acid except proline. The different categories of *N*-linked

glycans, such as high mannose and complex types, contain a common core-structure but differ in the terminal elaboration that extend from this core.

It is convenient to divide the biochemical pathway for *N*-linked glycan synthesis into three stages (Fig. 2A): (1) formation of a lipid-linked precursor oligosaccharide; (2) en bloc transfer of the oligosaccharide to the polypeptide; and (3) processing of the oligosaccharide. Processing steps include removal of some of the original sugar residues (trimming) followed by addition of new sugars at the non-reducing termini of the glycan (Fig. 2B).

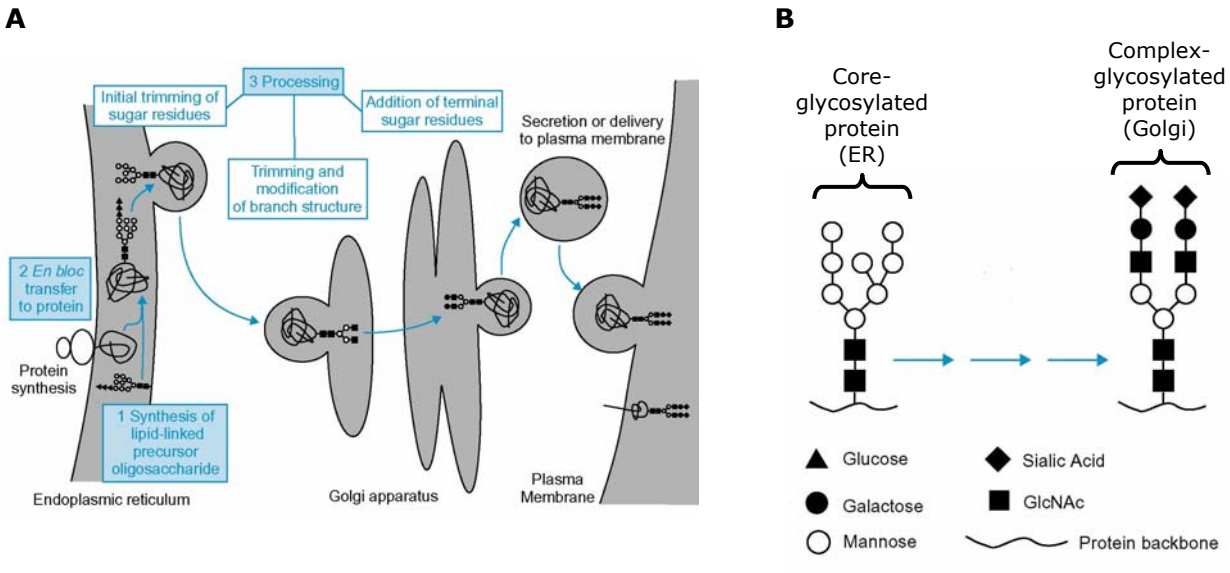


**Fig. 2: (A) Overview of the pathway for glycoproteins biosynthesis and its location within a cell. (B) Processing of an initial high mannose *N*-linked glycan to generate complex glycans (Taylor and Drickamer, 2003).**

## I-2. P2X receptors

P2X receptors are ligand-gated membrane ion channels that when activated by extracellular ATP mediate fast excitation in various cells, including central and peripheral neurons. P2X receptors belong to the superfamily of purine receptors, which is divided in two sub-families: the adenosine receptors called P1 receptors and the P2 receptors, recognizing

primarily ATP, ADP, UTP and UDP (Ralevic and Burnstock, 1998). P2 receptors divide into two families, the P2X ligand-gated ion channels and the P2Y G protein-coupled receptors.

## 2.1 Structure of cloned P2X receptors

The first cDNAs encoding P2X receptor subunits were isolated in 1994, their expression in heterologous cells substantiated the view that P2X receptors were ion channels gated by ATP.

There are seven genes for P2X receptor subunits. The P2X subunits proteins are 384 ($cP2X_4$) to 595 ($rP2X_7$) amino acids long (for recent review, see (North, 2002)).

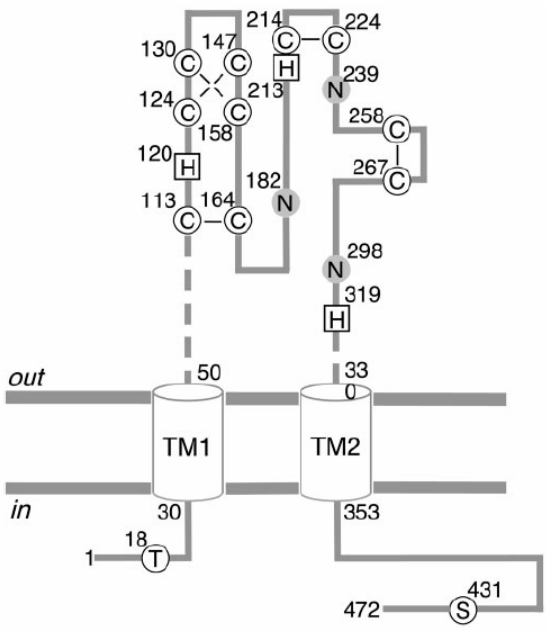


**Fig. 3: Membrane topology of $P2X_2$ receptors showing glycosylation, phosphorylation and possible disulfide bonding (North, 2002)**. Solid circles (N): indicate glycosylated sites in the native $P2X_2$ receptor. Open circles (T, S): indicate positions phosphorylated by protein kinases (PKC, PKA). Open circles (C): indicate the 10 conserved cysteines. Open squares (H): indicate histidine residues involved in zinc (His-120, His-213) and proton binding (His-319).

Structural features of P2X receptors have been predicted from the amino acid sequences of cloned P2X receptor subunits (Brake et al., 1994). Each has two hydrophobic regions of sufficient length to cross the plasma membrane; the first of these extends from residue 30 to 50, and the

second from residue 330 to 353 (numbers refer to the rat $P2X_2$ receptor, see Fig. 3). These hydrophobic regions are separated by a large extracellular loop (Newbolt et al., 1998). The $NH_2$ and COOH termini are presumed to be cytoplasmic (Torres et al., 1998b). The COOH-terminal regions diverge in sequence considerably (Fig. 4).

```
|P2X1|     H-------------------ILPKRHYYKQKKFKYAEDMGPGEGEHDPVATSSTLGLQEN  395
|P2X2|     T------------------FMNKNKLYSHKKFDKVRTPKHPSSRWPVTLALVLGQIPPPP  395
|P2X3|     N------------------FLKGADHYKARKFEEVTETTLKGTASTNPVFASDQATVEKQ  382
|P2X4|     Y-------------------CMKKKYYYRDKKYKYVEDYEQGLSGEMNQ             389
|P2X5|     Y------------------LIRKSEFYRDKKFEKVRGQKEDANVEVEANEMEQERPEDEP  401
|P2X6|     Y------------------VDREAGFYWRTKYEEARAPKATTNSA                 379
|P2X7|     TYASTCCRSRVYPSCKCCEPCAVNEYYYRKKCEPIVEPKPTLKYVSFVDEPHIWMVDQQL  416

|P2X1|      MRTS                                                        399
|P2X2|      SHYSQDQPPSPPSGEGPTLGEGAELPLAVQSPRPCSISALTEQVVDTLGQHMGQRPPVP  454
|P2X3|      STDSGAYSIGH                                                 393
|P2X5|      LERVRQDEQSQELAQSGRKQNSNCQVLLEPARFGLRENAIVNVKQSQILHPVKT       455
|P2X7|      LGKSLQDVKGQEVPRPQTDFLELSRLSLSLHHSPPIPGQPEEMQLLQIEAVPRSRDSPD  475

|P2X2|      EPSQQDSTSTDPKGLAQL                                          472
|P2X7|      WCQCGNCLPSQLPENRRALEELCCRRKPGQCITTSELFSKIVLSREALQLLLLYQEPLL  534

|P2X7|      ALEGEAINSKLRHCAYRSYATWRFVSQDMADFAILPSCCRWKIRKEFPKTQGQYSGFKY  593

|P2X7|      PY                                                          595
```

**Fig. 4: Amino acid sequence alignment of the C-terminal part of the seven cloned rat P2X receptors subunits.** Sequences and genes structure are deduced from NCBI accession numbers P47824 ($P2X_1$), 2020424A ($P2X_2$), CAA62594 ($P2X_3$), CAA61037 ($P2X_4$), CAA63052 ($P2X_5$), CAA63053 ($P2X_6$), and CAA65131 ($P2X_7$). The alignment was made using the ClustalW program available in the Internet (http://clustalw.genome.ad.jp/). Identical amino acids are highlighted by shaded boxes.

The amino acid identity between P2X receptors subunits is distributed throughout the extracellular domain, in which residues are involved in ligand binding (Jiang et al., 2000). A striking feature of this extracellular domain is the conservation of 10 cysteine residues among all known receptors. Disulfide bonds are known to play an important role in the formation and maintenance of ion channel structures (Ennion and Evans, 2002).

All P2X receptor subunits have consensus sequences for *N*-linked glycosylation (Asn-X-Ser/Thr), and some glycosylation is essential for trafficking to the cell surface (Rettinger et al., 2000a). The $P2X_2$ receptor primary sequence, for example, contains three consensus sites for N-glycosylation, these are $^{182}$Asn, $^{239}$Asn, $^{298}$Asn. All are glycosylated in oocytes (Newbolt et al., 1998), and HEK293 cells (Torres et al., 1998a). All the three glycosylation consensus sequences become complex glycosylated en route to the plasma membrane in oocytes (unpublished results, Ph.D. thesis S. Aschrafi; Frankfurt, 2002). The other P2X receptors subunits also have consensus sequences for *N*-linked glycosylation; these are well conserved in their positions among species variants, but incompletely conserved among the receptors ($P2X_1$, five sites; $P2X_3$, four sites; $P2X_4$, six sites; $P2X_5$, two sites; $P2X_6$, three sites; $P2X_7$, three sites) (North, 2002).

Evidence for heteromultimeric receptors has come from functional expression studies. The pharmacological properties (see below) of endogenous P2X receptors in smooth muscle and PC12 cells correlate well with those of the recombinant receptors cloned from these tissues, $P2X_1$ and $P2X_2$ receptors, respectively. However, this is not always the case. All P2X receptors except $P2X_7$ are expressed in sensory glia, but ATP-gated currents at endogenous P2X receptors in rat nodose neurons present a pharmacological profile that does not correspond to any of the homomeric P2X receptors cloned (Lewis et al., 1995). It was suggested that a new heteromeric receptor, $P2X_2P2X_3$, is formed from the $P2X_3$ and $P2X_2$ subunits.

In attempt to determine the number of P2X subunits contributing to the formation of oligomers or heteromers, different biochemical approaches have been used. Kim et al. purified a His-tagged form of the ectodomain of $P2X_2$ expressed in *E.coli* (Kim et al., 1997). Using the equilibrium sedimentation centrifugation technique they proposed a tetrameric assembly of $P2X_2$. In contrast, Nicke et al. using the Blue-native PAGE technique and performing cross-linking experiments showed that $rP2X_1$

and $rP2X_3$ subunits assemble into stable trimers (Nicke et al., 1998; Nicke et al., 2003). The trimeric structure of P2X receptors were confirmed many times in our group, particularly for the homomeric $rP2X_1$ receptor. Jiang et al. proposed recently a "head-to-tail" subunit arrangement in the quaternary structure of P2X receptors and suggested that trimeric $P2X_{2/3}$ receptor would have the composition $P2X_2(P2X_3)_2$ (Jiang et al., 2003).

## 2.2 Signal transduction mechanisms

P2X receptors mediate the rapid (onset within 10 ms) non selective passage of cations ($Na^+$, $K^+$, $Ca^{2+}$) across the cell membrane resulting in an increase in intracellular $Ca^{2+}$ and depolarization (for review, see (Ralevic and Burnstock, 1998)). The response time is very rapid, which explains the important role that P2X receptors play in fast neuronal signaling and regulation of muscle contractility.

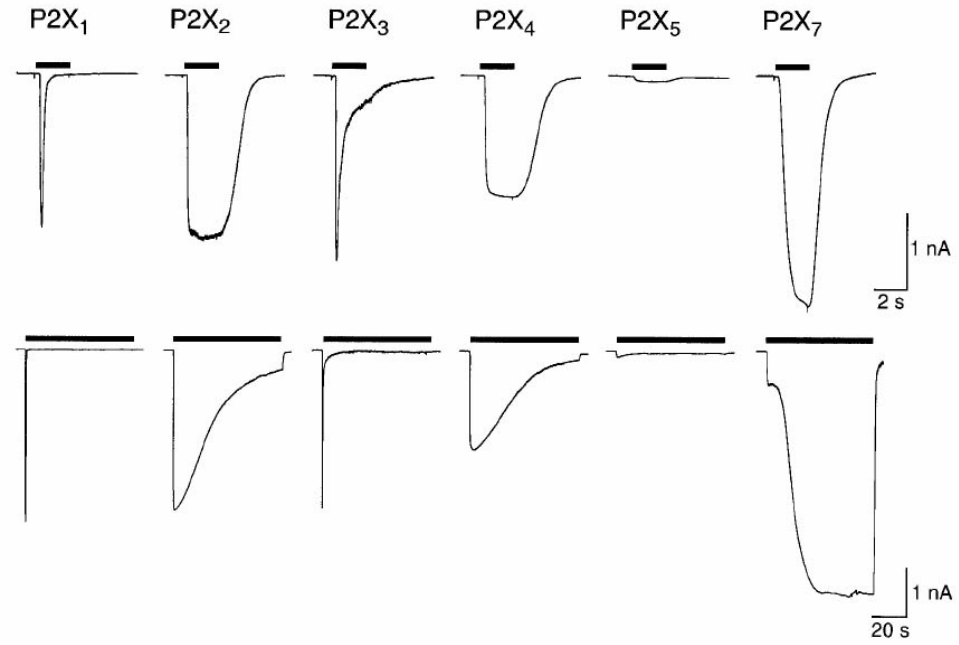


**Fig. 5: Fast (*top*) and slow (*bottom*) desensitization compared for homomeric rat P2X receptors (North, 2002).** Note 10-fold difference in time scale. HEK293 cells were transfected with 1 μg/ml cDNA 48h before these whole cell recordings were made. ATP (30 μM, except 1 mM for $P2X_7$) was applied either for 2s (*top*) or for 60s (*bottom*).

Cations can modulate ATP-activated currents in native and endogenous P2X receptors. $Mg^{2+}$ and $Ca^{2+}$ generally inhibit P2X receptors currents, probably by decreasing the affinity of the ATP binding site by an allosteric change in the receptor (Nakazawa et al., 1990; Li et al., 1997). $Zn^{2+}$ potentiates the cation conductance induced by ATP at most P2X receptors, excepted the $P2X_7$ receptor, which is inhibited by $Zn^{2+}$ and $Cu^{2+}$ (Virginio et al., 1997). Modulation of the affinity of the ATP-binding site also occurs by extracellular protons; acid pH causes an increase, and alkaline pH causes a decrease in currents (King et al., 1996). This may be particularly significant for P2X-receptor-mediated signaling in pathophysiological conditions where injury or inflammation can profoundly alter extracellular pH. Fig. 5 shows the electrophysiological response of the different homomeric P2X receptors transfected in HEK293 cells and their desensitization profile.

P2X receptors can be divided into two broad groups according to whether they desensitize rapidly, that is, within 100 to 300 ms as the rat $P2X_1$ receptor (Rettinger and Schmalzing, 2003; Rettinger and Schmalzing, 2004), or slowly if at all (see table 1).

| P2X receptors | Desensitization | α-β-meATP sensitivity | PPADS sensitivity | Suramin sensitivity |
|---|---|---|---|---|
| $P2X_1$ | Rapid | Yes | Yes | Yes |
| $P2X_2$ | Slow | - | Yes | Yes |
| $P2X_3$ | Rapid | Yes | Yes | Yes |
| $P2X_4$ | Slow | - | - | - |
| $P2X_5$ | Slow | - | Yes | Yes |
| $P2X_6$ | Slow | - | - | - |
| $P2X_7$ | Slow | - | N.D. | Yes |
| $P2X_2P2X_3$ | Slow | Yes | N.D. | N.D. |

-, weak or inactive; N.D., not determined

**Table 1: Distinguishing pharmacological characteristics of P2X receptors.**

α-β-meATP is a subtype-specific P2X receptor agonist. Electrophysiological studies at recombinant P2X receptor subtypes established the existence of two phenotypes of receptors for α-β-meATP (Table 1), which is a relatively potent agonist at $P2X_1$, $P2X_3$ and heteromeric $P2X_2P2X_3$ and $P2X_1P2X_5$ receptors. α-β-meATP is a weak partial agonist or inactive at homomeric $P2X_2$, $P2X_{4-7}$ and heteromeric $P2X_{4/6}$ receptors (Ralevic and Burnstock, 1998; Lambrecht, 2000).

PPADS was first considered to be a P2 receptor antagonist selective for native $P2X_1$-like receptor (Lambrecht et al., 1992), but it is now accepted that PPADS is a non-selective (but universal) P2 antagonist (Ralevic and Burnstock, 1998). It was shown by Dunn et al., that suramin antagonizes $P2X_1$-like receptor-mediated effects (Dunn and Blakeley, 1988). In many studies, suramin has been found to be a non-selective antagonist at native P2X and P2Y receptors with relatively low potency (Ralevic and Burnstock, 1998). However, NF279 and NF449, two suramine analogues, are potent and selective analogues of $P1X_1$ receptors. NF279, incubated prior to ATP or simultaneously with ATP, was much more potent for $P2X_1$ and $P2X_3$ receptors than for $P2X_2$ receptors. $P2X_4$ receptors were the least sensitive subtypes for this compound (Rettinger et al., 2000b). NF449 showed inhibitory potency for $rP2X_1$ at subnanomolar concentrations and the rank order of potency was $P2X_1 >> P2X_3 > P2Y_1 > P2Y_2$ (Braun et al., 2001; Hülsmann et al., 2003).

## 2.3 Distribution and biological effects

In this chapter it will only be focused on $P2X_2$, $P2X_5$, and $P2X_7$ which were the subunits investigated in this study. Detailed information about $P2X_1$, $P2X_3$, $P2X_4$, and $P2X_6$ are available in a recent review written by R. Alan North (North, 2002).

a- *$P2X_2$ receptor*

The rat $P2X_2$ receptor subtype was originally isolated from PC12 rat pheochromocytoma cell (Brake et al., 1994) and displays only 41% amino acid homology with the rat vas deferens $P2X_1$ receptor. This receptor undergoes little or no desensitization. However, currents at $P2X_2$ receptors in outside-out patches decline much more rapidly than in whole cell configuration (Ding and Sachs, 1999; Ding and Sachs, 2000). This observation implies that the decline of current is prevented in the whole cell configuration because of the presence of some intracellular modulator, which is lost slowly in the whole cell recording but lost rapidly in outside-out patches (Ding and Sachs, 2000).

$P2X_2$ receptor mRNA is distributed in bladder, brain, spinal cord, superior cervical ganglia, adrenal medulla, intestine, and vas deferens, with the highest levels found in the pituitary gland and vas deferens (Brake et al., 1994). Distinct but restricted patterns of distribution of $P2X_2$ mRNA have been described within the rat brain (Collo et al., 1996). Three cDNAs encoding splice variants of the $P2X_2$ receptor were isolated from rat cerebellum, $P2X_{2b}$, $P2X_{2c}$, and $P2X_{2d}$ (Simon et al., 1997). $P2X_{2b}$ was the only one splice variant which was functional when expressed in either *Xenopus* laevis oocytes or in HEK 293 cells (Simon et al., 1997). $P2X_{2b}$ has a 69-amino acid (207-pb) deletion starting at the Val-370 codon (Brändle et al., 1997). A serine- and proline-rich region is thus deleted, shortening the carboxyl-terminal region. In contrast to the nondesensitizing $P2X_{2a}$ receptor, prolonged application of ATP produced a more rapid desensitization of the $P2X_{2b}$ receptor. Functional studies have suggested that alternative splicing of the receptor serves to modulate the response of the receptor to prolonged agonist exposure (Brändle et al., 1997; Simon et al., 1997; Koshimizu et al., 1998). The human homologue of the $P2X_2$ receptor has been isolated in 1999 by Lynch et al. (Lynch et al., 1999). Like the rat gene, the human $P2X_2$ gene produces multiple transcripts in a variety of tissues.

Extracellular ATP has been implicated in the function of the neuroendocrine system. ATP induces secretion of hormones, including prolactin and leuteinizing hormone from cells of the pituitary gland. The existence of high levels of human $P2X_2$ message in the pancreas and in the pituitary gland suggest a role of $P2X_2$ receptors in the modulation of pancreatic functions and in the regulation of hormone release (Lynch et al., 1999).

b- *$P2X_5$ receptor*

The $P2X_5$ receptor was first cloned from rat coeliac ganglia (Collo et al., 1996). In situ hybridization shows $P2X_5$ mRNA in motoneurons of the ventral horn of the cervical spinal cord, and in neurons in the trigeminal and dorsal root ganglia. Rat $P2X_5$ was also cloned from rat heart (Garcia-Guzman et al., 1996). With the exception of the mesencephalic nucleus of the trigeminal nerve, the *brain does not express $P2X_5$* mRNA. A chicken P2X receptor cDNA ($cP2X_8$) homologous to mammalian $P2X_5$ subunit but showing sequence divergence at the C-terminal end has been cloned from embryonic skeletal muscle (Bo et al., 2000). Ruppelt et al. isolated the same cDNA from chicken heart (Ruppelt et al., 2001) and considered $cP2X_8$ the chicken orthologue of $rP2X_5$. Moreover, the authors showed in this study that $cP2X_5$ is permeable not only to cations but also to $Cl^-$. These data suggest, that chicken $P2X_5$ receptors are expressed in developing muscle and might play a role in early muscle differentiation.

c- *$P2X_7$ receptor*

The $P2X_7$ receptor, which was cloned from rat macrophages and brain (Surprenant et al., 1996), is the cytolytic "$P_{2Z}$ receptor" previously described in mast cells, macrophages, fibroblasts, lymphocytes,

erythrocytes, and erythroleukemia cells. Human and mouse cDNAs were cloned from monocytes and microglial cells respectively (Rassendren et al., 1997; Chessell et al., 1998).

One of the striking features of the $P2X_7$ receptors is that they need concentrations of ATP greater than 100 μM to be activated, and that BzATP, an ATP analog, is 10-30 times more potent than ATP. Moreover, in low divalent cation solutions, agonists induce sustained currents and the channel becomes permeable to molecules up to 900 daltons, although in normal solution selectivity for small cations is observed (Surprenant et al., 1996). This pore formation involves the cytoplasmic C-terminus of the protein because it does not occur with a truncated $P2X_7$ receptor lacking the last 177 residues, although cation function of the receptor is retained (Ralevic and Burnstock, 1998).

$P2X_7$ mRNA and protein are distributed in bone marrow cells, including granulocytes, monocytes/macrophages and B lymphocytes (Klapperstuck et al., 2000; Boldt et al., 2003), and in macrophages in brain (Collo et al., 1997). Functional studies have shown that $P2X_7$ receptor distribution is generally limited to cells of hemopoietic origin. $P2X_7$ receptors are also present on hepatocytes and parotide and salivary gland acinar cells (for review, see (Ralevic and Burnstock, 1998)).

In murine and human macrophages activation of $P2X_7$ receptors causes activation of phospholipase D, and activation of $P2X_7$ receptors of human macrophages triggers the release of the inflammatory cytokine IL-1β, which may provide a clue to the physiological and/or pathophysiological role of this receptor (Ralevic and Burnstock, 1998). The increased permeability caused by activation of the $P2X_7$ receptor results in large ion fluxes and leakage of small metabolites. On prolonged stimulation it may cause cell swelling, vacuolization, and cell death by necrosis or apoptosis. Finally, ATP or BzATP induces remarkable changes in the appearance of HEK293 cells transfected with the rat P2X7 receptor (Virginio et al., 1999). After ~30 s of continuous application of BzATP (30 μM), the plasma

membrane begins to develop large blebs, and after 1 or 2 min, these become multiple and sometimes coalesce.

## 2.4 Methods to characterize protein complexes and aim of the experiments performed with the P2X receptors

The aim of the experiments performed with P2X receptors was to identify proteins that are involved in the intracellular transport and localization of these receptors in the brain.

In the nervous system, efficient signalling depends critically on the precise positioning of ligand-gated ion channels (LGICs) in high density in the cell membrane at sites postsynaptic to nerve terminals releasing neurotransmitters. Among the intracellular proteins which are enriched in the postsynaptic density and provide a link to the cytoskeleton are gephyrin (Kneussel and Betz, 2000), rapsyn (Kassner et al., 1998), and GABARAP (Wang et al., 1999). The tubulin binding protein *gephyrin* (Fig. 12), for example, is crucial for the clustering and post-synaptic localization of inhibitory glycine receptors at synapses of the spinal cord by linking the heteropentameric $\alpha\beta$ glycine receptor complex through the $\beta$ subunit with microtubules (Kirsch et al., 1991; Kirsch and Betz, 1993). In addition, gephyrin mediates the post-synaptic clustering of $GABA_A$ receptors in the brain (Essrich et al., 1998; Kneussel and Betz, 2000). Likewise, GABARAP (Fig. 6), a 17 kDa protein, has been shown to associate with $GABA_A$ receptors and to bind to microtubules (Wang et al., 1999; Wang and Olsen, 2000) by serving as a linker between $GABA_A$ and gephyrin (Kneussel et al., 2000). In contrast to gephyrin, however, GABARAP appears to play a role in intracellular transport of GABAA receptor rather than in receptor anchoring at the synapse (Kneussel et al., 2000; Kittler et al., 2001).

It is becoming increasingly clear that an important level of organization is provided by multi protein complexes. Proteins interact with each other

and form larger assemblages in a time- and space-dependent manner. To identify protein-protein interactions on a large scale, two types of approaches can be used: the two-hybrid system, which is used to detect binary interactions *in vivo*, and biochemical co-purification of complexes using affinity tags, coupled with protein identification using mass spectrometry, which defines the total spectrum of complexes for a particular tagged protein. These two approaches will be shortly presented and discussed in this chapter.

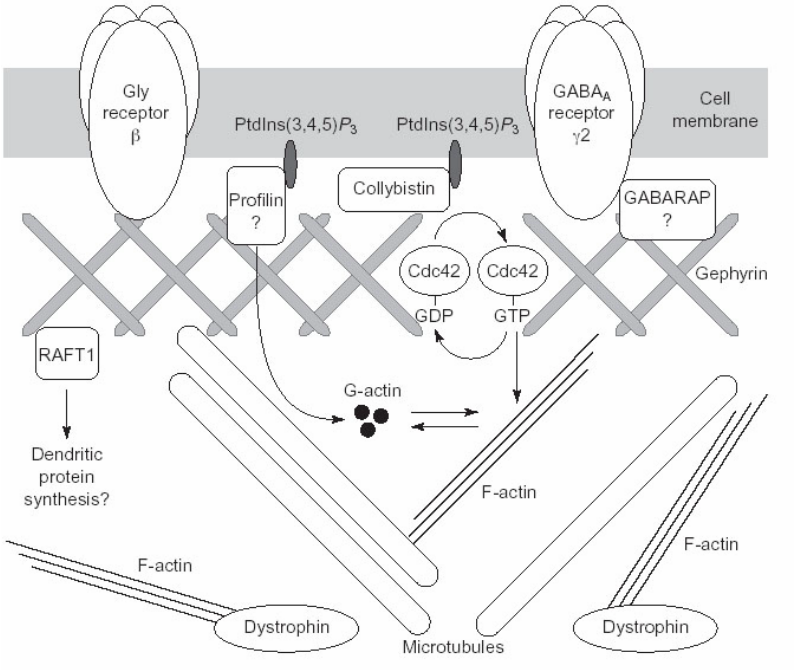


**Fig. 6: Post-synaptic gephyrin and its binding partners (Kneussel and Betz, 2000).**

The yeast two-hybrid assay provides a genetic approach to the identification and analysis of protein-protein interactions. In this assay, hybrid proteins are generated that fuse a protein X to the DNA binding domain and protein Y to the activation domain of a transcription factor. Interaction between X and Y reconstitutes the activation of the transcription factor and leads to expression of reporter genes with recognition sites for the DNA-binding domain.

Key advantages of the two-hybrid system assay are its sensitivity and flexibility. This sensitivity leads to the detection of interactions with dissociation constants around $10^{-7}$M, in the range of most weak protein interactions found in the cell, and is more sensitive than co-purification, which requires stability of a complex through dilution from cell lysis, and through subsequent purification steps (Phizicky et al., 2003).

Disadvantages of the yeast assay include the unavoidable occurrence of false negatives and false positives. False negatives include proteins such as membrane proteins and secretory proteins that are not usually amenable to a nuclear-based detection system, proteins that activate transcription when fused to a DNA binding domain, proteins that fail to fold correctly, and interactions dependent on domains occluded in the fusion or on post-translational modifications. False positive seem to be due to spurious transcription that does not derive from any interaction occurring between the hybrid proteins (Phizicky et al., 2003).

The combination of biochemistry and mass spectrometry is driving progress in the field of functional proteomic today. The purification of protein complexes has been accomplished by a multitude of different techniques ranging from classical methods such as size exclusion or ion exchange chromatography to different varieties of affinity chromatography. Affinity-based methods include one highly discriminating separation step, which is essential considering the samples complexity. In these methods, one of the molecules is immobilized on a solid support and the interacting molecules can be purified from e.g. a cell lysate along with associated proteins. The immobilized molecules are most of the time recombinant proteins, epitope-tagged proteins and antibodies. For more specialized applications, peptides and nucleic acids have also been used (Bauer and Kuster, 2003).

A classical approach is the co-immunoprecipitation experiment using antibodies. It is probably the most frequently employed method for testing whether two proteins are associated *in vivo* but the method can also be successfully used for the discovery of novel interacting partners in a

protein complex. A retrieved complex is washed extensively to remove non-specifically bound proteins and is subsequently eluted from the resin prior identification by mass spectrometry. There are several arguments that would favor an antibody approach. Importantly, antibodies allow the retrieval of protein complexes from endogenous components of cells and tissues which is obviously closest to resembling physiological conditions as there is no need for ectopic expression of the bait protein that could lead to variety of problems (see below). One limitation of antibody immunoprecipitation is that an individual antibody is needed for every bait protein. There are some other, more technical, limitations to the method: even mouse monoclonal antibodies might exhibit cross-reactivity with proteins other than the immunogen, leading to the generation of false positive. Cross-reactivity of the antibody aside, very abundant proteins might non-specifically bind to the resin. Specificity is typically increased by washing the immobilized protein complex briefly before elution using high stringency conditions (200-500 mM salt). However, components that are not tightly bound might be lost during this procedure. Although this point is raised in this section, other affinity approaches will suffer from the same limitation. Loss of particular components of a protein complex might be overcome by chemical cross-linking (Bauer and Kuster, 2003).

Antibodies can be used in a more generic way for the isolation of protein complexes that circumvents the need for producing specific antibodies. For this purpose, bait proteins can be fused to an epitope-tag and an antibody directed against the tag instead of the bait protein is used for complex retrieval. A variety of different epitope tags (e.g. Myc, HA, Flag, KT3) have been used successfully in the past and antibodies against these tags are commercially available. The underlying advantage of the approach is the high degree of reproducibility of the results because standardized technical procedures can be used that do not need to be optimized for each individual case. The downside of epitope-tagging is obviously the need to ectopically express proteins in cells which largely limits this approach to cell culture systems. Tight control over the expression level of

bait proteins must be exercised as overexpression might adversely affect the assembly of the protein complex. In addition, overexpression can occasionally cause cytotoxicity. In addition, the artificially introduced tag may interfere with protein folding, protein function, or the ability to interact with other proteins. Despite some of these limitations, co-immunoprecipitation via epitope tags is used extensively on a normal lab scale to identify protein complexes (Bauer and Kuster, 2003).

The standard precipitation experiment with the aid of a recombinant GST fusion protein has been widely used for the discovery and analysis of individual protein interactions and, to a lesser extent, protein complexes. In this approach, the protein of interest is expressed in *Escherichia coli* as a recombinant fusion protein and immobilized on a solid support. Interacting proteins can then be precipitated (or "pulled-down") by applying a cellular lysate to the column. An obvious advantage of this method is that it is robust, easy to use and capable of retrieving even weakly interacting and low abundant proteins owing the fact that large amounts of recombinant protein are present on the column. However, not all proteins can be easily overexpressed in a soluble form in *E. coli*. Furthermore interactions that may be dependent on the correct post-translational processing of the bait protein may not be provided by the expression system used.

TAP (tandem affinity purification), a method that was recently developed, is highly discriminating against unspecific protein background and nevertheless retain essential components of the complex. First, the "TAP-tagged" protein is expressed in cells to form a complex with the endogenous components. The tagged protein along with associated partners is retrieved via interaction of the ProteinA tag with immunoglobulins that are immobilized on agarose beads. In order to remove proteins that are non-specifically bound to the column, the retrieved protein complex is released by protease cleavage using the TEV (Tobacco etch virus) protease. This enzyme is a site specific protease that cleaves a seven amino-acid recognition sequence located between the first

and the second tag. This sequence is only found in very few human proteins known so far thus ensuring that components of retrieved complexes are not themselves cleaved by the protease. In the second affinity step, the complex is immobilized to calmoduline coated beads via the calmoduline binding peptide (CBP) tag. This step removes the TEV protease and further contaminants that may be present. The CBP-calmoduline interaction is calcium dependent and, hence, the removal of calcium ions with chelating agents can be used as a second specific elution step that yields the final protein complex preparation (Fig. 7). Aside some of the limitations associated with epitope tagging mentioned earlier, the two step TAP approach has several advantages over traditional single step methods. Probably the most useful asset is the massive reduction of sample complexity through very efficient reduction of unspecific protein background. Stringent purification conditions (high salt or detergent concentrations) which tend to result in the loss of associated proteins can be avoided and the complex can be kept under close to physiological conditions all along the purification procedure. The results of TAP purifications are highly reproducible and comparable for different bait proteins which render the approach applicable to small- and large-scale studies alike (Bauer and Kuster, 2003).

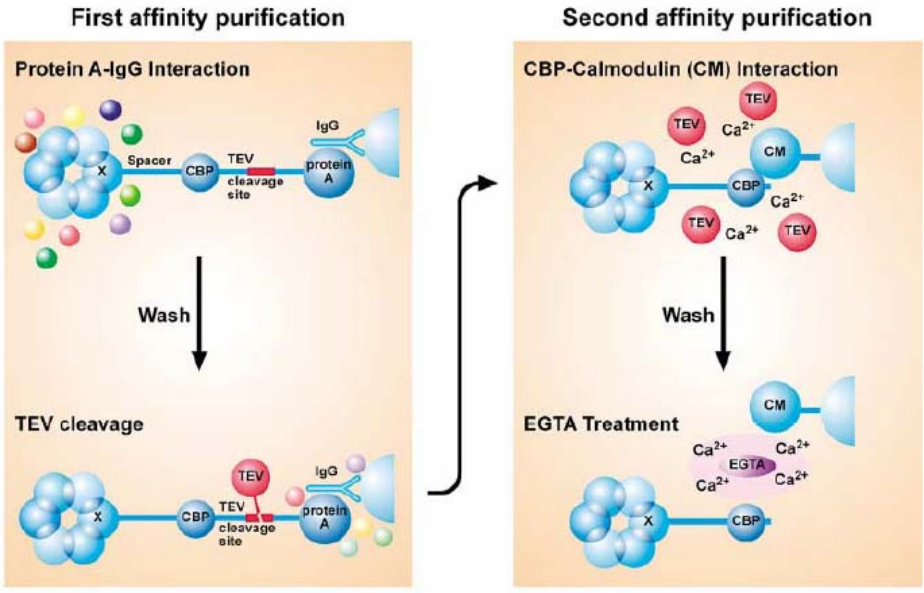


**Fig. 7: Schematic representation of the tandem affinity purification method (Bauer and Kuster, 2003).**

To isolate proteins interacting with P2X receptors, GST fusion proteins containing the intracellular C terminal tail of $P2X_2$, $P2X_5$, or $P2X_7$ were used as bait to screen detergent extracts of rat brain synaptosomes by affinity chromatography. Proteins were resolved by 1D- or 2D SDS-PAGE, and bands/spots of interest were analysed by MALDI-TOF mass spectrometry.

## I-3. Glutamate transporters

### 3.1 Roles of amino acid transporters

Intracellular communication in the central nervous system requires the precise control of the duration and the intensity of neurotransmitter action at specific molecular targets. After they have been released at the synapse, neurotransmitters activate pre- and/or postsynaptic receptors. To terminate synaptic transmission, neurotransmitters are in turn, inactivated by either *enzymatic degradation* or *active transport* in neuronal and/or glial cells by **neurotransmitter transporters**. These processes are responsible for homeostasis of neurotransmitter pools within nerve endings

Both at the plasma and the vesicular membranes, neurotransmitter influxes are directly coupled to *transmembrane ion gradients* which provide the energy for the retrotransport (Kanner and Schuldiner, 1987).

Neurotransmitter transporters can be classified in two superfamilies (for review see (Masson et al., 1999)): 1) the plasma membrane transporters and 2) the vesicular membrane transporters. The superfamily of plasma membrane transporters can be further divided into two families depending on their ionic dependence: 1) the $Na^+/Cl^-$-dependent transporters and 2) the $Na^+/K^+$-dependent transporters. In this chapter only the plasma membrane $Na^+/K^+$-dependent neurotransmitters transporters will be taken into consideration.

A few words about the $Na^+/Cl^-$-dependent transporters: the classical members of this family are the dopamine transporter (DAT), the 5-HT transporter (SERT), the GABA transporter [GAT(1-3)], the norepinephrine transporters (NET), the proline transporter (PROT), the taurine transporter (TaurT), and the glycine transporter [GLYT(1a, -b, -c, and –2)]. All share the same topology and are 40 to 60% homologous. The hydropathicity analysis of these clones revealed 12 stretches of 15 to 25 hydrophobic amino acids which have been interpreted as forming $\alpha$-helical

transmembrane domains. The N- and C-terminal regions are intracellular and the second large extracellular loop contains two to four potential *N*-glycosylation sites (Masson et al., 1999).

## 3.2 Sodium- and potassium-coupled glutamate transporters

### a- *The importance of glutamate uptake*

The amino acid L-amino acid L-glutamate (Fig. 8) is considered to be the major mediator of excitatory signals in the mammalian central nervous system and is probably involved in most aspects of normal brain functions including cognition, memory and learning (Danbolt, 2001). Glutamate also plays major roles in the development of the central nervous system, including synapse induction and elimination, and cell migration, differentiation and death.

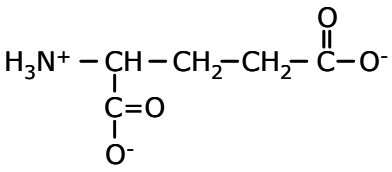

**Fig. 8: Chemical structure of glutamate.**

Brain glutamate is abundant, but mostly intracellular. The concentration gradient of glutamate across the plasma membranes is several thousand-fold and the highest concentrations are found inside nerve terminals (Danbolt, 2001). Glutamate is continuously being released from cells and is continuously being removed from the extracellular fluid.

Glutamate exerts its signaling role by acting on glutamate receptors. It is of critical importance that the extracellular glutamate concentration is kept low. This is required for a high signal to noise (background) ratio in synaptic transmission. Further, excessive activation of glutamate receptors is harmful, and glutamate is thereby toxic in high

concentrations. Finallly, for economic reasons it is necessary to conserve the glutamate released. In contrast, intracellular glutamate is generally considered non-toxic (Danbolt, 2001).

b- *The EAAT family*

The members of the glutamate transporter family that have been functionally characterized can be classified in three groups based on their substrate specificity: C4-dicarboxylate transporters (found in bacteria), glutamate/aspartate transporters (found in bacteria and eukaryotes) and neutral amino acid transporters (found in bacteria and eukaryotes) (Slotboom et al., 1999). A phylogenetic tree of the glutamate transporter family is presented in Fig. 9.

Five different eukaryotic "high-affinity" glutamate (excitatory amino acid) transporters have been cloned so far: EAAT1 (Storck et al., 1992), EAAT2 (Pines et al., 1992), EAAT3 (Kanai and Hediger, 1992), EAAT4 (Fairman et al., 1995) and EAAT5 (Fairman et al., 1995). All five proteins catalyze $Na^+$- and $K^+$-coupled transport of L-glutamate as well as L- and D-aspartate. Originally, these transporters were referred to as the "sodium-dependent high-affinity transporters" to distinguish them from the "low-affinity transporters". The "low-affinity" uptake exhibits $K_m$ values above 500 μM and, in contrast to the "high affinity system" is described as sodium independent and sensitive to inhibition by D-glutamate and L-homocysteate. This uptake system has been suggested to supply brain cells with amino acids for metabolic purposes, but is poorly characterized (Danbolt, 2001).

The five cloned EAAT glutamate transporters (within a single species) share 50-60% amino acid sequence identity with each other, 30-40% identity with some carriers for neutral amino acids, and about 20-30% identity with proton-dependent bacterial glutamate and dicarboxylate transporters.(Danbolt, 2001). Between mammals, the five proteins are about 90% identical to the equivalent protein of another species.

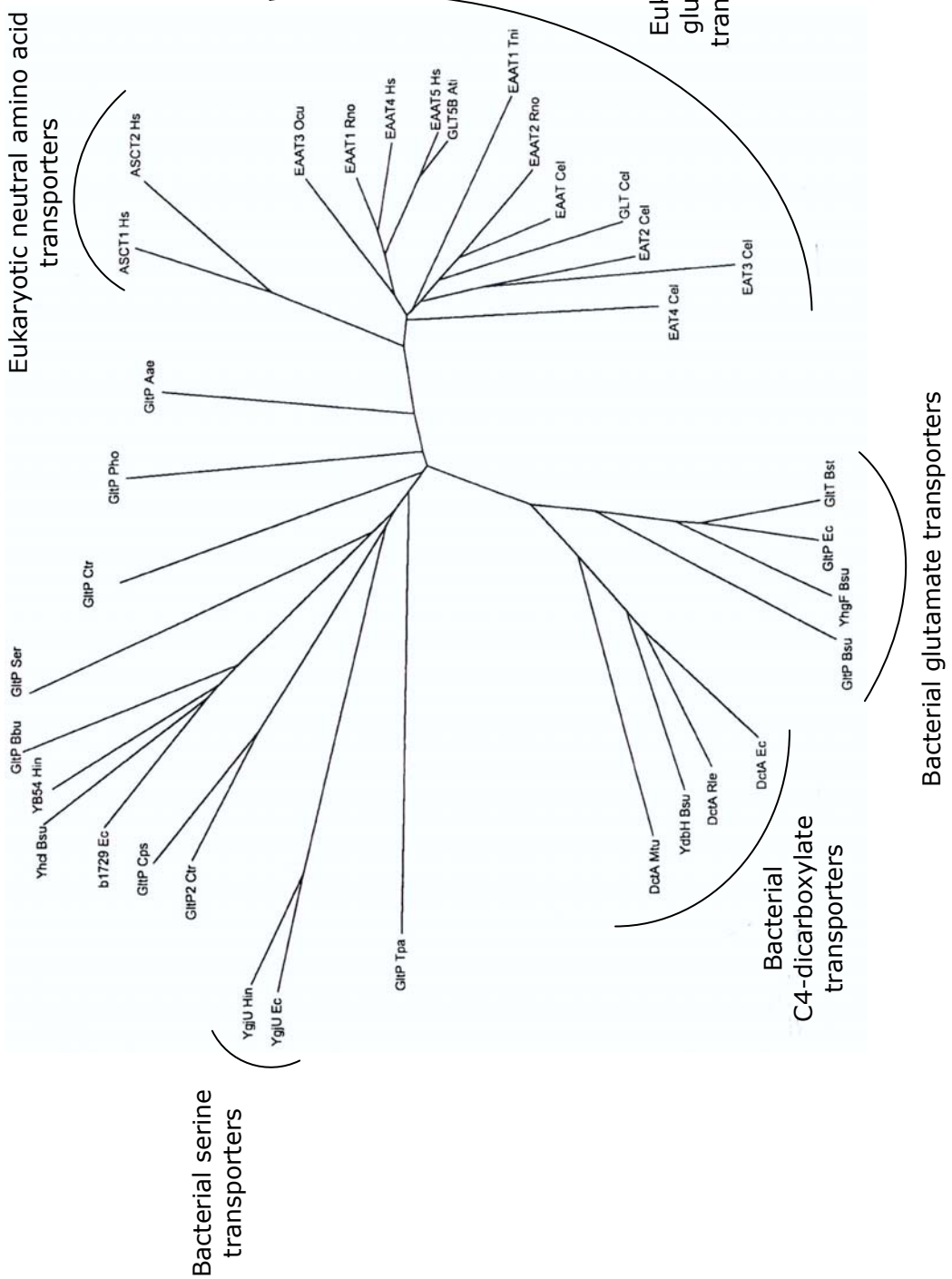


**Fig. 9: Phylogenetic tree of 35 members of the glutamate transporter family (Slotboom et al., 1999).** The set of 35 members does not contain pairs of sequences with more than 70% identical residues. Abbreviations: Hs, *Homo sapiens*; Mmu, *Mus musculus*; Rno, *Rattus norvegicus*: Bta, *Bos Taurus*; Cel, *Caenorhabditis elegans*; Ec, *Escherichia coli*; Bca, *Bacillus caldotenax*; Bsu, *Bacillus subtilis*.

c- *Molecular structure of glutamate transporters*

The glutamate transporter topology is still debated. The first six transmembrane domains are clearly indicated by hydropathy plots, but there is not consensus with regard to the C-terminal one-third of the sequence (Danbolt, 2001). A proposed membrane topology for glutamate transporters is presented in Fig. 10. Four groups have tried to uncover the topology of the mammalian glutamate transporters, but have arrived at different results (for review, see (Danbolt, 2001)). All groups agree about the first six transmembrane (TM) domains (which they all believe are $\alpha$-helices) and about the long stretch between TM3 and TM4. They also agree with the immunocytochemical data showing that both N- and C-terminals are intracellular. There is a relatively large intracellular stretch (residues 339-390 in EAAT2) between TM6 and TM7. Part of this stretch (the 20 residues in the middle) is not thought to be a true intracellular domain, but to form a reentrant loop, which resides in the membrane without forming an usual transmembrane segment. Residues 422-443 (in EAAT2) are suggested to make up a second reentrant loop, while the rest may form an extracellular superficial membrane associated linker to the last $\alpha$-helix. After the last TM, all models contain a long intracellular C-terminus.

The fact that affinity chromatography on a wheat germ lectin has been successfully used to isolate EAAT2 and that this lectin also binds EAAT1 as well as EAAT3, show that the glutamate transporters are glycosylated (Danbolt, 2001). The sugar groups are at least on EAAT2 N-linked because treatments of purified EAAT2 with PNGase F reduces the apparent molecular mass by about 10 kDa (Danbolt et al., 1992). Consensus sites for N-linked glycosylation are encoded in the large hydrophilic loop between putative TM3 and TM4 in all the cloned human glutamate transporters (EAAT5: one site; EAAT1, EAAT2, and EAAT3: two sites; EAAT4: three sites) (Danbolt, 2001). The two N-glycosylation sites in EAAT1 ($^{206}$N, $^{216}$N) have been modified by site-directed mutagenesis, but

the glycosylation was reported to be without functional significance (Conradt and Stoffel, 1995).

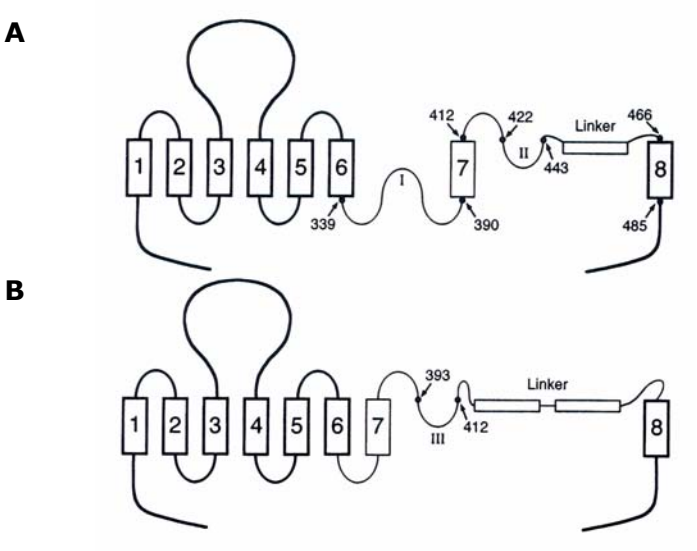


**Fig. 10: Topology of glutamate transporters (Danbolt, 2001).** (A) The proposed topology of rat EAAT2 (Grunewald and Kanner, 2000). (B) The proposed topology of human EAAT1 (Seal et al., 2000).There is consensus (thick line) with regards to the first six transmembrane domains (which are thought to be $\alpha$-helices) and the intracellular localization of the termini. Although there is still debate concerning the last transmembrane domain, most of the investigators seem to favor the notion that this is an $\alpha$-helix too. There is as yet no consensus with regard to the other part of the proteins (thin line).

In addition to all types of ion channels (Nicke et al., 1999), also a variety of transport proteins have been shown to exist as oligomer. These include the glucose transporter GLUT1 (Hebert and Carruthers, 1992), the rat serotonin transporter (Jess et al., 1996; Schmid et al., 2001), the GABA transporter (Schmid et al., 2001), and erythrocyte band 3 (Blackman et al., 1998). When fresh brain tissue is directly homogenized and solubilized in SDS and the proteins immediately separated by SDS-polyacrylamide gel electrophoresis in the absence of reducing agents, only glutamate transporters monomers are seen (Danbolt et al., 1992). This can only imply that the subunits of putative oligomers in the brain must be non-covalently attached. When fresh brain membranes (prior to solubilization) are exposed to chemical crosslinkers (in the presence of DTT) and then

solubilized in SDS, oligomer bands appear on the gel (Haugeto et al., 1996). Further, the different glutamate transporters subtypes do not form oligomeric complexes with each other suggesting that they are homo-oligomers (Haugeto et al., 1996).

Multiple glutamate transporter subunits seem to contribute to the transporter pore (Kavanaugh, 1999). A freeze-fracture electron microscopical study (Eskandari et al., 2000) of human EAAT3 expressed in *Xenopus laevis* oocytes suggests that EAAT3 is a pentamer with a cross-sectional area of 48 $\pm$ 5 $nm^2$ in the plasma membrane. EAAT3 particles are pentagonal in shape in which five domains could be identified.

d- *Mechanism of glutamate uptake*

The transporters utilize the ion gradients of both $Na^+$ and $K^+$, and also $H^+$ as energy sources for the transport process (Zerangue and Kavanaugh, 1996). According to studies of human EAAT3, expressed in *Xenopus laevis* oocytes (Zerangue and Kavanaugh, 1996) and rat EAAT2, stably and inducibly expressed in a mutant CHO cell line with deficient endogenous glutamate transport (Levy et al., 1998), the EAAT3 and EAAT2 glutamate transporters have the following stoichiometry: one glutamate is taken up together with three $Na^+$ and one $H^+$ in exchange for one $K^+$ (Fig. 11). It cannot be taken for granted that the stoichiometry of EAAT1, EAAT4, EAAT5 and the glutamate transporter in glutamatergic nerve terminals are the same. Fig 12 shows the possible mechanism of the role of Arg447 (EAAT2) in the sequential interaction with glutamate and potassium.

Based on this stoichiometry it has been estimated that the energy consumed by the glutamate transporters in the cerebral cortex represents only about 2% of the total energy consumption of the tissue (Attwell and Laughlin, 2000).

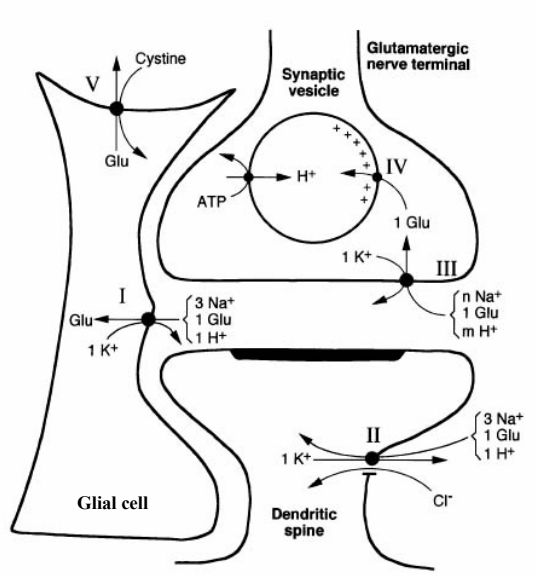


**Fig. 11: Types of glutamate transporters at glutamatergic synapses (Danbolt, 2001).** I. Glutamate transporters in glial cells plasma membranes, EAAT1 and EAAT2 as well as some EAAT3. II. Glutamate transporters are also found post-synaptically in the plasma membrane of dendritic spines: EAAT3 and EAAT4 (only in cerebellar Purkinje cells). These transporters have a relatively high associated $Cl^-$ channel activity. III. The glutamate transporter in glutamatergic nerve terminals has still not be molecularly identified. IV. Synaptic vesicles are loaded with glutamate from cytosol by means of a glutamate transporter located in the plasma membrane of synaptic vesicles. V. Cystine, which is essential for the synthesis of glutathione is transported into cells in exchange with glutamate.

### e- *Localization of glutamate transporters*

The localization of only EAAT2 will be detailed in this chapter. Data about the other EAAT transporters are very well reviewed in (Danbolt, 2001).

EAAT2 is the quantitatively dominating glutamate transporter in the forebrain, or to be more precise: it dominates in all regions of the mammalian central nervous system except in those regions where EAAT1 is the major transporter (Fig. 13). So far the EAAT2 protein has only been found in astrocytes (fibrous as well as protoplasmic) in the normal adult rat brain and spinal cord (Danbolt et al., 1992) as well as in the adult human brain. EAAT2 protein has neither been detected in neurons nor in other cell types (oligodendrocytes, epithelial cells of the choroids plexus and tanycytes). If EAAT2 protein is expressed in neurons, then the

expression must be far lower than that of astroglia or the neurons must express an EAAT2 variant not recognized by the antibody used so far.

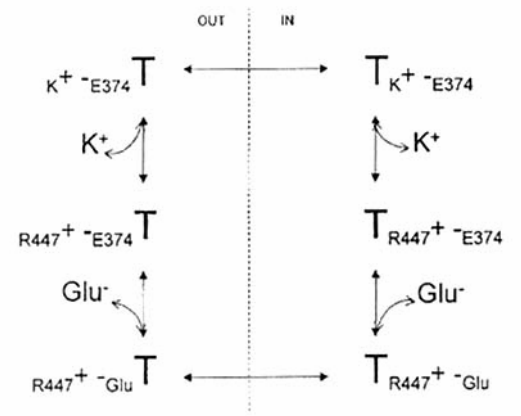


**Fig. 12: Possible mechanism of the role of Arg$^{447}$ (R447$^{+}$) in the sequential interaction with glutamate and potassium (Kanner et al., 2001).** The transporter (T) is shown in its unloaded form (middle level), glutamate bound form (lower level), and its potassium bound form (upper level).

The mRNA encoding EAAT2 is expressed in astroglial cells in agreement with the localization of the protein, but the mRNA is also expressed in several populations of neurons including the pyramidal cells in CA3 hippocampus and in layer VI of the parietal neocortex (Torp et al., 1994). In the the normal and mature mammalian retina, EAAT2 protein is not expressed in retina glial cells. It is exclusively expressed in neurons (cone photoreceptors and bipolar cells) (Rauen, 2000). Fig. 13 shows the subcellular distribution of EAAT2 and the other transporters at two different glutamatergic synapses.

Glutamate uptake also takes place in peripheral organs and tissues. Most cells and tissues have the ability to take up glutamate. Sodium-dependent glutamate uptake systems have been identified in fibroblasts from various tissues, in erythrocytes, in macrophages, in platelets, in muscle, in prostate, in liver, in taste bud, in mammalian oocytes, as well as in the heart, intestine, kidney, pancreas, placenta, bone and mammary gland (for review, see (Danbolt, 2001)). EAAT2 mRNA has been detected in the kidney (Welbourne and Matthews, 1999), but there are no published

reports on the protein. The EAAT2 protein has been identified in placenta (Matthews et al., 1998) and in the lactating mammary gland (Martinez-Lopez et al., 1998).

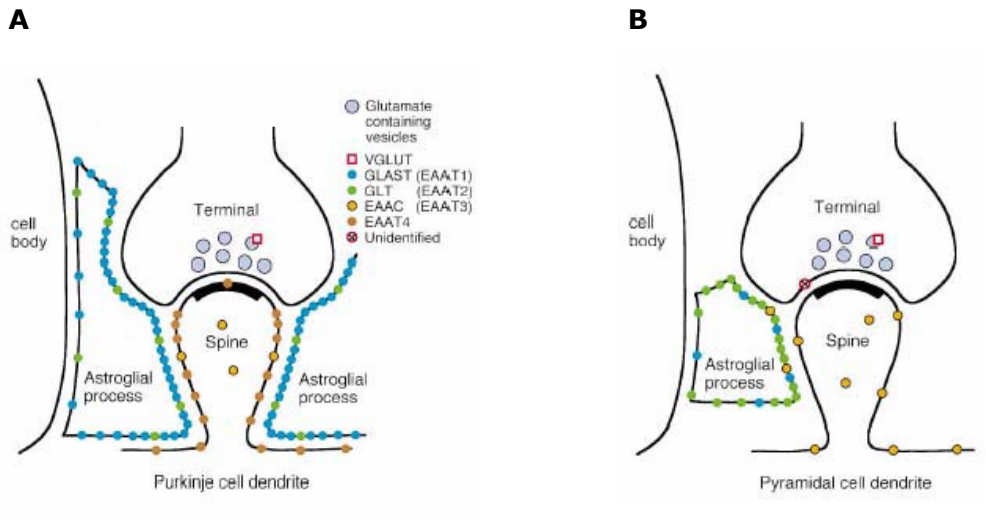


**Fig. 13: Schematic representation of the detailed localization of glutamate transporters in the vicinity of the glutamatergic synapses (Danbolt, 2001).** (A) Parallel fiber to Purkinje cell dendritic spine synapses in the cerebellar molecular layer. (B) Glutamatergic synapse in the hippocampus (e.g. Schaffer collateral to pyramidal cell synapse).

f- *Ion channel activities*

Activation of the excitatory amino acid carriers generates an electrogenic current attributable to the ion-coupled cotransport. In addition to this transport-associated current, a substrate-gated thermodynamically uncoupled anion flux has been identified that has been proposed to dampen neuronal excitability. In 1995, Fairman et al. demonstrated that EAAT4 has an intrinsic $Cl^-$ conductance gated by glutamate, and subsequent studies showed that this property is shared by other EAAT transporters (Fairman et al., 1995; Wadiche et al., 1995). Sodium-dependent glutamate binding to the transporters triggers the anion conductance, which has the following rank order of selectivity: $SCN^- > ClO_4^- > NO_3^- > I^- > Br^- > Cl^- > F^- >>$ gluconate (Wadiche et al., 1995). This anion conductance is thermodynamically independent of the transport process. The transport rate does not depend on the anion concentration (as long as

the anions do not change the pH or membrane potential) and the transport occurs in the absence of these anions. Under conditions where no net glutamate transport is expected, the anion conductance is still observed (Danbolt, 2001). Consequently, the anions pass through glutamate transporters down their electrochemical gradients as if the anions were passing through a glutamate-gated channel. This property is particularly prominent in EAAT4 and EAAT5.

### 3.3 Roles of glutamate transporters in disease

When neurons are exposed to a high concentration of glutamate, the neurons are excessively excited, causing acute and delayed degeneration, and finally necrosis (Ikematsu et al., 2002). This phenomenon is known as "neuroexcitotoxicity". A link between glutamate transporter dysfunction, increased extracellular levels, and onset of excitotoxic neuronal damage has been established in animal models (Rothstein et al., 1996) and in some human neurodegenerative diseases such as amyotrophic lateral sclerosis (Rothstein et al., 1992; Rothstein et al., 1995). Altered glutamate transport has been implicated in Alzheimer's disease, with biochemical studies showing reduced numbers of high-affinity glutamate uptake sites in Alzheimer's disease in many cortical areas (for review, see (Scott et al., 1995)). It has also been suggested that under certain pathophysiological circumstances such as acute cerebral ischemia and epilepsy, glutamate neurotoxicity is propagated due to failure or reversal of glutamate transport. Even when the primary defect in epilepsy is nor of glutamatergic origin, reduced expression of glutamate transporters has been shown to cause or be associated with seizures in animal models. Mutant mice lacking the major glutamate transporter EAAT2 develop spontaneous seizures (Tanaka et al., 1997).

## 3.4 Methods to investigate the oligomeric structure of membrane proteins and aim of the experiments performed with the EAAT2 and ecgltP glutamate transporters in this study

Experimental determination of the physiologically relevant oligomeric state of a protein is technically demanding, but several complementary techniques can be used to probe the structures of proteins either in detergent solution or embedded in membranes.

*a- Quaternary structure in detergent solution*

Although the quaternary structure of membrane proteins is analyzed more easily in the detergent-solubilized rather than the membrane embedded state, the structure of the protein in detergent might not be biologically relevant. Generally, enzyme activity is a good indicator of structural integrity. However, in the case of detergent-solubilized secondary transport proteins, the best that can be measured is ligand-binding activity. It possible that the oligomeric complexes might dissociate during analysis. Whether oligomeric species are then observed depends on the strength of the protein-protein interactions, which can be influenced by the type of detergent used to solubilized the protein. The techniques to study the quaternary structure of membrane proteins in detergent solutions are gathered in Table 2.

The method which is used routinely in our laboratory to investigate the oligomeric structure of membrane proteins is the blue-native PAGE technique. Blue-native electrophoresis is a discontinuous electrophoretic system developed for the isolation of native membrane protein complexes from biological membranes (Schägger et al., 1994). Coomassie dyes are added to purified proteins to induce a charge shift and aminocaproic acid serves to improve solubilization of membrane proteins (Schägger and von Jagow, 1991).

| Techniques | Principles and unique features | Prerequisites and drawbacks |
|---|---|---|
| **Analytical ultracentrifugation** | **Sedimentation velocity**<br>In combination with the frictional coefficient, a reasonable estimate of the molecular mass can be obtained<br>Rigorous assessment of sample heterogeneity | **General**<br>Amount of bound detergent/lipids needs to be determined<br>Sedimentation velocity is dependent on the shape of the protein; does not allow accurate mass determination<br>Highly purified proteins that is homogeneous and stable for at least a few days |
| | **Sedimentation equilibrium**<br>Independent of protein shape<br>Determination of protein (or protein complex) size, stoichiometry and strength of the interactions between the subunits<br>Determination of protein-protein interactions over a wide range of protein concentrations in a single experiment without perturbing the chemical equilibrium | |
| **Size-exclusion-chromatography** | In combination with a sediment coefficient, a reasonable estimate of the molecular mass can be obtained | Amount of bound detergent/lipids needs to be determined<br>Dependent on protein shape<br>Calibration is problematic for membrane proteins<br>$K_D$ of the complex needs to be relatively low |
| **Blue-native PAGE electrophoresis** | Protein stops migrating when trapped at region of appropriate pore size<br>Many different samples can be analyzed simultaneously | Protein solubility and stability in the presence of Coomassie brilliant blue<br>Non-equilibrium method<br>$K_D$ of the complex needs to be relatively low |
| **Co-purification and co-immuno-precipitation** | Truncated proteins can be used to define the protein parts that are involved in oligomerization | Hetero-oligomer formation<br>Differently tagged protein species are needed<br>When association constants in detergent solution are high, these experiments depend on hetero-oligomer formation in the membrane and thus on co-expression in one and the same host |

**Table 2: Techniques to study quaternary structure of membrane proteins in detergent solution (taken from (Veenhoff et al., 2002)).** $K_D$, dissociation constant.

*b- Quaternary structure in the membrane*

The oligomeric state of a membrane protein is best determined when it is embedded in the membrane. However, low expression levels and interference by endogenous proteins complicate *in vivo* analyses. *In vitro*, there are the problems of membrane reconstitution, which can be inefficient, and correct insertion of the protein into the membrane, which can be difficult to achieve. The dimensions of a protein in the membrane can be estimated from high magnification electron-microscope images, the rotational mobility of the molecule, and multicolor co-localization experiments.

Cross-sectional area of freeze-fracture particles of $\alpha$-helical membrane proteins varies linearly with the number of transmembrane $\alpha$-helices (Eskandari et al., 1998). On average, each transmembrane $\alpha$-helix occupies 1.4 $nm^2$. This value has been used to estimate the quaternary structure of membrane proteins that contain a known number of transmembrane $\alpha$-helix in each subunit. The freeze-fracture technique involves rapid freezing, followed by fracture of the membrane and shadowing with metal-carbon to replicate the specimen. One drawback of this technique relates to the thickness of the metal film, which can be as thick as the difference between the diameter of a monomeric and dimeric 12-transmembrane $\alpha$-helix subunit (Veenhoff et al., 2002). Problems can also arise if the secondary structure differs from the assumed $\alpha$-helical organization, such as occurs with "reentrant loops" (elements that line water-filled cavities but do not span the membrane).

The motional time scales of measurements using saturation-transfer electron-spin resonance (ST-ESR) ($10^{-6}$-$10^{-3}$s) are appropriate to observe the rotational mobility of labeled proteins in membranes. The effective radius of the protein can be derived from the rotational diffusion coefficient, provided the viscosity of the protein is known (Spooner et al., 2000). The rate of rotational motion is related to the size (effective volume) as well as to the shape, and assumptions must be made to

accommodate these parameters. Membrane viscosity can be estimated by calibration with a membrane protein of known shape and structure.

Whether the monomeric or oligomeric structure represents the minimal functional unit can be deduced from the activity of a system after co-expression of mutant alleles or coreconstitution of mutant proteins (Laube et al., 1998). Using this system, the presence of a nonfunctional mutant will not affect the activity of a wild-type protein that is fully functional as a monomer. However, if two or more subunits form the active molecule, the presence of the nonfunctional mutant will decrease the activity.

Finally, chemical cross-linking at the plasma membrane (or on purified proteins) is a simple method to demonstrate the close proximity of proteins in their native state. However, the target sites have to be accessible.

In this study, the subunit stoichiometry and processing of two distantly related glutamate transporters, the human glial glutamate transporter, hEAAT2 and the bacterial ecgltP from *E. coli* were investigated. For this purpose these two proteins were expressed in *Xenopus laevis* oocytes, purified under non-denaturing conditions and analyzed by blue-native or SDS-polyacrylamide gel electrophoresis. The results obtained with the blue native PAGE technique were confirmed by chemical cross-linking experiments followed by SDS-PAGE analyses.

# II/ Materials and methods

## II-1. Materials

Chemicals: If not further specified, the chemicals were purchased from Merck (Darmstadt, Germany).

## II-2. Cloning of cDNAs in expression vectors

### 2.1 PCR amplification

a- *PCR amplification using a pure plasmid as template*

Most DNA constructs were amplified in the same way. A pair of primers flanking a region of interest, or a complete coding sequence, were designed. Each was composed of a portion, which annealed completely with the template, and at the 5´end a non-annealing sequence, which contained a stop-codon if necessary, a restriction site and three adenosines to facilitate cleavage by restriction enzymes close to the end of the DNA.

Example: Reverse primer 944 used to amplify the Carboxyl-terminal tail of the $P2X_2$ receptor

Stop codon  Annealing part

5´AAAGAATTCTTATCAAAGTTGGGCCAAACCTTTGGG 3´

EcoRI

For the PCR the Pfu turbo® DNA polymerase (delivered with the appropriate buffer; Stratagene, La Jolla, USA) was used. Different template dilutions (miniprep plasmid) were tried to find the optimal one. The deoxy-nucleotides (dNTPs, Stratagene, La Jolla, USA) were used at a final concentration of 0.15 mM, each. The final primer (Qiagen; Hilden,

Germany) concentration was 0.25 μM, each and 5 units of enzyme were used to catalyze the chain reaction. The elongation time was calculated on the basis of 2 minutes/kb of DNA to amplify. The annealing temperature was between 55 and 72°C, and was calculated as an average of the annealing temperature of the two primers used according to:

$$[((\%\ GC)Tm_1 - 5°C) + ((\%\ GC)Tm_2 - 5°C)]/2.$$

b- *PCR amplification from a cDNA library*

The PCR principle was the same as in 2.1.a, but instead of one purified DNA template, the amplification was performed on a cDNA library, which corresponded to the total mRNAs expressed in a selected organ. To perform this type of PCR, the FailSafe™ PCR PreMix Selection Kit from Epicentre (Madison, USA) was used. This kit contains twelve 2x "Premixes" (100 mM Tris-HCl, pH 8.3; 100 mM KCl; 0.4 mM of each dNTPs) with $MgCl_2$ ranging between 3 and 7 mM and a Failsafe PCR Enhancer (betaine) in various concentrations. This kit allows one to find the best conditions to amplify the sequence coding for the protein of interest. The amplification protocol was designed according to the same rules as in 2.1.a.

## 2.2 Digestion with restriction enzymes, ligation, transformation, and DNA purification

I worked with three types of vectors:

✓ **pNKS** vectors (pNKS2 (Gloor et al., 1995), pNKS 3 and 4 are modified versions of pNKS2) for the cRNA translation and expression in *Xenopus* oocytes,

✓ **pGEX-2T** (Amersham Biosciences; Freiburg, Germany) for the production of GST fusion proteins in *E.coli* or

✓ **pcDNA3.1** (Invitrogen; Karlsruhe, Germany) for the expression in eukaryotic cells.

I always performed directional cloning with cohesive ("sticky") ends, i.e. two different restriction enzymes were used in 5´ and in 3´of the fragment to be inserted. All restriction enzymes were purchased from New England Biolabs (Frankfurt am Main, Germany). Digested DNA fragments were purified from 1% agarose gels using the Jetsorb® extraction kit (Genomed, Bad Oeynhausen, Germany) according to the instructions of the manufacturer. Ligations were performed for 2 h minimum at 16°C, or overnight, using a T4-DNA ligase (New England Biolabs; Frankfurt am Main, Germany). Then competent *E.coli* K12 (Top 10 or DH 5α) were transformed, and spread on LB-plates in the presence of an antibiotic corresponding to the resistance gene carried by the vector. The plates were incubated overnight at 37°C. Some colonies were picked, and 10 ml aliquots of LB-medium supplemented with an antibiotic (mostly ampicillin, 0.05 mg/ml) were inoculated and incubated overnight under continuous shaking at 37°C. On the next day the bacteria were harvested and DNA was isolated using a miniprep kit (Sigma; Taufkirchen, Germany) following the protocol of the manufacturer.

## 2.3 Mutagenesis

To carry out point mutations or DNA insertions, I used the QuickChange™ site-directed mutagenesis kit from Stratagene (La Jolla, USA) consisting of a PCR, followed by a Dpn I digestion and transformation in XL1-Blue supercompetent *E.coli* (for more details, see the instructions of the manufacturer).

## 2.4 Deletion and ligation with primers

To delete more than one codon from a plasmid, the DNA portion to be removed was excised by digestion with two different restriction enzymes. The obtained linear vector was then "re-ligated" with the help of two primers. These primers (Qiagen; Hilden, Germany) were not fully overlapping, and corresponded to a DNA fragment missing in the linear plasmid to achieve the ready construct. The primers were solubilized at a concentration of 100 μM and annealed together (5 μM primer 1, 5 μM primer 2, 10 mM NaCl) for 1 min at 95°C, 2 min at 90°C, thereafter the temperature was decreased by 5°C every 5 min until a final temperature of 5°C was reached. Ligation between the linearized vector and the annealed primers was performed with T4-DNA ligase.

## 2.5 Sequencing of DNA

All the DNA constructs were tested first with restriction enzymes to identify positive clones and then sequenced. The sequencing reaction is a PCR using only one primer in the presence of fluorescent dNTPs (BTRRM mix from Applied Biosystem). The PCR was followed by DNA precipitation with ethanol and sodium-acetate. The DNA pellet obtained by this method was washed once with 70% ethanol, dried by air and resuspended in HPLC water. This sample was then placed in a sequencing instrument (Applied Biosystem), which combines electrophoretic separation of DNA fragments through acrylamide gels with a laser detection of the fluorescent nucleotides. The sequence thus obtained was compared with a sequence generated by the VNTi (Vector Nti) program of the protein. This was achieved by alignment of the two sequences with the "Clustal" alignment program available in the Internet (http://clustalw.genome.ad.jp/).

Note: All the cloned constructs are listed in a table presented in the appendix (chapter VI-2), which also indicates the cloning sites and the primers used for amplification or mutagenesis.

## II-3. Protein expression and purification

### 3.1. Expression and purification in *E.coli*

All the proteins produced in *E.coli* were GST fusion proteins cloned in the pGEX-2T vector.

a- *Small-scale expression*

The aim of this protocol is to find the best conditions (time, temperature, or concentration of IPTG) to express a new fusion protein in *E.coli*. First, *E.coli* BL21 cells, a protease-deficient strain, were transformed and spread on LB-plates containing 0.05 mg/ml ampicillin. All the following culture steps were done in LB medium supplemented with 0.05 mg/ml ampicillin at 37°C.

LB medium (1 liter): Selected Pepton 140 (Gibco BRL): 10g; Yeast extract (ICN): 5g, NaCl: 5g.

Two or three colonies were picked and cultured overnight at 37°C in 10 ml LB-Amp. On the next day 500 µl of this pre-culture were dispensed into many reaction tubes, diluted to 5 ml and grown until an optic density at 600 nm of 0.5 was reached. At this step IPTG (PeqLab; Erlangen, Germany) was added to different final concentrations ranging between 0.05 and 0.8 mM. Some cultures were induced for 1, 2, and 3 h and one culture was also induced overnight with 0.2 mM IPTG at 29°C. At the end of the induction period 1.5 ml of each culture (including sample without

IPTG, as control) were centrifuged (14,000 rpm, 2 min, 4°C). The obtained bacterial pellet was washed once with PBS, and centrifuged once again (14,000 rpm, 2 min, 4°C). The washed pellet was resuspended with 50 µl SDS-PAGE loading buffer and incubated for 5 min at 96°C. The samples were centrifuged for 5 min at 14,000 rpm and room temperature. A volume between 5 and 10 µl was applied on a SDS-PAGE gel (acrylamide concentration: 10% or 12.5%), which after running was stained with Coomassie Blue.

b- *Larger cultures*

This protocol (Zhao et al., 2001) was adapted to the production of milligram amounts of GST fusion proteins. The principle was almost the same as for the small scale expression. BL21 bacteria containing a positive clone were preserved in 50% of glycerol at –80°C. 20 ml of LB medium were inoculated and incubated under continuous shaking overnight at 37°C. This small scale culture was diluted on the next day to 1 liter. The culture was allowed to grow until an optic density at 600 nm of 0.5 was reached, and was then induced with IPTG (usually 0.2 mM for 3 h). At the end of the induction period the cells were centrifuged (6,000 rpm, 10 min, 4°C), and the pellet was resuspended in 20 ml of lysis buffer. The protein lysate, which was maintained permanently on ice, was sonicated 6 times for 30 s, with 30 s rest in-between (Sonifier 450, Branson). The lysate was cleared by centrifugation at 12,000 rpm for 10 min and 4°C. Before usage the glutathione-Sepharose 4B beads (Amersham Biosciences; Freiburg, Germany) were washed 3 times with lysis buffer to remove ethanol. The supernatant was incubated with 0.5 ml glutathione-Sepharose beads for 1 h at 4°C by end-over-end mixing.

**Table 1: Composition of the buffers used for purification of GST-fusion proteins.**

| Compound | Lysis buffer | Washing buffer |
|---|---|---|
| PBS | 200 ml | 25-50 ml |
| Tris-HCl | 50 mM (1.2114g) | |
| $MgCl_2$ | 0.5 mM (20.3 mg) | |
| pH | 8.0 (HCl) | |
| At the last time: | | |
| Triton X-100 10% (Roche) | 0.5% (v/v) | 0.1% (v/v) |
| Lysozyme (Boehringer) | 1 μg/μl | - |
| Pefabloc (BioMol) | 100 μM | - |
| DTT | 5 mM | - |

At the end of the incubation time, the beads were washed 5 times with washing buffer. After the last washing step, the supernatant was entirely removed, and the beads were resuspended in fresh washing buffer containing 50% of glycerol (v/v) and stored in aliquots at –80°C.

For a semi-quantitative determination of protein concentrations, the GST fusion proteins were released from the beads by boiling in SDS-PAGE loading buffer and resolved on linear SDS-polyacrylamide gels (12.5% acrylamide) in parallel with known amounts of bovine serum albumin (2.5-15 μg per lane) as standards. After staining the gel with Coomassie Blue, the concentration of the various GST fusion proteins were estimated by visual comparison of the intensity of the protein bands.

## 3.2 Expression and purification in Xenopus laevis oocytes

### a- *In vitro cRNA synthesis*

The cDNAs of the proteins to be expressed in the oocytes were cloned into pNKS vectors. A first step before the transcription of cRNAs in vitro is linearization of the plasmid. This step is achieved using restriction enzymes such as Not I, Eco RI, Xba I, or Sph I, which cleave the plasmid

behind the poly(A) tail only. The linearized "template" was then purified by using the QIAquick Nucleotide Removal Kit (Qiagen; Hilden, Germany), following the instructions of the manufacturer. Finally, the template was eluted with RNase-free 10 mM Tris-Cl, pH 8.5 and precipitated with ethanol (67% v/v), and sodium acetate (3.3% v/v) (3M, pH 4.6) at -20°C. The DNA template was then centrifuged, washed, and dissolved in 0.5x TE-buffer (TE 100x (Sigma; Taufkirchen, Germany): Tris-Base 1M, EDTA 0.1M, pH 8.0). 0.5-3 μg were used for the cRNA synthesis with SP6-RNA polymerase (Epicentre; Madison, USA) and cap-nucleotides (Epicentre; Madison, USA). The synthetized cRNAs were then purified through Sepharose G50 columns (Amersham Biosciences; Freiburg, Germany) to remove the nucleotides, extracted with phenol-chloroform, and dissolved in 5 mM Tris/HCl, pH 7.2. The quantification of the cRNA quantity was achieved by measuring the absorbance at 260 nm in an Eppendorf photometer.

b- *Isolation and maintenance of Xenopus laevis oocytes*

*Xenopus laevis* females were anesthetized by immersion for 5-15 min in a 0.2% solution of 3-aminobenzoic acid ethyl ester (Tricaine=MS 222 (Sigma; Taufkirchen, Germany) in water; pH 7.4 adjusted with Hepes). The animal was laid down on the back, and an incision was made on the lateral side of the abdomen. The desired amount of ovary was pulled out and immediately transferred into ORi (Oocyte Ringer solution). The incisions in the abdominal muscles and in the skin were sutured separately.

To separate the oocytes that are enclosed and bound to each other by follicle cells, the ovary lobes were manually separated into small pieces and incubated for about 15 h at 19°C in a collagenase solution (1.5 mg/ml Ori supplemented with gentamycin; sterile filtered). The next day, the oocytes were first washed several times with ORi, and then incubated for 10 min in nominally calcium free ORi to remove the follicle cells. The

oocytes were finally washed with ORi until the supernatant was clear. Oocytes of the same size and stage of development (stages V-IV) were manually selected by means of a fire polished Pasteur pipette and injected with cRNAs. Until used, the oocytes were stored at 19°C.

**Table 2: Oocytes Ringer solutions composition.**

| Compound | ORi | Calcium free ORi |
|---|---|---|
| NaCl | 90 mM | 90 mM |
| KCl | 1 mM | 1 mM |
| $CaCl_2$ | 1 mM | - |
| $MgCl_2$ | 1 mM | 1 mM |
| Hepes | 10 mM | 10 mM |
| Gentamycin (optional) | 50 μg/ml | - |
| pH | 7.4 | 7.4 |

c- *Micro-injections of cRNA in Xenopus laevis oocytes*

The oocytes were injected, one at a time, with 50 nl (about 0.5 μg/μl) of one cRNA or a mixture of two, occasionally three cRNAs (with various ratios). The injection setup was composed of one stereo microscope, one micromanipulator, and one microinjector (World of Precision Instruments). For each cRNA a new glass capillary filled with mineral oil was used, whom tip was broken under the microscope to permit to suck up a cRNA droplet. After injections, the oocytes were stored for 1 h at 19°C to allow them to recover from injections and to allow the cRNA(s) diffusion inside the cell before labeling with radioactive methionine was started. Non injected oocytes were used as control group, and were subjected to the same treatment as the other injected oocytes.

d- *Metabolic labeling with [$^{35}$S]methionine*

For metabolic labeling, the oocytes were incubated for 4h or overnight with Revidue™ L[$^{35}$S]methionine (Amersham Biosciences; Freiburg,

Germany), at about 0.1 MBq/oocyte (for 10 oocytes: 250 µl ORi, 1 MBq methionine, 2.5 µl NaCl) and 19°C. For each cRNA, at least 10 oocytes were injected, and labeled together in specially coated tubes. After this "pulse" period, the oocytes were homogenized for protein purification, or let alive for the desired time at 19°C in non-radioactive ORi to perform a so called "chase" period.

e- *Purification of $(His)_6$-tagged proteins*

**Table 3: Buffers used for purification of $(His)_6$-tagges proteins.**

| Compounds | Homogenization | Incubation | Washing |
|---|---|---|---|
| Sodium Phosphate Buffer 0.1M, pH 8.0 | + | + | + |
| Purified digitonin (Fluka) | 1% (w/v) | 1% (w/v) | 0.2% (w/v) (non purified) |
| Protease inhibitors* | 0.1% (v/v) | 0.1% (v/v) | 0.1% (v/v) |
| Iodacetamide | 50 mM | - | 1 mM |
| Imidazole | - | 10 mM/tube | 25 mM |

*Protease inhibitors: Antipain (10 mM), Pepstatin A (5 mM), Leupeptin (50 mM), Pefabloc SC (100 mM) (all from BioMol, Hamburg, Germany).

Iodacetamide (Sigma; Taufkirchen, Germany) prevents the formation of artificial disulfide bonds by alkylating thiols that may form by oxidation. Imidazole was used to reduce non-specific binding to the nickel agarose beads. When dodecylmaltoside (Biomol, Hamburg, Germany) was employed as a detergent instead of digitonin, the following concentrations were used: homogenization/incubation: 0.5% (≈ 10 mM); washing: 0.1%; elution: 0.05-0.1%.

After labeling, oocytes were washed with nominally calcium free ORi. Each group of oocytes (10/group) was homogenized with 200 µl of ice-cold homogenization buffer (10 µl/oocyte). The homogenate was vortexed (3 times for 15 s) and incubated for 15 min on ice before being cleared by two centrifugation steps (16,000g, for 10 min, 4°C). After each centrifugation step, the layer between the pellet and the lipids (located at the surface) was pipetted, and was transferred into a new tube.

**Table 4: Sodium phosphate buffer and elution buffer composition.**

| Compound | Sodium Phosphate Buffer pH 8.0 | Elution buffer |
|---|---|---|
| $Na_2HPO_4$ | 93.2 mM | - |
| $NaH_2PO_4$ | 6.8 mM | - |
| Imidazole | - | 250 mM |
| Lyophilized digitonin | - | 0.5% (w/v) |
| HCl | - | pH 7.4 |

The incubation reaction mix was composed of 100 µl homogenate, 30 µl $Ni^{2+}$-NTA agarose beads (Quiagen, diluted 1:1 with phosphate buffer), 400 µl incubation buffer and 10 mM imidazole. The affinity chromatography took place for 45 min by end-over-end mixing at room temperature. Then the beads were washed 6 times with 1 ml washing buffer pro tube and pro washing step. At the last washing step, the complete supernatant was removed. Proteins were eluted from the $Ni^{2+}$-NTA agarose by addition of 50 µl elution buffer and shaking at room temperature for 15 min. This step was repeated once and the two aliquots were mixed. After elution, the proteins were ready for deglycosylation, Blue-Native and SDS-PAGE analyses.

f- *Chemical cross-linking*

Chemical cross-linking is an effective method to covalently link proteins, which are close enough to each other that the cross-linker can bridge the space between them. This holds true for example for oligomers, which consist of monomers noncovalently linked. Covalent cross-linking allows then to visualize the protein of interest in its oligomeric state of the on SDS-polyacrylamide gels.

Three different cross-linkers were used: DMA (Pierce, Rockford, USA), DMS (Uptima) and DTSSP (Pierce, Rockford, USA), which differ from the length of their spacer arm.

**Fig. 1: Structures of the different cross-linkers used in this study.**

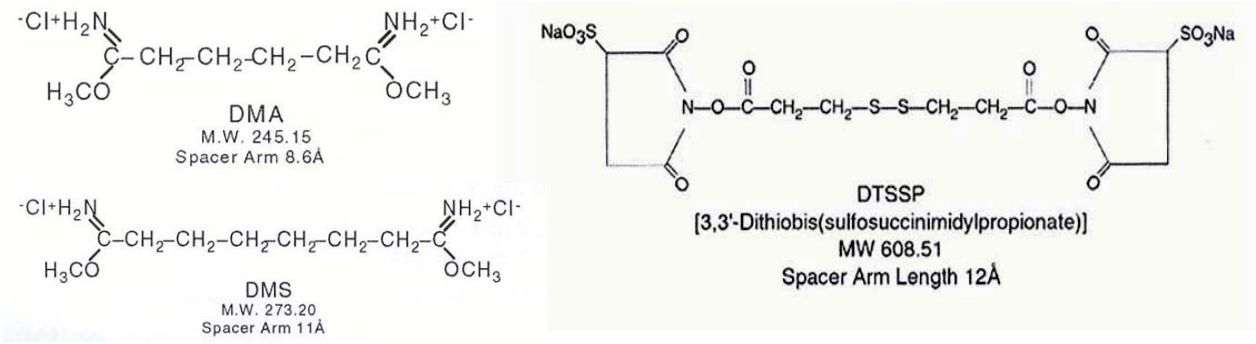


Chemical cross-linking was performed on purified His-tagged proteins still bound on $Ni^{2+}$-NTA agarose beads. His-tagged proteins were purified from cRNA-injected radiolabeled oocytes as described in 2.2.e. The beads were washed five times with 0.1 M sodium phosphate buffer pH 8.0-0.2% digitonin, containing 25 mM imidazole, and 10 mM iodacetamide, and then two times with 0.1 M phosphate buffer pH 8.0-0.2% digitonin. After the last washing step all the washing buffer was carefully removed and the cross linking reaction was performed in a volume of 50 µl. Each cross-linker was dissolved just before use. *DMA and DMS* were dissolved in 0.2 mM triethanolamine pH 8.0-0.5% digitonin, and 50 µl were added to the beads. *DTSSP* was dissolved in 0.1 M sodium phosphate buffer pH 7.4-0.5% digitonin, and 50 µl were added to the beads. At the desired time the beads were centrifuged, and the cross-linker was removed by pipeting. Before elution a washing step with 0.1 M phosphate buffer pH 8.0-0.2% digitonin was performed. The proteins were eluted from the $Ni^{2+}$-NTA agarose beads by two rounds of incubation, both for 15 min at room temperature: first with 50 µl of 250 mM imidazole pH 7.4-0.5% digitonin, and second with 50 µl of 1x SDS-loading buffer containing 20 mM DTT. DTSSP was an exception, because the second elution had to be

performed in 50 µl 1x SDS-loading buffer without DTT. Both elutions were kept separated.

2.5 µl of 5x SDS-loading buffer (with or without 0.1 M DTT) were added to 10 µl of the first elution. The remaining 40 µl left were preserved for BN-PAGE analysis. The samples in SDS-loading buffer from the first and the second elution were denatured for 10 min at 56°C and proteins were then resolved on SDS-polyacrylamide gradient gels.

*g- Deglycosylation*

Deglycosylations of glycoproteins were performed using two endoglycosidases: EndoH (Endoglycosidase H) and PNGase F (Peptide: N-glycosidase F) (both form New England Biolabs, Frankfurt am Main, Germany). EndoH is only able to remove high mannose chains formed in the endoplasmatic reticulum (ER), whereas PNGase F removes high mannose chains formed in the ER, and complex oligosaccharides formed in the Golgi apparatus. The enzymatic reaction was performed in 1 x SDS-PAGE loading buffer for 3h at 37°C. 10 µl of protein sample (in elution buffer) were supplemented with 2.5 µl of 5x SDS-PAGE loading buffer (containing 0.1 M DTT) and incubated with 2 µl enzyme diluted 1:10. EndoH was diluted in 1 x SDS-PAGE loading buffer, and PNGase was diluted in 1% (w/v) NP-40 to counteract SDS inactivation of this enzyme. Before loading the samples on SDS-PAGE, 1% NP 40 was added to the control samples (without enzyme) and to the samples digested with EndoH.

## II-4. Rat brain Synaptosomes preparation and interaction assays using GST fusion proteins

### 4.1 Rat brain Synaptosomes preparation

This protocol describes the preparation of a protein detergent extract from a rat brain, which is suited for affinity chromatography assays.

**Table 5: Sucrose buffer and detergent phosphate buffer composition.**

| Compounds | "Sucrose" buffer | Detergent-phosphate buffer |
|---|---|---|
| Sucrose | 0.32 M | - |
| Tris-HCl | 10 mM | - |
| $Na_2HPO_4$ | - | 77.4 mM |
| $NaH_2PO_4$ | - | 22.6 mM |
| Triton X-100 10% | - | 0.1% (v/v) |
| Protease inhibitors | 0.1% (v/v) | 0.1% (v/v) |
| pH | 7.4 | 7.4 |

If digitonin was chosen instead of Triton X-100, the following concentrations were used: homogenization: 1% (w/v); washing: 0.2% (w/v).

An adult Sprague-Dawley rat was anaesthetized with isoflurane (Abbot) and killed by decapitation. The brain was rapidly removed, and dropped into ice-cold PBS.

All the following steps (4.1, 4.2 and 4.3) except elution, were performed on ice and the different buffers were maintained cold.

The complete rat brain was homogenized with 10 ml of sucrose buffer with the help of a Potter-Elvehjem tissue homogenizer, at slow speed. The formation of air bubbles during the homogenization was avoided as far as possible. This homogenate was centrifuged for 10 min at 1,000g.
The resulting supernatant is once again centrifuged for 15 min at 15,000 g (Schmalzing, 1985). At the end of this centrifugation, the pellet was resuspended with 1 ml sucrose buffer and diluted with 4 ml phosphate buffer. This homogenate (= "synaptosomal detergent extract") was incubated by end-over-end mixing for 15 min at 4°C.
The synaptosomal detergent extract was centrifuged for 10 min at 15,000g, and the supernatant was used for the pull-down experiments.

## 4.2 Rat brain Synaptosomes purification through a Ficoll gradient

In some experiments, myelin was removed from the synaptosome preparation. For this purpose a supplementary step consisting of a centrifugation through a discontinuous Ficoll/sucrose gradient was added to the protocol described above (Booth and Clark, 1978).

As previously, the brain tissue was homogenized in sucrose buffer and centrifuged for 10 min at 1,000g, and the resulting supernatant was centrifuged for 15 min at 15,000g to obtain a crude mitochondrial/synaptosomal P2 pellet. The P2 pellet was resuspended with 2.5 ml of a sucrose solution (0.32 M sucrose, 50 μM EDTA, pH 7.4) and diluted to 15 ml with 12% Ficoll/sucrose: 12% (w/w) Ficoll$^{TM}$ PM 400 (Amersham Biosciences; Freiburg, Germany) 0.32 M sucrose, 50 μM EDTA, pH 7.4. This suspension was transferred into a centrifugation tube and carefully overlaid with 11.75 ml of 7.5% Ficoll/sucrose (7.5% (w/w) Ficoll, 0.32 M sucrose, 50 μM EDTA, pH 7.4) and 11.75 ml sucrose solution (0.32 M sucrose, 50 μM EDTA, pH 7.4). The tube was centrifuged for 30 min at 99,000 g and 4°C (SW 28 rotor, Beckman). At the end of the centrifugation, the purified synaptosomes are located at the border between 12% and 7.5% Ficoll (see Fig.2).

The synaptosomal layer was collected with a Pasteur pipette, diluted to 15 ml with sucrose buffer and centrifuged for 10 min at 15,000 g and 4°C. The pellet was then subjected to the same detergent treatment as in 3.1.

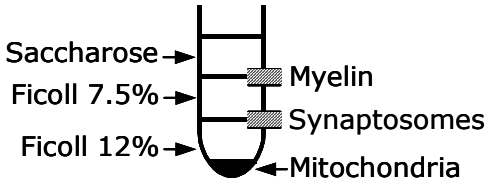


**Fig. 2: Scheme of the fractionation of a crude mitochondrial pellet trough a Ficoll-Sucrose gradient.**

### 4.3 "Pull-down" experiments: Interaction assays using GST fusion proteins

The complete synaptosomal detergent extract was pre-cleared by a 30 min incubation with about 200 μg of GST protein alone, immobilized on glutathione-Sepharose. The beads were centrifuged (for 2 min, 10,000g and 4°C) and discarded. 1 ml of the pre-cleared supernatant (about 3 mg of synaptosomal proteins) was incubated with about 50 μg of one of the various GST-P2X fusion proteins (immobilized on glutathione-Sepharose) for 1 h at 4°C. The beads were washed 5 times with detergent-phosphate buffer, and proteins were then eluted by a 15 min incubation with 1x SDS-PAGE loading buffer at 56°C. The samples were resolved by SDS-PAGE, and proteins were visualized by staining with Coomassie Blue.

## II-5. Protein separation: PolyAcrylamide Gel Electrophoresis

### 5.1. SDS-PAGE

a- *Linear SDS-PAGE*

To pour the SDS-polyacrylamide gels, a vertical slab glass cuvette from Phase (Lübeck, Germany) was used, and the following volumes (in ml) are calculated for 1 gel of 1 mm thickness using this cuvette:

**Table 6: 5x SDS-loading buffer composition.**

| Compound | Vol. or weight (concentration) |
|---|---|
| 1M Tris/HCl pH 6.8 | 3.1 ml (310 mM) |
| SDS | 1 g (10%) |
| 87% glycerol | 7g (50%) |
| Bromophenol blue | 50 mg (0.5%) |
| $H_2O$ | Adjust vol. to 10 ml |

Just before use: add 5 μl of 2M DTT to 100 μl of 5x SDS-PAGE loading buffer

Protein mass marker: [$^{14}$C]-labeled molecular mass marker (Rainbow, Amersham Biosciences; Freiburg, Germany)

**Table 7: Preparation of linear SDS-polyacrylamide gels.**

| Compounds | 1 gel 10% | 1 gel 12.5% | 1 stacking gel (4%) |
|---|---|---|---|
| $H_2O$ | 3.635 | 3.167 | 3.17 |
| 40% acrylamide* | 1.875 | 2.343 | 0.5 |
| 1.5M Tris-HCl pH 8.8 | 1.875 | 1.875 | - |
| 0.5M Tris-HCl pH 6.8 | - | - | 1.25 |
| 20 % SDS | 0.0375 | 0.0375 | 0.025 |
| 10 % APS | 0.075 | 0.075 | 0.05 |
| TEMED | 0.003 | 0.003 | 0.005 |

* 40% acrylamide/Bis-acrylamide solution (29:1) Bio-Rad

Running buffer: 10xTris/glycine/SDS

250 mM Tris, pH 8.3, 1.92 M glycine, 1% SDS

It is not necessary to adjust the pH, this is achieved automatically, furthermore chloride ions would disturb the migrations of proteins.

Fixing solution to facilitate the drying of a SDS-polyacrylamide gels:

65% $H_2O$; 25% Isopropanol; 10% acetic acid

Coomassie Blue staining :

**Table 8: Staining and destaining solutions composition for Coomassie blue staining.**

| Solution | Compound | Weight, or vol. |
|---|---|---|
| Staining (200 ml) | Coomassie Brilliant Blue R250 | 0.3 g |
| | Methanol | 1.5 ml |
| | TCA | 198.5 ml |
| Destaining (2 l) | Methanol | 300 ml |
| | Acetic acid | 150 ml |
| | $H_2O$ | 1550 ml |

b- *Gradient SDS-PAGE*

The gradient SDS-polyacrylamide gels are poured with the same gel solutions as for the linear SDS-PAGE system, but consist of a mixture of two preparations with different acrylamide concentrations. The volumes are calculated such that when the gradient gel is poured there is no solution left. The stacking gel is exactly the same as in 4.1.a-.

**Table 9: Preparation of gradient SDS-polyacrylamide gels.**

| Compounds | 1 gel 4 % | 1 gel 10 % |
|---|---|---|
| $H_2O$ | 2.699 | 2.061 |
| 40% acrylamide* | 0.4254 | 1.0635 |
| 1.5M Tris-HCl pH 8.8 | 1.0635 | 1.0635 |
| 20 % SDS | 0.0213 | 0.0213 |
| 10 % APS | 0.0425 | 0.0425 |
| TEMED | 0.0017 | 0.0017 |

* 40% acrylamide/Bis-acrylamide solution (29:1) Bio-Rad
Volumes in ml.

The gels are run at 100V when the proteins are in the stacking gel, and at 125V when the proteins are in the running gel.

c- *Tricine-SDS-PAGE*

The Tricine-SDS-PAGE system is a discontinuous SDS-PAGE method, which enhances the resolution for small proteins (Schägger and von Jagow, 1987). Tricine is used instead of glycine as trailing ion. The gels are run at 70V when the proteins are in the stacking gel, and at 100V when the proteins are in the running gel.

**Table 10: Buffers used in the tricine-SDS-PAGE system.**

| Compounds | Gel buffer | Anode buffer | Cathode buffer |
|---|---|---|---|
| Tris | 3 M | 0.2 M | 0.1 M |
| Tricine | - | - | 0.1 M |
| % SDS | 0.3 | - | 0.1 |
| pH* | 8.45 | 8.9 | 8.859 (automatic) |

pH* : The pH values are adjusted with HCl

**Table 11: Preparation of tricine-SDS-polyacrylamide gels.**

Volumes in ml for 1 gel (1mm)

| Compound | Spacer gel 10% | Running gel 16.5% (optional) | Stacking gel 4% |
|---|---|---|---|
| Gel buffer | 1.67 | 1.67 | 0.62 |
| 40% acrylamide* | 1.26 | 2.079 | 0.25 |
| $H_2O$ | 2.07 | 0.761 | 1.63 |
| Glycerin | - | 0.6 g | - |
| 10% APS | 0.025 | 0.025 | 0.013 |
| TEMED | 0.0025 | 0.0025 | 0.0013 |

*40% acrylamide/Bis-acrylamide solution (29:1) Bio-Rad

**Table 12: 5x tricine-SDS-loading buffer.**

| Compound | %/concentration |
|---|---|
| Tris/HCl pH 6.8 | 250 mM |
| SDS | 20% |
| Glycerol | 60% (w/v) |
| Serva Blue G | 0.05% |

Just before use: add 5 µl of 2M DTT to 100 µl of 5x SDS-PAGE loading buffer

d- *Tris-Borate-EDTA SDS-PAGE*

This protocol is inspired from the work of J.F. Poduslo (Poduslo, 1981). Glycoproteins often behave anomalously in SDS-PAGE systems, because the binding of constant amounts of SDS per protein molecule is not

achieved compared with non-glycosylated proteins. The glycoprotein migrates at a higher apparent molecular mass.

During my experiments I was confronted to the problem that some glycoproteins were not migrating as sharp bands in SDS-PAGE. For this reason borate salt was included in the gel solutions. Borate ions can react with neutral sugars converting them to charged complexes at alkaline pH. The formation of borate complexes could increase the net negative charge of glycoproteins which would compensate for the decreased binding of SDS, resulting in a charge density consistent with an electrophoretic migration of glycoproteins that now correlates with their molecular mass.

Proteins were purified from injected oocytes as described in 2.2.e. Elution was performed as usual with 100 µl of 250 mM imidazole, pH 7.4, and 0.5% digitonin. 9 µl of protein sample in 1x SDS-loading buffer was incubated overnight at 4°C with 1 µl of a borate solution (1 M Tris, 1 M boric acid, 25 mM EDTA, pH 8.3). The next day the sample was applied on a borate SDS-polyacrylamide gel prepared as follows. The gel was poured like a conventional SDS-PAGE, the only difference is the composition of the gel solutions.

Borate gel buffer: 1 M Tris, 1M boric acid, 25 mM EDTA, 1% SDS, pH 8.3

**Table 13:. Preparation of Tris-Borate-EDTA-SDS-polyacrylamide gels.**

| Compounds | 1 gel 10% | 1 stacking gel (4%) |
|---|---|---|
| $H_2O$ | 4.800 | 4.195 |
| 40% acrylamide* | 1.875 | 0.5 |
| Borate gel buffer | 0.750 | 0.250 |
| 10 % APS | 0.075 | 0.05 |
| TEMED | 0.003 | 0.005 |

* 40% acrylamide/Bis-acrylamide solution (29:1) Bio-Rad

Running buffer: 0.1 M Tris, 0.1 M boric acid, 2.5 mM EDTA, 0.1% SDS, pH 8.5

The gel run 4.5 h at constant power (15W) with a cooling system.

## 5.2. BN-PAGE

Blue native (BN) PAGE analysis permits gel electrophoresis under non denaturing conditions (Schägger et al., 1994) and thus the determination of the oligomeric structure of proteins. BN acrylamide gels are gradient polyacrylamide gels. The gels were let run for 3 h, or overnight to allow the proteins to reach their equilibrium migration point.

**Table 14: Buffers used in the BN-PAGE system.**

| Compounds | Gel buffer 3 x | Anode buffer | Cathode buffer |
|---|---|---|---|
| Tricine | - | - | 50 mM |
| Bistris | 150 mM | 50 mM | 15 mM |
| Aminocaproic acid (Sigma) | 1.5 M | - | |
| pH* | 7.0 | 7.0 | 7.0 |
| Serva Blue G | - | - | 0.005% just before use |

pH* : The pH values were adjusted with HCl

**Table 15: Preparation of BN-Polyacrylamide gels.**

| Compound | Gel 4% | Gel 16% | Gel 6% | Gel 20% | Stacking gel 4% |
|---|---|---|---|---|---|
| Gel buffer | 1.362 | 1.362 | 1.09 | 1.09 | 1.67 |
| 30% acrylamide* | 0.575 | 2.265 | 0.86 | 3 | 0.667 |
| $H_2O$ | 2.3 | - | 2.35 | - | 2.64 |
| Glycerin | - | 0.903 g | - | 0.72 g | |
| 10% APS | 14.875 µl | 14.875 | 14.875 µl | 14.875 µl | 20.µl |
| TEMED | 2.875 µl | 2.875 | 2.875 µl | 2.875 µl | 4 µl |

Gel run for 3h  Gel run for 12h

*30% acrylamide/Bis-acrylamide solution (29:1) Bio-Rad

Protein mass marker: Combithek II (Boehringer Ingelheim, Germany), calibration proteins in native conformation for chromatography (MW 18,000-300,000 kDa).

**Table 16:. 5x BN-loading buffer.**

| Compound | %/concentration |
|---|---|
| Serva Blue G | 1% |
| Aminocaproic acid | 100 mM |
| Glycerol | 50% (w/v) |

2.5 µl BN-loading buffer 5x were added to 10 µl of protein sample.

Before being loaded on the BN-gel, some samples were subjected to treatments (in BN-loading buffer) that might denature proteins such as heating (1h-37°C or 1h-56°C) or incubation with urea (4M or 8M), DTT (0.1M), or SDS (0.01 to 1%). Urea (Sigma; Taufkirchen, Germany) was freshly dissolved in 2.5 µl 5x BN-loading buffer by flickering, then 10 µl sample were added. For samples in native condition, BN-loading buffer was added just before loading on the gel.

It is important to wash the pockets of the BN-gel with buffer before loading the samples, because there is still non-polymerized acrylamide inside after removing the comb.

**Table 17: Staining and destaining solutions composition for Coomassie blue staining of BN-polyacrylamide gels.**

| Solution | Compound | Weight, or vol. |
|---|---|---|
| Staining 1 l | Coomassie Brilliant Blue R250 | 1 g |
| | methanol | 450 ml |
| | acetic acid | 100 ml |
| | $H_2O$ | 450 ml |
| Destaining 1 l | methanol | 100 ml |
| | acetic acid | 100 ml |
| | $H_2O$ | 800 ml |

The radioactive SDS-polyacrylamide gels were dried for 2h at 80°C, and the tricine- or BN-gels were dried for 3 h at 70°C (Gel dryer model 583, Bio-Rad). The signal on the gels was then revealed either with BioMax MS films (Kodak), or by using PhosphorImager screens (Amersham Biosciences; Freiburg, Germany) in combination with a Storm 820 PhosphorImager. Kodak films were developed manually using fixing and developing solutions from Kodak according to the instructions of the manufacturer.

## 5.3. 2D-electrophoresis

Two-dimensional electrophoresis is a powerful method for the analysis of complex protein mixtures extracted from cells, tissues or other biological samples. This technique separates proteins according to two independent properties in two steps:

✓ the first dimension step: isoelectric focusing (**IEF**) separates the proteins according to their isoelectric point (pI)

✓ the second-dimension step, **SDS-PAGE**, separates proteins according to their molecular mass.

Each spot on the resulting two-dimensional array is assumed to correspond to a single protein species in the sample.

For IEF (first dimension), the Multiphor™ II apparatus and immobilized non-linear pH gradients (18 cm IPG strips, pH 3-10; Amersham Biosciences, Freiburg, Germany; ordering number: 17-1235-01) were used. For the second dimension large SDS-polyacrylamide gels (18x16 cm plates) were poured according to the recipe described in 4.1.a, and were run with a Biometra Maxigel apparatus (Göttingen, Germany). The complete protocol, including solution compositions is extremely well described in a booklet available through Amersham Biosciences (Berkelman and Stenstedt, 1998).

2-D electrophoresis was performed after pull-down experiments (3.3.). After the washing steps, proteins were eluted with reduced glutathione (Amersham Biosciences; Freiburg, Germany) instead of 1x SDS-loading buffer. The elution solution contained 10 mM glutathione freshly solubilized in Tris-HCl 50 mM, pH 8.0. For elution proteins were incubated for 1h at room temperature by end-over-end mixing with 1 ml of glutathione solution per 50 µl beads. Proteins were then precipitated with 3 ml of ice cold acetone per ml of protein solution in glutathione for at least 2 h at -20°C. Proteins were collected by centrifugation (20,000g for 15 min at 4°C), the pellet was dried by air and finally solubilized in rehydration solution for IPG strips (Amersham Biosciences; Freiburg, Germany), which volume depended on the size of the protein pellet and ranged between 500 µl and 1 ml. IPG strips were rehydrated overnight at room temperature with IPG rehydration solution in which eluted proteins were dissolved. Details of the electrophoretic separation in the first and second dimensions are well described in the reference cited above.

## II-6. Other techniques

### 6.1. Silver staining

The 2-D polyacrylamide gels were stained with silver nitrate to visualize the protein spots. The following protocol is adapted from (Blum et al., 1987), and is compatible with tryptic digestion for mass spectrometry analysis.

For the sensitization step a 10% $NaS_2O_3$ (pentahydrate) solution was prepared, which was diluted 500 fold before use (2 ml of 10% stock solution in 1l) because the 0.8 mM $NaS_2O_3$ solution is stable for 1 week only.

The staining protocol was the following: The gels were fixed 3 times for 30 min in fixing solution and rinsed 4 times for 10 min with water. The sensitizing step lasted only 1 min (1 gel at a time).

**Table 18: Composition of the solutions used for silver staining.**

| Compound | Fixation | Sensitizing | Staining | Developing | Stop |
|---|---|---|---|---|---|
| $NaS_2O_3$ (pentahydrate) | - | 0.8 M | - | 0.00125% | - |
| NiAg | - | - | 2 g/l | - | - |
| $K_2CO_3$ | - | - | - | 3% | - |
| 37% formaldehyde solution | - | - | - | 0.00925 | - |
| Tris | - | - | - | - | 4% |
| Absolute ethanol | 30% | - | - | - | |
| Acetic acid | 5% | - | - | - | 2% |

Immediately thereafter the gels were rinsed twice for 1 min with water, incubated in silver nitrate for 30-60 min, and rinsed once for 5-15 s with water. Development was performed by an incubation for 10-20 min with the developing solution. The development was stopped by immerging the gels into the stop solution for 30-60 min. Finally the gels were rinsed several times with water.

After silver staining the gels were dried (see 5.2.) and scanned using the Snapscan 1236 scanner from Agfa. Protein spots of interest were excised from the gels after drying, subjected to proteolytic digestion with trypsin (Promega; Mannheim, Germany) in the gel matrix and fragments were analysed by Maldi-TOF mass spectrometry by the group of K. Aktories (Institute of Experimental and Clinical Pharmacology and Toxicology, Albert Ludwigs-University, Albertstrasse 25, D-79104 Freiburg, Germany) using a Bruker Biflex mass spectrometer (Schmidt et al., 1999).

## 6.2 Western-Blotting

The first step of a Western-blot is the transfer of the proteins from acrylamide gels onto nitrocellulose membranes. The transfer was performed with a semi dry blotter (Pegasus blotter, Phase, Lübeck, Germany). The transfer buffer contained 25 mM Tris, 192 mM glycine, and 20% methanol. PVDF nitrocellulose membrane (Millipore) was used, which was soaked in methanol before use. The advantage of this type of membrane is that proteins are trapped on the membrane and can not pass through it. The transfer was performed for 2 h at ~2 mA/cm$^2$ of gel surface, and a maximum of 40 volts.

**Fig. 3: Protein transfer principle.**

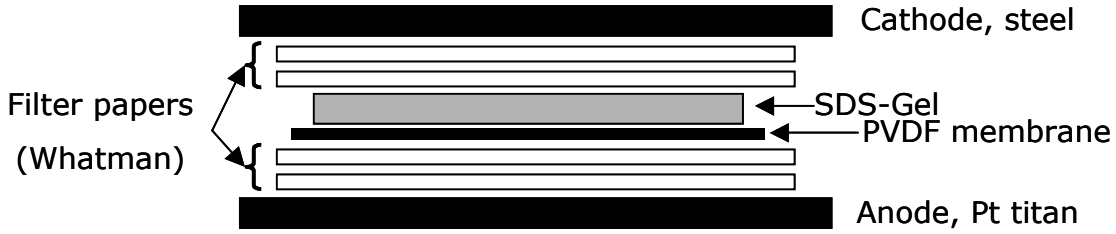


The main buffer used for Western-blot is called TBST (10 mM Tris pH 8.0, 150 mM NaCl, 0.05% Tween 20 (Sigma; Taufkirchen, Germany)). All the steps of the Western-blot were performed at room temperature. After transfer, the membrane was blocked for 1 h with TBST supplemented with 1% (w/v) of non-fat dry milk and 1% (w/v) of BSA, and then incubated for 1 h with the "primary" antibody diluted in TBST/1% milk/1% BSA. The membrane was then washed 3 times for 10 min with TBST/1% of milk/1% of BSA. The incubation (for 1 h) with the "secondary" antibody (HRP-conjugated antibody, diluted with TBST/1% milk/1% BSA) was followed by 3 washing steps (15 min each) with TBST. The membrane was at this step ready for enhanced chemiluminescence (ECL), which is a method to detect the bound antibodies. During this study the following antibodies were used: antibody anti-ßIII tubulin

(1:400, Sigma), anti-MBP (1:400, PharMingen), and goat antibody anti-mouse IgG HRP-conjugated (1:5000, Amersham Biosciences).

The ECL-solution was composed of 0.1 M Tris-HCl, pH 8.5, 25 μM Luminol (Sigma), and 0.44 μM Comaric acid (Sigma). At the last time 6.25 μl of $H_2O_2$ were added to 10 ml of ECL solution. For ECL, the membrane was incubated in ECL-solution for 1 min in a dark room, and placed between two plastic sheets. A film (Hyperfilm$^{TM}$MP, Amersham Biosciences; Freiburg, Germany) was then exposed to the membrane. The time of exposure was adjusted to the intensity of the signal. The film was then developed with a developing machine (Optimax Type TR, MS Laborgeräte).

## 6.3. Overlay assays

This protocol for overlay assays was adapted from the work of McPherson et al. (McPherson et al., 1994), all the steps were performed at room temperature. *GST fusion proteins* were produced as described in 2.1.b, but after the washing steps, directly eluted with a 10 mM glutathione solution (in Tris 50 mM, pH 8.0). Glutathione solution was exchanged against sodium phosphate buffer (0.1 M, pH 8.0) by size exclusion chromatography using Hi-Trap desalting columns (Amersham Biosciences; Freiburg, Germany).

After determining the protein concentration with a BCA protein assay reagent kit from Pierce (Rockford, USA; for details see the instructions of the manufacturer), the GST fusion protein was stored in aliquots at -80°C.

A Triton X-100 extract of synaptosomes was supplemented with reducing SDS-PAGE loading buffer, boiled for 2 min (95°C), and then resolved on an SDS-polyacrylamide gel (10% acrylamide). After semi-dry protein transfer, the PVDF membrane was blocked by overnight incubation with Blotto buffer. The membrane was then washed and incubated for 1 h in

buffer B containing 3% BSA, 1 mM DTT and 4.5 μg/ml of one of the GST fusion proteins.

**Tables 19, 20: Composition of the buffers used for overlay assays**

| Blotto Buffer | |
|---|---|
| Compound | Concentration |
| NaCl | 150 mM |
| $Na_2HPO_4$ | 50 mM |
| Non-fat dry milk | 5% (w/v) (at the last time) |
| pH | 7.5 |

| Buffer B | |
|---|---|
| Compound | Concentration |
| Tris | 20 mM |
| Tween 20 | 0.1% |
| pH | 7.4 |
| At the last time: | |
| DTT (optional) | 1 mM |
| BSA | 3% (w/v) |
| GST fusion protein (optional) | 4.5 μg/ml |

The membrane was washed three times with buffer B containing 3% BSA, and then incubated with an antibody against GST (Amersham Biosciences; 1:10,000) in buffer B, 3% BSA. Subsequently, the membrane was washed twice with buffer "C" (10 mM Tris-HCl, pH 7.4, 150 mM NaCl), four times with buffer "D" (0.2% SDS, 0.5% Triton X-100, 0.5% BSA, 0.9% NaCl, pH 7.0), and twice with buffer C. Bound GST-antibody was labeled by incubation with [$^{125}$I]protein A (Amersham Biosciences; 30,000 cpm/ml) for 1 h in buffer C, followed by a series of washing steps (2x buffer C, 5x buffer D, 3x buffer C). Visualization of bound radioactivity was achieved by PhosphorImaging.

# III/ Results

## III-1. Identification of proteins interacting with the C-terminal tail of P2X receptors

To isolate proteins interacting with the C-terminal tail of P2X receptors, GST fusion proteins containing the C-terminal portion of rat $P2X_2$, $P2X_5$ and $P2X_7$ were produced and used as baits to screen detergent extracts of rat brain synaptosomes by affinity chromatography. To identify potential interacting partners, proteins were resolved by SDS-PAGE and/or 2D-electrophoresis. Protein bands/spots of interest were excised from the gels, digested with trypsin and proteolytic fragments were analyzed by MALDI-TOF mass spectrometry. The proteolytic profiles were then compared with those deposited in databases.

### 1.1 Design and expression of GST-rP2X$_2^{356-472}$, GST-rP2X$_5^{364-457}$ and GST-rP2X$_7^{433-596}$ fusion proteins

The members of the P2X receptor family share a common membrane topology with two membrane spanning segments linked by a large, glycosylated ectodomain (Fig. 1). The first transmembrane segment is preceded by an intracellular N-terminal domain, which has a similar length of 24-31 amino acids on all P2X subunit isoforms. In contrast, the C-terminal tails show no apparent sequence homology and their lengths vary considerably between the various P2X isoforms ranging from 27 ($P2X_6$) to 239 amino acids ($P2X_7$). These characteristics suggest that the C-terminal tails may carry isoform-specific information important for the *subcellular targeting and membrane clustering of the receptor*.

For a search of putative binding proteins, we focused on the three P2X subunits that possess the longest C-terminal domains within the P2X family: $P2X_2$, $P2X_5$, $P2X_7$, assuming that they have the highest probability to be involved in protein-protein interactions. Three GST-P2X fusion proteins were engineered all consisting of glutathione S-transferase fused

N-terminally to the *C-terminal tail of one of the three rat P2X isoforms* (see Fig.2).

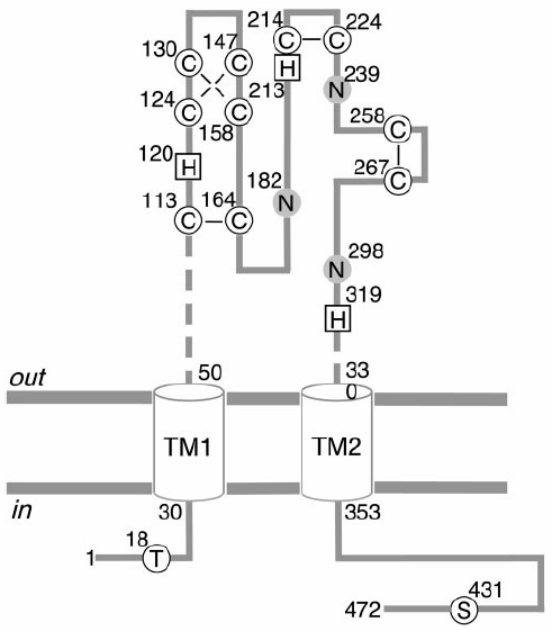


**Fig. 1: Membrane topology of $P2X_2$ receptors showing glycosylation, phosphorylation and possible disulfide bonding (North, 2002)**. Solid circles (N): indicate glycosylated sites in the native $P2X_2$ receptor. Open circles (T, S): indicate positions phosphorylated by protein kinases (PKC, PKA). Open circles (C): indicate the 10 conserved cysteines. Open squares (H): indicate histidine residues involved in zinc (His-120, His-213) and proton binding (His-319).

a- *Expression of the three GST-rP2X fusion proteins*

Small quantities of GST fusion proteins were first produced to find the optimal culture and induction conditions and to see the pattern of expression of the different proteins. Fig. 3 shows GST-$P2X_2$ fusion protein resolved by SDS-PAGE after small scale expression, and Fig. 4 shows the pattern of expression of the three GST-P2X fusion proteins expressed in *E.coli* BL21. The optimal induction conditions for all the fusion proteins were 0.2 mM IPTG for 3h at 37°C. These culture and induction conditions were also used for the expression of large amounts of fusion proteins. As shown in Fig. 4, the full-size GST-$P2X_2$ and GST-$P2X_5$ were produced as full-length proteins in *E.coli* BL 21 as judged from the correct mass of the

major protein species. In addition, several degradation products were observed in small quantities.

Unfortunately GST-P2X$_7$ was degraded either during the protein synthesis or during the purification steps. Reducing the temperature of culture from 37°C to 25°C or using *E.coli* K-12 TG1 as a bacterial host strain did not eliminate this problem. Also usage of a milder detergent (digitonin) or reducing the intensity of ultrasonication did not reduce GST-P2X$_7$ degradation (results not shown). Pull-down experiments were nevertheless performed with these samples.

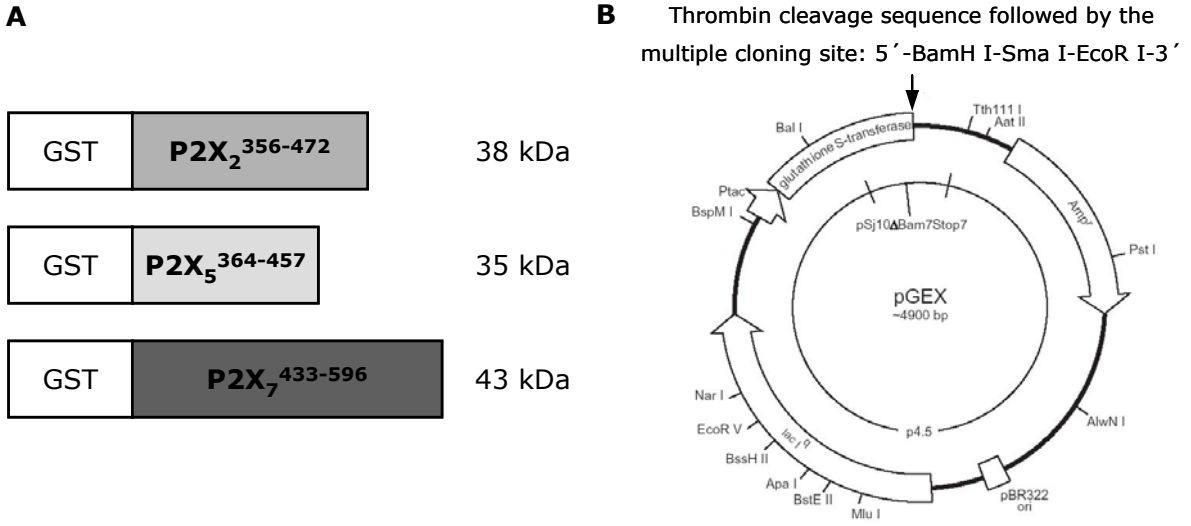


**Fig. 2: Design of the GST-P2X fusion proteins and map of the pGEX-2T vector.** (A) Superscripts refer to the amino acid sequence of the corresponding full length P2X subunit. The total mass of the fusion protein including the GST portion is indicated. (B) Map of the pGEX-2T vector (Amersham Biosciences). All the P2X sequences were cloned between the BamH I and EcoR I cleavage sites of this vector.

An upper band of approximately 70 kDa was always observed to co-purify with the fusion proteins. A protein of an apparently identical mass has already previously been observed to co-purify in pull-down experiments and has been identified to represent the product of the gene *dna*K from *E.coli* (Amersham Biosciences, 2001). This protein is involved in the degradation of "abnormal" proteins in *E.coli* and binds to GST or the Sepharose matrix.

b- *Pull-down experiments: Tubulin binds specifically to the $P2X_2$ subunit*

To identify possible interacting proteins, the GST fusion proteins incorporating the C-terminal domains of the rat $P2X_2$, $P2X_5$ and $P2X_7$ isoforms were incubated with a detergent extract of rat brain synaptosomes. After washing and centrifugation, bound proteins were eluted from the glutathione-Sepharose beads and resolved by tricine-SDS-PAGE followed by Coomassie blue staining.

For each fusion protein, two samples were treated identically: one sample consisted of fusion protein (immobilized on glutathione-Sepharose beads) and detergent extract of synaptosomes, the other sample (control) consisted of the same quantity of immobilized GST-P2X fusion protein and the detergent buffer used for the synaptosome preparation and extraction (sucrose/phosphate buffer, see II-4.1). After finishing the pull-down experiment, the two samples were resolved on the same tricine-SDS-polyacrylamide gel. Protein bands present in the sample incubated with synaptosome detergent extract, and absent in the control sample were considered to represent potential interacting proteins. These bands were excised from the gel, digested with trypsin in the gel matrix, and analyzed by MALDI/TOF mass spectrometry. MALDI/TOF analyses were performed by Dr. J. Schirmer from the Institute of Experimental and Clinical Pharmacology and Toxicology in Freiburg, Germany. As additional control, pull-down experiments were performed (-/+ synaptosome extracts) with glutathione-Sepharose beads loaded with the GST moiety alone to distinguish proteins that interact non-specifically with the GST part of the fusion protein.

Pull-down experiments were performed with synaptosome extracts prepared either with Triton X-100, or with digitonin, which is considered to be a milder detergent than Triton X-100. The results are presented in Fig. 5 and 6. A protein band of approximately 55 kDa was detected in the

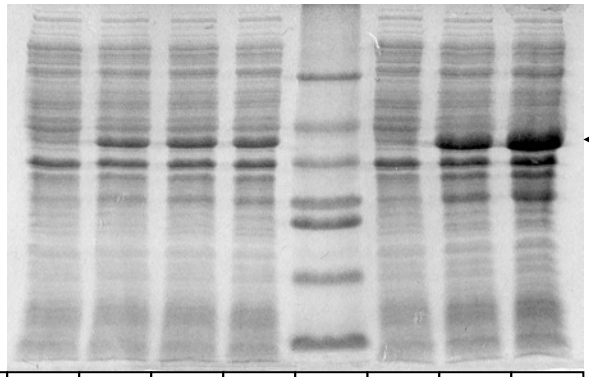


| IPTG (mM) | 0 | 0.1 | 0.2 | 0.4 | MW | 0 | 0.2 | 0.2 |
|---|---|---|---|---|---|---|---|---|
| Time (h) | - | 1 | 1 | 1 | | - | 2 | 3 |

**Fig. 3: Small-scale expression of GST-P2X$_2$.** BL21 bacteria were induced by IPTG for different time periods and at different concentrations as indicated (for further details see Materials and Methods 3.1.a). After the induction the bacteria were harvested and lysed with 1x SDS-loading buffer and the proteins were resolved on a 12.5% SDS-polyacrylamide gel. Arrow, GST-P2X$_2$ polypeptide.

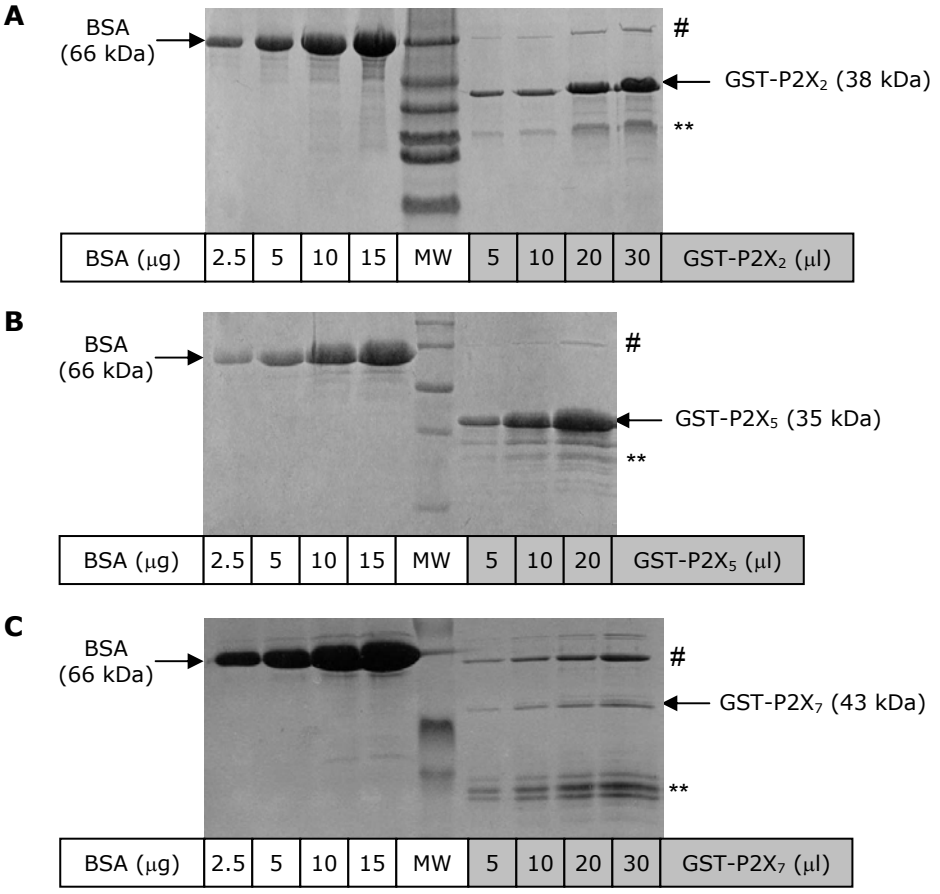


**Fig. 4: Pattern of expression of GST-P2X$_2$ (A), GST-P2X$_5$ (B), and GST-P2X$_7$ (C) in *E.coli*.** The different fusion proteins were expressed in *E.coli* BL21, and purified with glutathione-Sepharose beads. For semi-quantitative determination of protein concentrations, the various GST fusion proteins were released from glutathione beads (different volumes) by boiling in SDS-loading buffer and resolved on linear 12.5% SDS-polyacrylamide gels in parallel with known amounts of bovine serine albumin as standards. The gels were stained with Coomassie blue, and the concentration of the various GST fusion proteins were estimated by visual comparison of the intensity of the protein bands. # Product of the gene dnaK from E.coli, which was consistently co-purify with the GST-fusion proteins; ** degradation products; arrow, indicated P2X fusion protein.

samples incubated with GST-P2X$_2^{356-472}$ (=GST-P2X$_2$) and brain detergent extract (Fig. 5 and 6, lane 2). In contrast, this band was neither observed when the brain detergent extract was incubated with GST alone (Fig. 5 and 6, lane 4), with GST-P2X$_5$ (Fig. 5 and 6, lane 7), nor with GST-P2X$_7$ (Fig. 5 and 6, lane 9). The 55 kDa band was identified by MALDI/TOF mass spectrometry as **ßIII tubulin** (accession number: P04691), a brain-specific ß tubulin isoform. These results were corroborated by immunoblot analyses (Fig. 7), which clearly demonstrate that tubulin was pulled-down with GST-P2X$_2^{356-472}$, but not with the two other GST-P2X fusion proteins nor with GST alone.

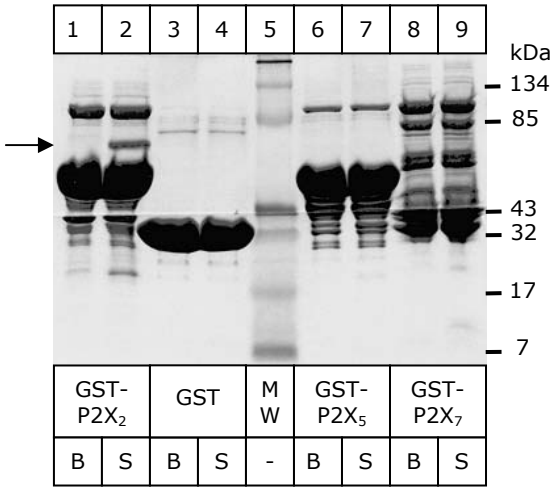


**Fig. 5: Pull-down of proteins from a Triton X-100 extract of rat brain synaptosomes with GST-P2X fusion proteins.** Proteins were pulled-down from a Triton X-100 extract of crude rat brain synaptosomes as described in Materials and Methods. Proteins were resolved in a tricine-SDS-polyacrylamide gel stained subsequently by Coomassie blue. Incubation conditions: (S): Synanaptosomes; (B): Buffer. Black arrow: interacting protein.

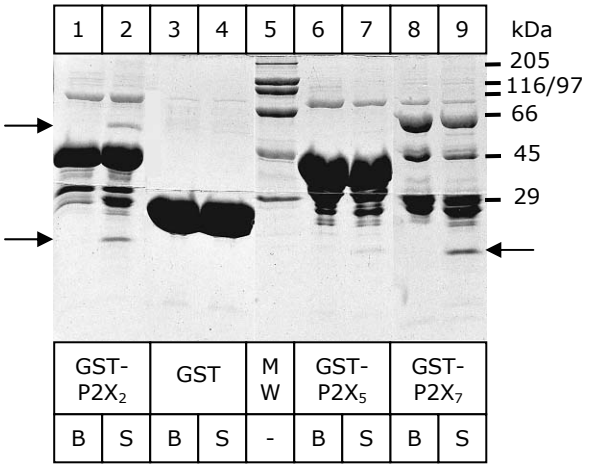


**Fig. 6: Pull-down of proteins from a Digitonin extract of rat brain synaptosomes with GST-P2X fusion proteins..** Proteins were pulled-down from a digitonin extract of crude rat brain synaptosomes as described in Materials and Methods. Proteins were resolved in a tricine-SDS-polyacrylamide gel stained subsequently by Coomassie blue. Incubation conditions: (S): Synaptosomes; (B): Buffer. Black arrow: interacting proteins.

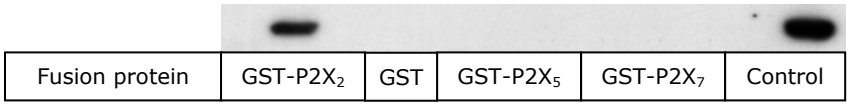


**Fig. 7: Immunoblot analysis after pull-down experiments with GST, GST-P2X$_2$, GST-P2X$_5$, and GST-P2X$_7$.** The samples used for Western-blot are the same as in Fig. 5, but only the samples incubated with synaptosomes were tested. The transferred proteins were probed with an antibody against ßIII tubulin followed by ECL. In the control lane a few µl of the crude synaptosome detergent extract was applied as a positive control of the blotting reaction.

c- *Results confirmed by 2D-electrophoresis*

Because of the limited resolution capacity of 1-D-SDS-PAGE, potential interacting partners of P2X receptors may be hidden behind the large amount of fusion protein. To address this problem, the 2D-electrophoresis technique was used. To this end, pulled-down proteins were eluted with reduced glutathione, and precipitated with acetone as described in the methods (4.3). The proteins were then resolved on immobilized pH gradients (IPG) gel strips between pH 3 and 10. The second dimension was performed with 12.5% SDS-polyacrylamide gels and the gels were stained with silver nitrate. This protocol was used only with GST-P2X$_2$ and GST as control. As in 1.1.b, two samples were handled in parallel, one with synaptosome detergent extract, and one with buffer as control. Two

2D-gels corresponding to pull-down with GST-$P2X_2$ are presented in Fig. 8. By comparison of the two gels, some news spots were detected (not detected after pull-down with GST, data not shown), which can correspond to new proteins interacting with the $P2X_2$ subunit. These spots are still to be analysed by mass spectrometry.

In experiments destined for detection of proteins by Western-blotting, the silver staining was omitted. Proteins were transferred onto nitrocellulose membranes and blotted with an antibody against ßIII tubulin. The ßIII tubulin was detected in the sample pulled-down with GST-$P2X_2$ in the acidic region of the strip, which is in agreement with the low isoelectric point (4.6) of ßIII tubulin (Fig. 8C).

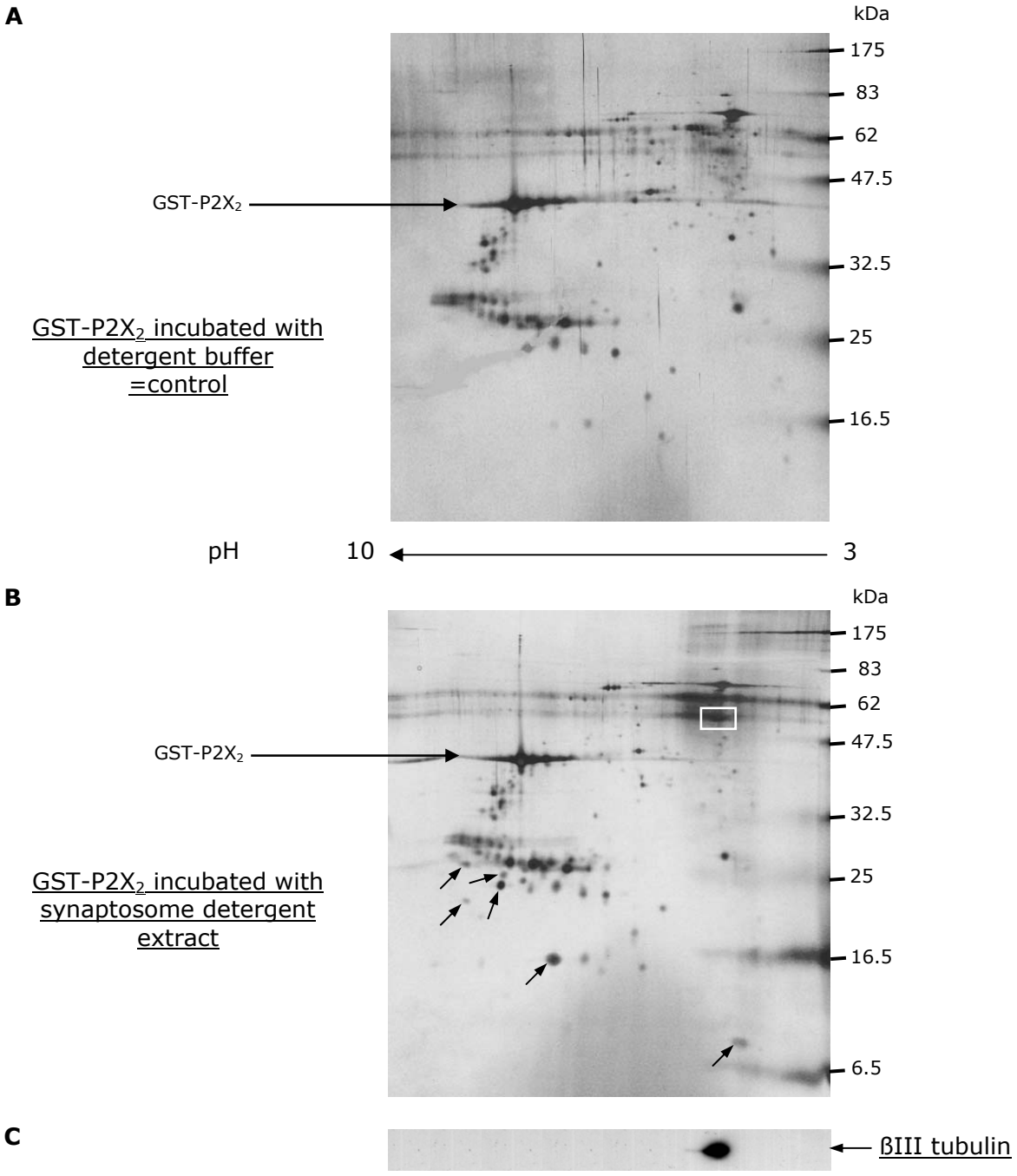


**Fig. 8: Pull-down of rat brain proteins with GST-P2X$_2$ fusion protein followed by 2D-electrophoresis and Western-blot analysis.** (A, B) Proteins were pulled-down from a Triton X-100 extract of crude rat brain synaptosomes and resolved by 2D-gel electrophoresis followed by silver staining. (A) GST-P2X$_2$ was incubated with detergent buffer (sucrose-phosphate buffer), (B) GST-P2X$_2$ was incubated with synaptosome detergent extract. (C) Same sample as in (B), proteins were resolved on a 2D-polyacrylamide gel, transferred onto a nitrocellulose membrane and blotted with an antibody against ßIII tubulin. The black arrows show the potential interacting proteins, and the white rectangle shows the position of the ßIII tubulin on the 2D-gel. All polyacrylamide gels were 12.5% SDS-gels.

## 1.2 All three GST-P2X fusion proteins bind MBP

An additional protein band of about 20 kDa was observed to occur with all three GST-P2X fusion proteins (Fig. 6) and identified by MALDI/TOF mass spectrometry to constitute myelin basic protein (MBP, accession number: CAA10807). Consistent with this result, probing of an immunoblot with an antibody against MBP labeled protein bands of about 20 kDa in the same samples (Fig. 9), supporting the view that MBP interacts with the three fusion proteins GST-$P2X_2$, GST-$P2X_5$, and GST-$P2X_7$. The antibody against MBP recognized several protein bands. This can be attributed to the occurrence of four major MBP isoforms of 21.5, 18.5, 17 and 14 kDa in rat generated by alternative splicing of a single primary MBP transcript (Boggs et al., 2000). The amount of MBP was greatly reduced when Triton X-100 instead of digitonin was used for protein extraction (Fig. 9), indicating that the interaction was more stable in the presence of a mild detergent.

To examine whether MBP isolated through the GST-P2X fusion proteins originates predominantly or exclusively from the large amount myelin present in the crude P2 synaptosome preparation, myelin was removed from the synaptosomes by Ficoll density gradient centrifugation as described in materials and methods. A pull-down experiment with a digitonin extract of the purified synaptosomes, followed by immunoblot analysis with the antibody against MBP showed that MBP could be isolated in significant amounts with GST-$P2X_2$ even when contaminating myelin was greatly reduced (Fig. 10B). This suggest that the interaction between P2X receptors and MBP is not an artefact due to the contamination of synaptosomes with myelin, but occurs with MBP present in the nerve terminals.

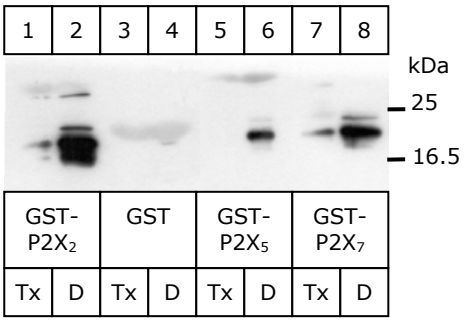


**Fig. 9: Immunoblot analysis of MBP after pull-down of rat brain proteins with GST-P2X fusion proteins.** The synaptosomal detergent extract was prepared either with Triton X-100 or with digitonin and proteins were pulled-down with the indicated GST-P2X fusion proteins. The Western-Blot was developed by ECL.

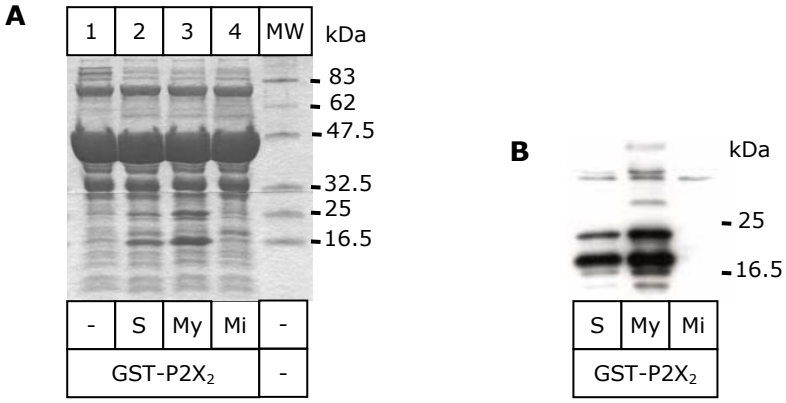


**Fig. 10: Pull-down experiments with GST-P2X$_2$ and purified synaptosomes.** The crude P2 synaptosome preparation was purified through a Ficoll gradient. (S) purified synaptosomes, (My) myelin, (Mi) mitochondria. Each fraction was pulled-down with GST-P2X$_2$. The proteins were resolved on tricine-SDS-polyacrylamide gels. (A) tricine-SDS-polyacrylamide gels stained with Coomassie blue. (B) Same samples as in (A), proteins were transferred on PVDF membrane and blotted with an antibody anti-MBP.

## 1.3 The P2X$_2$ subunit binds tubulin directly

To examine whether tubulin binds directly to the C terminus of the P2X$_2$ subunit or requires a linker protein, an *overlay assay* was carried out. A Triton X-100 (0.1%) extract of synaptosomes was resolved by SDS-PAGE, transferred to a PVDF membrane, and overlaid with GST-P2X$_2^{356-472}$. Binding of the fusion protein was then revealed with a GST antibody and [$^{125}$I]protein A (Fig. 11).

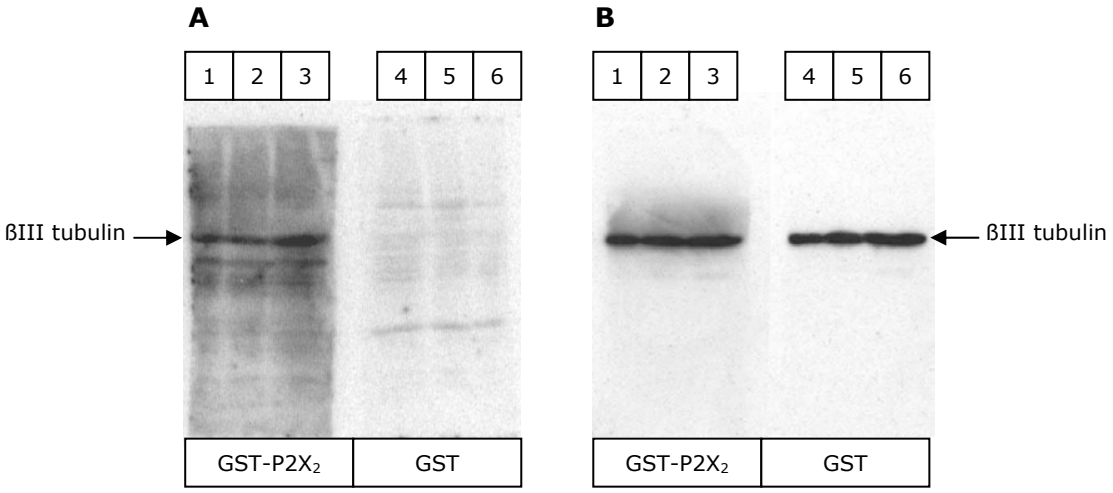


**Fig. 11: Overlay assay with GST-P2X$_2^{356-472}$.** Synaptosomal proteins (lane 1/4, 25 μg; lane 2/5, 50 μg; lane 3/6, 75 μg) solubilized with Triton X-100 were resolved on a SDS-polyacrylamide gel (10% acrylamide) and then transferred on a PVDF membrane. (A) Synaptosomal proteins were overlaid with GST-P2X$_2^{356-472}$ or GST alone as indicated, and then probed by a GST antibody and [$^{125}$I]protein A. Radioactivity was detected by PhosphorImaging. (B) The same membranes as in (A) were probed with the antibody against ßIII tubulin to confirm the identity of the band labeled in (A), and to verify that the both membranes contained the same amount of synaptosomal proteins.

The protein that became labeled corresponded in molecular mass to tubulin (Fig. 11A, lanes 1-3). The identity of this protein band with ßIII tubulin was verified by immunoblot analysis of the same membrane, which led to the labeling of exactly the same protein band(Fig. 11B, lanes 1-6). GST alone did not exhibit any binding (Fig. 11A, lanes 4-6). These results suggest that *ßIII tubulin binds directly to the C-terminal tail of the P2X$_2$ receptor subunit*.

## 1.4 Tubulin binding is mediated by a prolin-rich segment of the P2X$_2$ C-terminal tail

In an attempt to map the ßIII tubulin binding motif of the P2X$_2$ subunit, four additional GST-P2X$_2$ fusion proteins were generated containing various portions of the intracellular C-terminal domain of the P2X$_2$ subunit. A sequence comparison of the P2X$_2$ portions of these proteins is shown in Fig. 12A. These GST-P2X$_2$ fusion proteins were used in pull-down

experiments with a Triton X-100 extract of synaptosomes, followed by immunoblot analysis with the antibody against ßIII tubulin. ßIII tubulin was isolated with a fusion protein including the first half of the $P2X_2$ C-terminal tail (Fig. 12B; construct B, amino acids 356-412), but not at all with the second half of the C terminus (Fig 12B; construct C, amino acids 406-472).The highly positively charged region of fusion protein B (amino acids 356-381 of the $P2X_2$ subunit, construct D) was therefore first considered as a possible tubulin binding motif similar to that of GABARAP (Simon et al., 1997). However, fusion protein D comprising the basic portion of construct B interacted only weakly with tubulin (Fig. 12B). In contrast, fusion protein E comprising the second half of construct B (amino acids 371-412) bound tubulin as efficiently as the full length $P2X_2$ C-terminal tail (construct A) or construct F, lacking the basic domain, but including all C-terminal proline residues (amino acids 371-472).

Two shorter constructs were finally designed each containing a half of the tubulin binding motif (construct E). These GST-fusion proteins (GST-$P2X_2^{371-390}$ and $P2X_2^{391-412}$) were used for pull-down experiments followed by Western-blot with the antibody anti ßIII tubulin. The two constructs (Fig. 13) failed to bind tubulin as efficiently as the complete binding motif. The first half still bound tubulin, whereas the second half showed almost no binding. These results suggest that the entire motif (amino acids 371-412) is needed for an efficient binding of $P2X_2$ to ßIII tubulin.

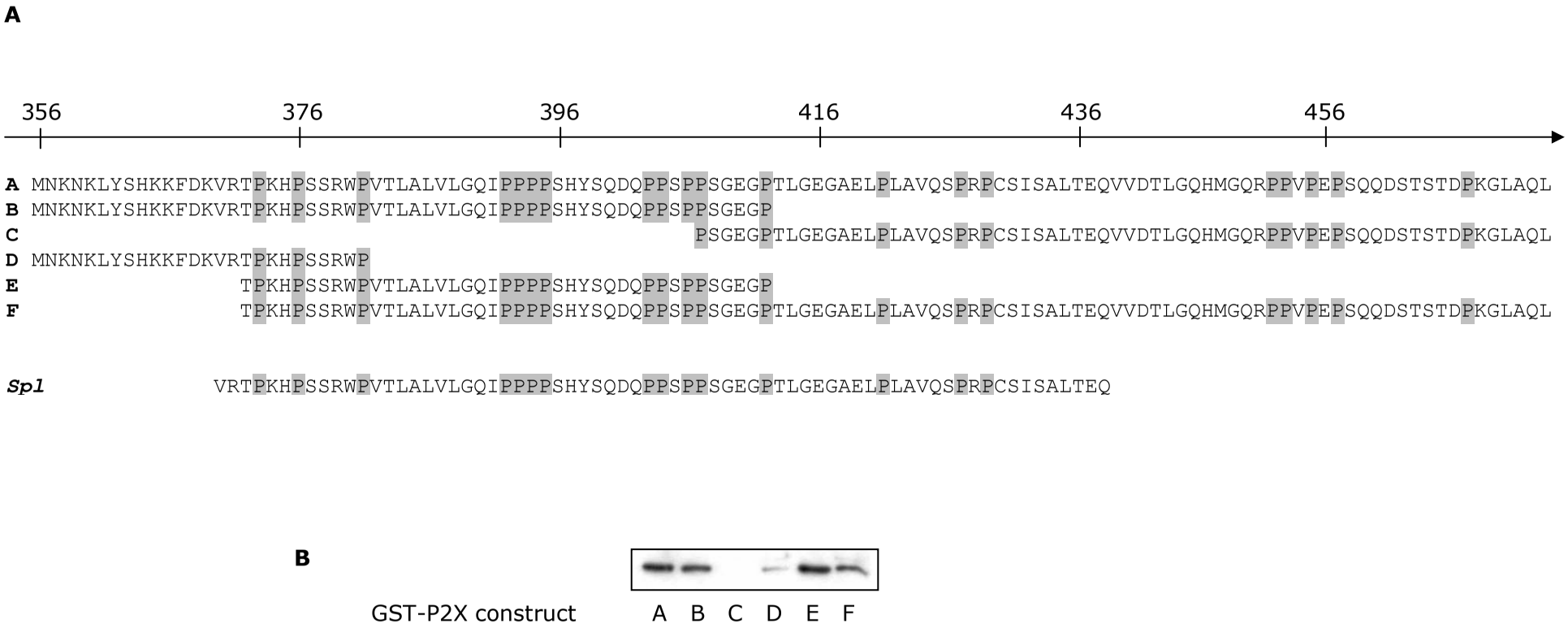


**Fig. 12: Mapping of the tubulin binding domain of $P2X_2$.** (A) Sequence comparison of the GST-P2X fusion proteins generated to map the tubulin binding domain. Proline residues are shown shadowed. *Spl*, 69 amino acid sequence lacking in the $P2X_{2B}$ subunit due to splicing (Simon et al., 1997). Residue numbers corresponding to the full length $P2X_2$ subunit are presented on the top. (B) Immunoblot detection of ßIII tubulin pulled down with different GST-$P2X_2$ fusion proteins from Triton X-100 extract of rat synaptosomes.

371-TPKHPSSRWPVTLALVLGQIPPPPSHYSQDQPPSPPSGEGP-412

371-TPKHPSSRWPVTLALVLGQI-390 391-PPPPSHYSQDQPPSPPSGEGP-412

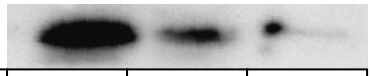

| $P2X_2$ portion in the GST-fusion protein | 371-412 | 371-390 | 391-412 |
|---|---|---|---|

**Fig. 13: Mapping of the tubulin binding domain of $P2X_2$.** Pull-down of ßIII tubulin from Triton X-100 extract of rat synaptosomes with two GST-$P2X_2$ fusion proteins, each containing one half of the tubulin binding motif identified in Fig. 12.

## 1.5 Co-injections of cRNAs coding for $P2X_2$ and tubulin in *Xenopus laevis* oocytes

The pull-down experiments described above suggest that $P2X_2$ subunits bind via their C-terminal tail to tubulin. To examine whether such an interaction also takes place between the full-length $P2X_2$ subunit and tubulin inside a cell, the two proteins were expressed by cRNA injection in *Xenopus* oocytes. To allow for pull-down of tubulin with the $P2X_2$ receptor or vice versa, one cRNA coding for a $(His)_6$-tagged protein and another coding for a protein without $(His)_6$-tag were co-injected. Co-purification of both proteins through the $Ni^{2+}$-NTA column may signify that they interact together and that this binding is strong enough to be preserved along the purification steps.

The cRNA-injected oocytes were metabolically labeled by overnight incubation with [$^{35}$S]methionine. The proteins were purified directly after the pulse period, because the oocytes became unhealthy when subjected to an additional chase period. The result of the co-expression of $(His)_6$-r$P2X_2$ with ßIII tubulin is shown in Fig. 14. $(His)_6$-ßIII tubulin was expressed alone (Fig. 14, lanes 2/7) to observe its position on the gel, thus allowing a comparison to be made with the sample corresponding to the co-expression of $(His)_6$-r$P2X_2$ with ßIII tubulin (Fig. 14, lanes 4/9). ßIII tubulin has a molecular mass of about 51 kDa (calculated from the cDNA sequence). $(His)_6$-r$P2X_2$ is a glycoprotein which contains three

consensus sequences for N-glycosylation (Asn-X-Ser/Thr) at the positions: $^{188}$N, $^{245}$N, and $^{304}$N (N=Asn=Asparagine). All these sites are core-glycosylated (Torres et al., 1998b; Newbolt et al., 1998) and all the three become complex-glycosylated en route to the plasma membrane (unpublished results, Ph.D. thesis S. Aschrafi; Frankfurt, 2002). The molecular mass of the $(His)_6$-rP2X$_2$ apoprotein is 53 kDa (including His-tag, mass calculated from the cDNA sequence), therefore the mass of the core-glycosylated $(His)_6$-rP2X$_2$ can be estimated to be 62 kDa, assuming that the three N-glycans have a mass of 3 kDa each.

This experiment shows that ßIII tubulin is co-purified with $(His)_6$-rP2X$_2$ (Fig. 14, lanes 4/9). As a positive control, $(His)_6$-ßIII tubulin was co-injected with gephyrin, a tubulin-binding protein essential for the recruitment of inhibitory glycine receptors and $GABA_A$ receptors to postsynaptic sites (Kirsch et al., 1991; Kneussel and Betz, 2000). Indeed, when co-expressed in Xenopus oocytes, gephyrin, a 93 kDa protein was co-purified with $(His)_6$-ßIII tubulin (Fig. 14, lanes 3/8). Two different detergents were tested, Triton X-100, and as a milder detergent, digitonin, to observe in which conditions the protein interactions are more stable. More $(His)_6$-ßIII tubulin was isolated in presence of Triton X-100, but the interaction $(His)_6$-rP2X$_2$/ßIII tubulin seemed to be more stable when digitonin was used as detergent.

An important control in co-injection/co-purification experiments is to verify that the protein, which does not posses a $(His)_6$-tag, does not bind non-specifically to the $Ni^{2+}$-NTA beads when it is expressed alone. Fig. 15 shows the result of the injection and expression of ßIII tubulin in comparison to the co-expression of $(His)_6$-rP2X$_2$ with ßIII tubulin. In this experiment, the combination $(His)_6$-ßIII tubulin/rP2X$_2$ was also injected. Three detergent were tested for the protein purification: Triton X-100 (Fig. 15, lanes 1-5), digitonin (Fig. 15, lanes 6-10), and dodecyl maltoside (Fig. 15, lanes 6-10). As shown in Fig. 15, lane 3, ßIII tubulin without $(His)_6$-tag was purified by the $Ni^{2+}$-NTA matrix in a quantity similar to that seen in lane 2, where ßIII tubulin was co-expressed together with

$(His)_6$-rP2$X_2$. In contrast, non-tagged rP2$X_2$ did not show non-specific binding (lane 4,9,14) , but was also not observed to co-purify with $(His)_6$-ßIII tubulin.

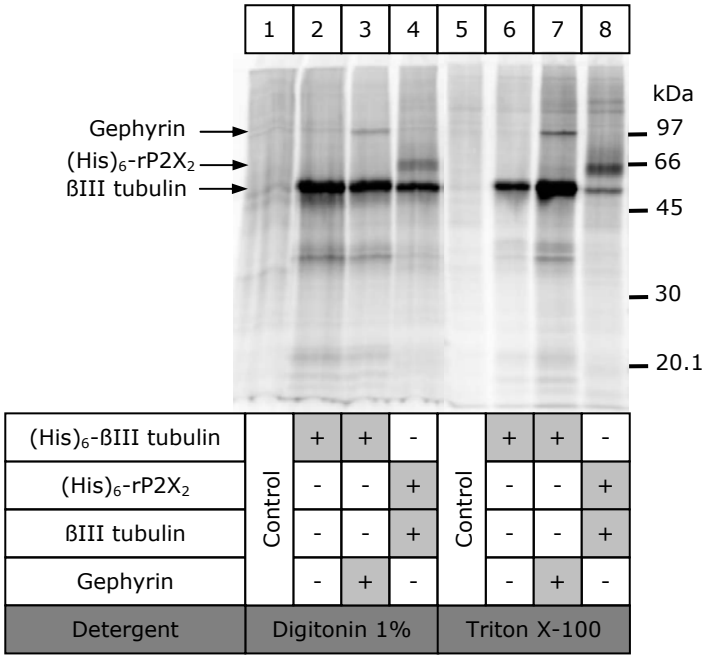


**Fig. 14: Protein expression in *Xenopus* oocytes. Co-expression of ßIII tubulin and rP2$X_2$.** The cRNAs coding for the indicated proteins were injected in *Xenopus laevis* oocytes (cRNAs were mixed to a ratio 1:1). The cells were metabolically labeled overnight with [$^{35}$S]methionine. The proteins were purified direct after the pulse period by affinity chromatography with $Ni^{2+}$-NTA agarose beads and eluted from the beads with 1x SDS-loading buffer. The purification steps were performed in the presence of the indicated detergent (the percentages indicate the concentrations used in the "homogenizing" buffer). The proteins were finally resolved on a 10% SDS-polyacrylamide gel, and the radioactivity was visualized by PhosphorImaging. Control lane: proteins from non injected oocytes that bound non-specifically to the $Ni^{2+}$-NTA agarose beads.

It is therefore likely, that the interaction between $(His)_6$-rP2$X_2$ and ßIII tubulin observed in Fig. 14 was at least partly due to non-specific binding of ßIII tubulin to the $Ni^{2+}$-NTA beads. In Fig. 14, lane 2, and in Fig. 15, lane 10, additional bands were observed in addition to the major band of $(His)_6$-ßIII tubulin. These bands represent either degradation products of ßIII tubulin, or proteins associated to the microtubules that co-purify with $(His)_6$-ßIII tubulin such as MAPs, microtubule-associated proteins, for example.

The conclusion of these results is that the interaction rP2$X_2$-ßIII tubulin could not be demonstrated reproducibly in *Xenopus* oocytes.

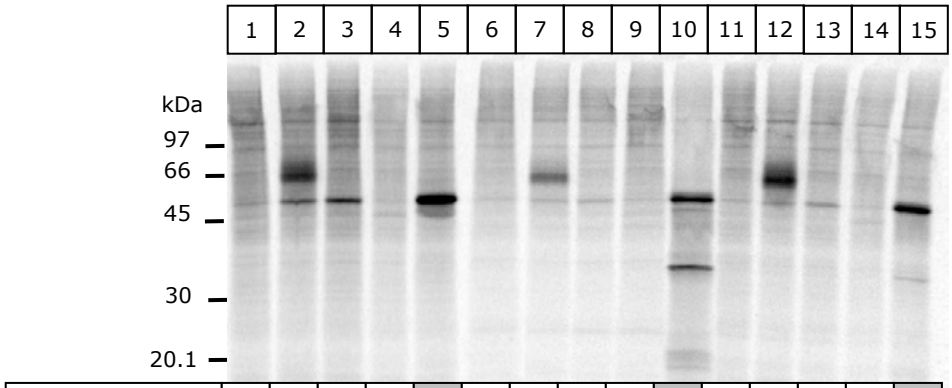


| | | | | | | | | | | | | | | | |
|---|---|---|---|---|---|---|---|---|---|---|---|---|---|---|---|
| $(His)_6$-ßIII tubulin | - | - | - | - | + | - | - | - | - | + | - | - | - | - | + |
| His-rP2X$_2$ | - | + | - | - | - | - | + | - | - | - | - | + | - | - | - |
| ßIII tubulin | - | + | + | - | - | - | + | + | - | - | - | + | + | - | - |
| rP2X$_2$ | - | - | - | + | + | - | - | - | + | + | - | - | - | + | + |
| Detergent | Triton X-100 0.5% | | | | | Digitonin 1% | | | | | Dodecyl maltoside 0.5% | | | | |

**Fig. 15: Protein expression in *Xenopus* oocytes. Co-expression of ßIII tubulin and rP2X$_2$.** The cRNAs coding for the indicated proteins were injected in *Xenopus laevis* oocytes. The cells were metabolically labeled overnight with [$^{35}$S]methionine. Proteins were purified direct after the pulse period by affinity chromatography with $Ni^{2+}$-NTA agarose beads and eluted from the beads with 1x SDS-loading buffer. The purification steps were performed in the presence of the indicated detergent (the percentages indicate the concentrations used in the "homogenizing" buffer). The proteins were finally resolved on a 10% SDS-polyacrylamide gel, and the radioactivity was visualized by PhosphorImaging. Control lane: proteins from non injected oocytes that bound non-specifically to the $Ni^{2+}$-NTA agarose beads.

## 1.6 Pull-down of ßIII tubulin expressed in *Xenopus* oocytes by the GST-P2X$_2^{356-472}$ fusion protein

To reproduce the results obtained with the synaptosome detergent extract (interaction P2X$_2$/ßIII tubulin), a series of experiments was performed in *Xenopus* oocytes. Purified GST-P2X$_2$ or GST (as control) proteins were pre-injected in *Xenopus* oocytes, then the same oocytes were injected with the cRNA coding for ßIII tubulin without hexahistidyl tag. After metabolic labeling with [$^{35}$S]methionine (overnight), the proteins were extracted with 1% digitonin, purified by affinity chromatography with glutathione-Sepharose beads, and resolved by SDS-PAGE. These experiments were done to examine whether GST-P2X$_2$ is able

to pull-down ßIII tubulin in intact cells rather than a detergent extract of rat brain synaptosomes. The results are presented in Fig. 16.

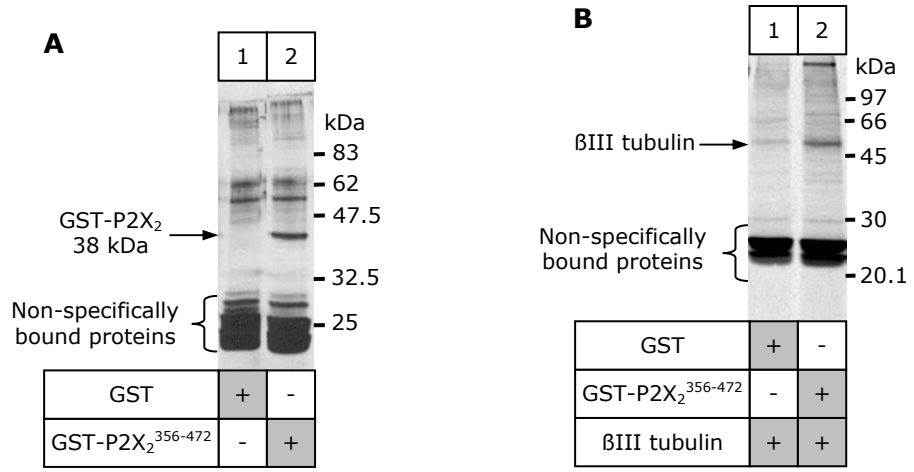


**Fig. 16: Co-injection of GST-P2X$_2^{356-472}$ and the cRNA coding for ßIII tubulin no His in *Xenopus laevis* oocytes.** GST-P2X$_2$ and GST (as control) fusion proteins were purified from *E.coli* and injected into Xenopus oocytes (about 40 ng/cell) together with the cRNA coding for ßIII tubulin without hexahistidyl tag. The cells were metabolically labeled overnight with [$^{35}$S]methionine. Proteins were purified directly after the pulse period by affinity chromatography with glutathione-Sepharose beads, eluted from the beads with 1x SDS-loading buffer and resolved on a 10% SDS-polyacrylamide gel. (A) Silver staining of the gel. (B) Autoradiography of the gel (PhosphorImager). Some endogenous proteins of oocytes interacted non-specifically either with the GST-fusion proteins or with the glutathione-Sepharose beads and are specified on both figures.

Fig. 16A shows a photography of the silver stained gel. On this gel the amount of fusion protein purified by this method can be observed. The re-isolated GST is masked by a large amount of oocyte proteins, which interact non-specifically either with the GST proteins or with the glutathione-Sepharose beads. Part of these oocytes proteins are also visible on the autoradiography of the same gel shown in Fig. 16B. On this figure a thin protein band was observed which co-purified with GST-P2X$_2$. This protein band has the same molecular mass as ßIII tubulin and was not co-purified with GST alone. These results show that it is possible to pull-down ßIII tubulin in *Xenopus* oocytes with GST-P2X$_2$.

I finally tried to isolate the [$^{35}$S]-labeled rP2X$_2$ receptor produced in *Xenopus* oocytes by purification of the intact microtubules from *Xenopus* oocytes. To this end, about 50 oocytes were injected with the cRNA coding for rP2X$_2$ subunit without hexahistidyl tag and metabolically labeled with

[$^{35}$S]methionine overnight. The next day the microtubules of all the oocytes were purified by the method of R.B. Vallee (Vallee, 1986): the oocytes were homogenized in PEM buffer (0.1 M PIPES-NaOH, pH 6.6, containing 1 mM EGTA and 1 mM $MgSO_4$), then GTP and taxol were added to initiate polymerization of all the endogenous tubulin in the cold. Microtubules were centrifuged and washed. The microtubule pellet was finally resuspended with 1x SDS-loading buffer and the proteins were resolved by SDS-PAGE. Unfortunately I was not able to co-isolate $rP2X_2$ and tubulin by this method.

## 1.7 Perspectives

This part of the results presents preliminary results, which lead to suggestions for further experiments. The aim of these experiments was to see in which compartments of eukaryotic mammal cells (COS-7 cell for example) the $rP2X_2$ receptor is localized and to observe if tubulin does affect its sub-cellular localization. For this purpose, we engineered a fusion protein consisting of the $rP2X_2$ subunit fused C-terminally to the green fluorescent protein (EGFP), which is a protein able to emit fluorescent light when excited with UV light. This construct was first cloned into the pNKS vector for expression in *Xenopus* oocytes, and then sub-cloned into the pcDNA3.1 vector for transfection of COS-7 cells.

$rP2X_{2A}$-GFP was first expressed in *Xenopus laevis* oocytes to confirm that the protein in produced is its full-length and that it is glycosylated on its three N-glycosylation consensus sequences. The results are presented in Fig. 17. Lanes 3/6 show the expression of $(His)_6$-$rP2X_{2A}$-GFP in *Xenopus* oocytes. $(His)_6$-$rP2X_2$-GFP migrated at a position in agreement with the calculated molecular mass of the core-glycosylated form of the protein of 90 kDa (81 kDa apoprotein and 3x3 kDa of N-glycans). The electrophoretic mobility of the $P2X_{2A}$-GFP subunit is similar to that of gephyrin, a 93 kDa protein (lanes 2 and 5). When $P2X_{2A}$-GFP was purified

with Triton X-100 as detergent instead of digitonin (lane 6), a second band with the same electrophoretic mobility as $P2X_{2A}$ (lane 7) appeared on the gel. This may suggest that $P2X_{2A}$-GFP was partially unstable and was cleaved between the $P2X_{2A}$ portion and the GFP portion of the fusion protein either in the oocytes or during protein purification.

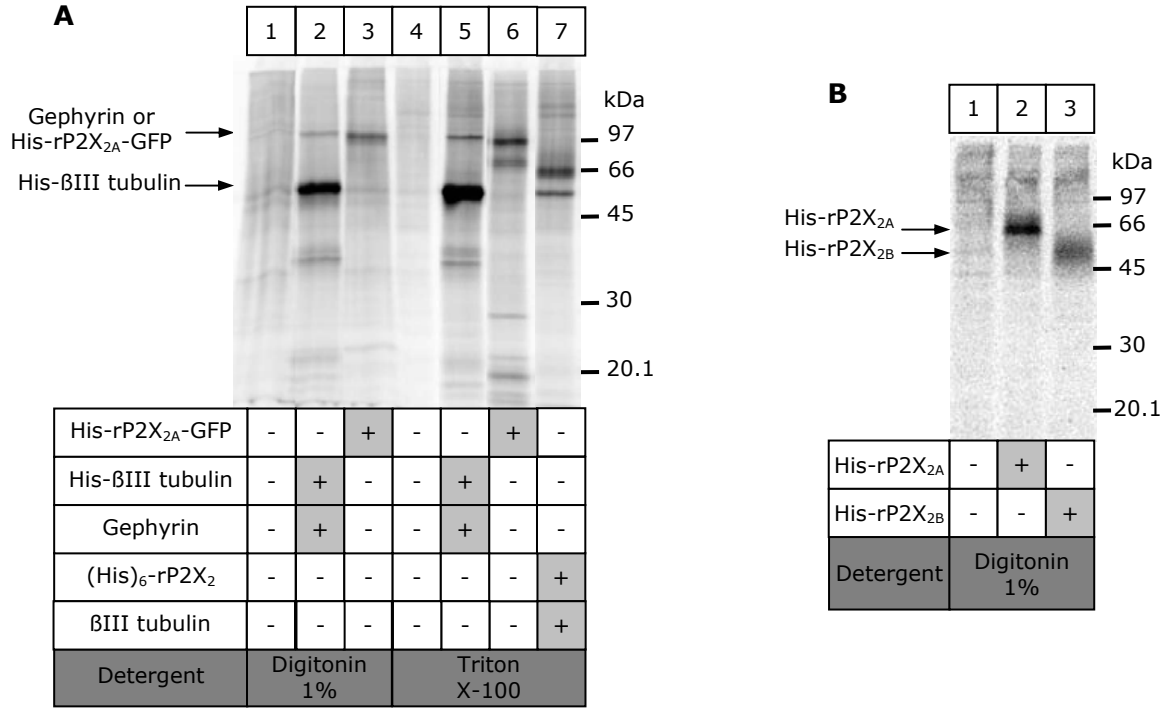


**Fig. 17: Expression of $rP2X_{2A}$-GFP (A) and $rP2X_{2B}$-GFP (B) in *Xenopus* oocytes.** The cRNAs coding for the indicated proteins were injected in *Xenopus laevis* oocytes (cRNAs were mixed in a ratio 1:1). The cells were metabolically labeled overnight with [$^{35}$S]methionine. The proteins were purified directly after the pulse period by affinity chromatography with $Ni^{2+}$-NTA agarose beads and eluted from the beads with 1x SDS-loading buffer. The purification steps were performed in the presence of the indicated detergent (the percentages indicate the concentrations used in the "homogenizing" buffer). The proteins were finally resolved on a 10% SDS-polyacrylamide gel, and the radioactivity was visualized by PhosphorImaging. Control lane: proteins from non injected oocytes that bound non-specifically to the $Ni^{2+}$-NTA agarose beads.

$P2X_2$-GFP was then expressed in COS-7 cells and the cells were observed in culture or fixed with paraformaldehyde using a conventional fluorescence microscope. Fig. 18 A and B show the fluorescence of $P2X_2$-GFP in living cells, Fig. C is a picture taken from fixed cells at a higher magnification. $P2X_{2A}$-GFP was very well expressed particularly in the intracellular compartments and was also present at the cell surface (Fig. 18C). An interesting experiment would be to compare the pattern of

localization of $P2X_{2A}$-GFP and $P2X_{2B}$-GFP, a splice variant of $P2X_2$ (Simon et al., 1997) in COS-7 cells. However, for unknown reasons, this second construct could not be observed in COS-7 cells, although it was synthesized as a protein of expected mass of 46.4 kDa in *Xenopus* oocytes (Fig. 17B, lane 3).

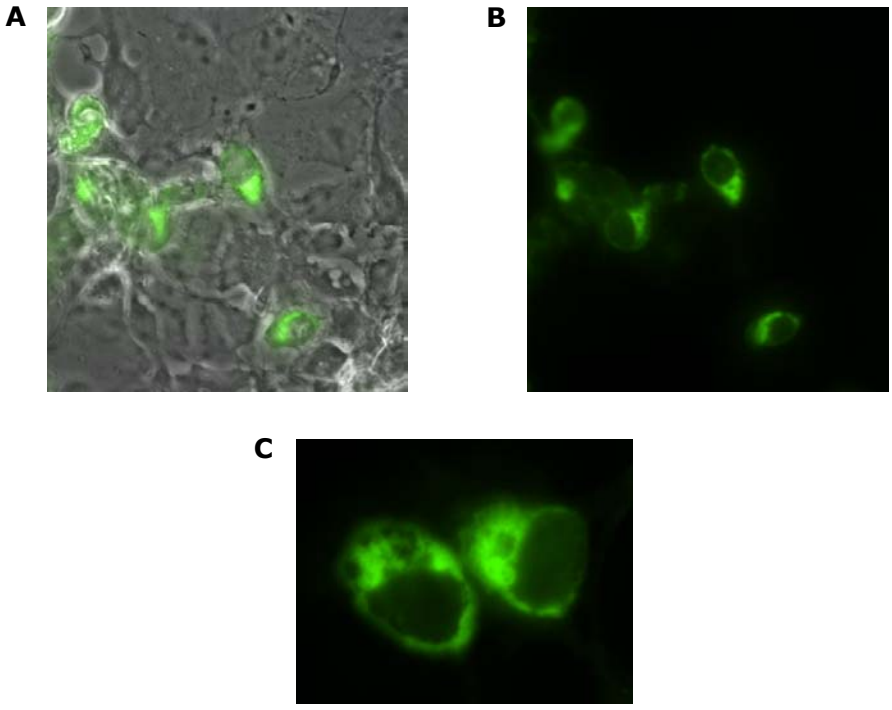


**Fig. 18: Expression of rP2X$_2$-GFP in COS-7 cells.** COS-7 cells were transfected with the cDNA coding for rP2X$_2$-GFP cloned in pcDNA 3.1 vector (transfection with FuGENE 6, Roche diagnostic). (A,B) COS-7 cells observed in culture using the Axiovert 200M fluorescence microscope (Zeiss). Cells were viewed through a 40x0.6 objective lens (Zeiss). (A) shows an overlay of phase contrast and fluorescence images, (B) shows only the fluorescence image of the same view. (C) COS-7 cells were fixed with 4% paraformaldehyde and observed using the same microscope. Cells were viewed through a 100x1.3 oil immersion objective lens (Zeiss).

Another point of interest would be the influence of microtubules on the expression of $P2X_{2A}$-GFP or $P2X_{2B}$-GFP at the plasma membrane. To answer this question it would be interesting to perform co-localization studies with tubulin or to disturb the microtubular network (with drugs like taxol or exposing the cells to cold temperatures), and observe with a confocal microscope the effects of these culture conditions on the subcellular localization of $P2X_2$-GFP and $P2X_{2B}$-GFP.

All these possibilities have still to be investigated.

## III-2. Investigations of the quaternary structure of two glutamate transporters: hEAAT2 and ecgltP

In the context of a collaboration work with the group of Prof. C.Fahlke from the Institute for Physiology (University Hospital of Aachen) I investigated the subunit stoichiometry of two distantly related glutamate transporters, the human glial glutamate transporter, **hEAAT2** and the *E.coli* bacterial glutamate transporter, **ecgltP**.

Glutamate transporters mediate glutamate uptake into neuronal and glial cells and play a central role in the termination of synaptic transmission and in extracellular glutamate homeostasis. To resolve the question of the quaternary structure of hEAAT2 and ecgltP, these two transporters were expressed in *Xenopus laevis* oocytes in a $(His)_6$-tagged form, and the native proteins were analyzed with the blue-native PAGE technique.

### 2.1 hEAAT2 and ecgltP transporters migrate as trimers in blue-native PAGE gels

cDNA constructs coding for $(His)_6$-hEAAT2 and $(His)_6$-ecgltP were provided by the group of Prof. C.Fahlke. cRNAs were synthetized *in vitro* and injected into *Xenopus laevis* oocytes. Hexahistidyl tags allow the purification of proteins by $Ni^{2+}$-NTA affinity chromatography and were placed either $NH_2$- or COOH-terminally.

#### *a- His-tagged hEAAT2 transporters exhibit unaltered functional properties*

The uptake process is driven by the electrochemical gradient across the cell membrane, sodium is required for glutamate binding while potassium is required for net transport (Danbolt, 2001). The process is **electrogenic** (positive charge moving in). The transporters utilize the ion gradients of

both sodium, potassium, and also protons; the transport of one glutamate requires a minimum of two $Na^+$ and one $K^+$ (Danbolt, 2001). It is possible to perform electrophysiological recordings from single cells expressing a single transporter subtype and thereby to exploit the electrogenic nature of the transport to measure the specificity and the kinetic of the uptake process. In addition, some transporters appear to have an extraordinary additional function as glutamate-gated chloride channel (Wadiche et al., 1995; Fairman et al., 1995); this anion conductance is thermodynamically independent of the transport process.

To test whether the addition of a hexahistidyl tag alters transport functions, oocytes expressing wild-type and His-tagged transporters were examined with two-electrode voltage clamp techniques (experiments realized by the group of Prof. C.Fahlke). When cRNA coding for $(His)_6$-tagged **ecgltP** was injected in *Xenopus* oocytes, neither glutamate-induced inward current nor glutamate-induced increase of anion currents were observed. As ecgltP is effectively translated in oocytes (see below), this result was most likely due to an *impaired surface targeting of the prokaryotic protein*. The His-tag in N-terminal or C-terminal left the stoichiometrically coupled and the pore-mediated current amplitudes of hEAAT2 unaffected (data not shown).

### *b- hEAAT2 and ecgltP transporters migrate as trimers in blue-native PAGE gels*

Blue-native (BN) PAGE analysis (Schägger et al., 1994) allows to study membrane proteins under non-denaturing conditions by gel electrophoresis. hEAAT2 and ecgltP were heterologously expressed in *Xenopus laevis* oocytes, metabolically labeled with [$^{35}$S]methionine, extracted with 1% (w/v) digitonin, and purified by metal affinity chromatography. Both proteins expressed at high levels in *Xenopus*

oocytes (Fig. 19A) and were metabolically stable during a sustained chase (data not shown).

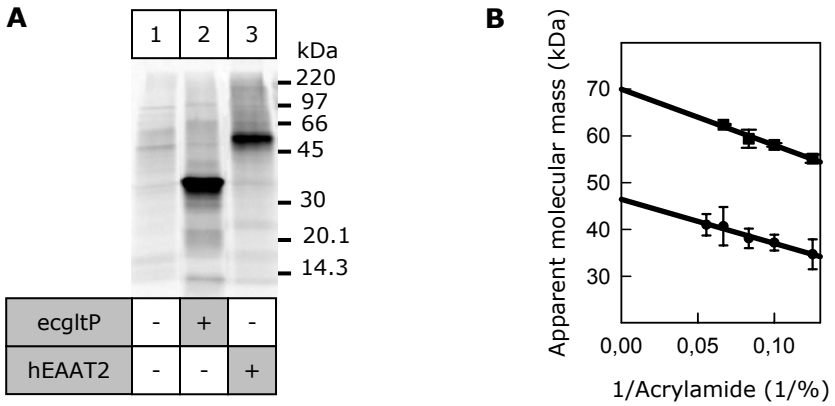


**Fig. 19: SDS-PAGE analysis of His-ecgltP and His-hEAAT2 in *Xenopus* oocytes.** (A) His-ecgltP and His-hEAAT2 were purified from *Xenopus* oocytes by Ni-NTA chromatography after a 4h [$^{35}$S]methionine pulse and were resolved by reducing SDS-PAGE (10% acrylamide) in parallel with [$^{14}$C]-labeled molecular mass markers. (B) Ferguson plot of molecular masses of the ecgltP and hEAAT2 polypeptides determined by SDS-PAGE at various polyacrylamide concentrations versus the polyacrylamide concentration. Solid circles: His-ecgltP; solid squares: His-hEAAT2.

When denatured by SDS and resolved by reducing SDS-PAGE, the ecgltP and the hEAAT2 polypeptides migrated both at 10-20% lower masses than calculated from their amino acid sequences, particularly in gels of low acrylamide concentration. To determine the correct molecular mass of these two polypeptides, a Ferguson analysis was performed (FERGUSON, 1964). To this end, His-ecgltP and His-hEAAT2 were resolved on SDS-polyacrylamide gels of different acrylamide percentages. When the derived apparent masses were plotted against the reciprocal of the acrylamide concentrations, straight lines were obtained with both proteins (Fig. 19B). According to Ferguson, the intercept point with the ordinate indicates the genuine mass of the protein of interest. This analysis yielded molecular masses of **46 kDa** and **69 kDa** for the **His-tagged ecgltP** and the **His-tagged hEAAT2**, respectively (calculated masses: 48 kDa for His-ecgltP and 63 kDa for non-glycosylated His-hEAAT2). Therefore, anomalous migration, as observed for many other hydrophobic membrane proteins,

likely caused the observed differences between the apparent and the calculated masses.

Both ecgltP and hEAAT2 transporters migrated predominantly as a single band when analyzed by BN-PAGE (Fig. 20A, lane 3; Fig. 20C, lane 2, respectively). The non-denatured ecgltP transporter and hEAAT2 transporter migrated at ~150 kDa (Fig. 20A, lane 3) and ~200 kDa (Fig. 20C, lane 2), respectively, when compared with the defined membrane protein complexes generated by partial denaturing of the homopentameric $\alpha$1 GlyR (calculated mass: 260 kDa including carbohydrates) (Griffon et al., 1999) or the homomeric $P2X_1$ receptor (calculated mass: 171 kDa including carbohydrates) (Nicke et al., 1998). These molecular masses are well above those of respective monomers, suggesting that both ecgltP and hEAAT2 exist exclusively as multimers in *Xenopus* oocytes.

The electrophoretic mobility is biased by dye binding and protein shape to an unclear extent, and therefore the exact number of monomers incorporated per protein complex cannot be readily deduced from the estimated masses alone. A reliable approach to determine the number of polypeptide chains incorporated in one transporter complex consists in weakening non-covalent subunit interactions by treatment with heat and low concentrations of SDS, thus inducing a dissociation the protein complexes into lower order intermediates (Griffon et al., 1999; Nicke et al., 1998). For **hEAAT2**, a 1h incubation at 56°C both in the presence (Fig. 20C, lane 4) and absence (lane 5) of Coomassie dye generated a ladder-like pattern of three protein bands. Incubation in the additional presence of increasing concentrations of SDS (lanes 6-10) led to a gradual disappearance of the ~200 kDa protein and an enhanced appearance of the two additional proteins of masses of ~130 kDa and ~65 kDa. At $\geq$0.05% SDS, the ~65 kDa band became the predominant one (lanes 9-10). No polypeptide migrated faster than the ~65 kDa band, suggesting that the ~65 kDa band corresponds to the hEAAT2 monomer with a calculated mass of 66 kDa in a high mannose form (see 2.4). Fig. 19D

shows PhosphorImager analysis of the gel shown in Fig. 20C. All the conditions that led to a dissociation of the hEAAT2 caused the appearance of a total of three bands with masses corresponding to the assembly of three, two and one minimal units. The monomer became the dominant species at high SDS concentrations (Fig. 20D).

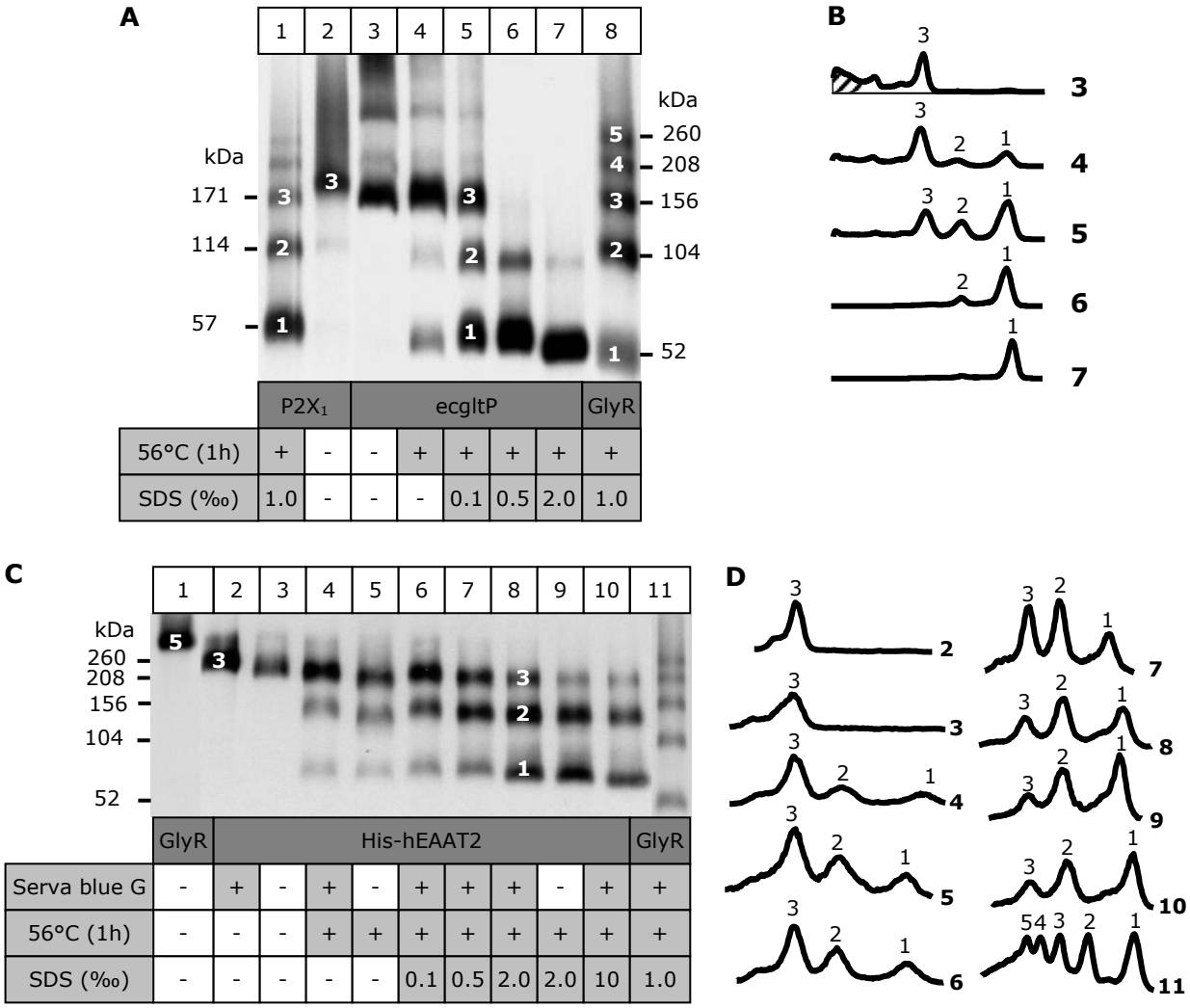


**Fig. 20: Oligomeric state of the ecgltP and hEAAT2 transporters in *Xenopus* oocytes determined by BN-PAGE.** Samples were treated as indicated to induce dissociation into lower order intermediates. (A), (C) Autography of the gels. (B), (D) Quantitative profiles of the gel lanes shown in (A) and (C), respectively, were obtained by PhosphorImager analysis and are marked by the same lane numbers. The origin of the abscissa corresponds to the top of the polyacrylamide gel. The five bands that became visible upon partial denaturing of the GlyR are consistent with the pentameric state of this class of ligand-gated ion channels. Numbers specify the oligomeric state of the corresponding peak. The mass markers shown on both sides of the gels were generated by partial dissociation of the ligand-gated ion channels with SDS as indicated.

The natively purified **ecgltP** protein migrated predominantly at ~150 kDa (Fig. 20A, lane 3) when compared with the homomeric $P2X_1$ receptor (lane 2) or the partially dissociated $\alpha$1 GlyR (lane 8). In addition, a slower migrating distinct band, presumably an ecgltP hexamer, and an amorphous mass of proteins, most likely ecgltP aggregates, were visible. Quantification of the various ecgltP forms by PhosphorImager analysis indicated that the 150 kDa band is the most prominent one (Fig. 20B). A 1h incubation at 56°C both in the absence (not shown) as well as in the presence of Coomassie dye (Fig. 20A, lane 4) and denaturing with increasing concentrations of SDS led to the dissociation of the 150 kDa band into the monomeric and dimeric ecgltP species (Fig. 20A, lanes 5-7).

## 2.2 Results obtained with a concatenated ecgltP dimer are consistent with a trimeric ecgltP structure

The results shown above demonstrate that **both hEAAT2 and ecgltP glutamate transporters are assembled into trimers** from a minimal unit that migrates close to the expected molecular mass of the monomer in BN-PAGE.

To rule out the possibility that the lowest molecular band corresponds to an unusually stable dimer and correspondingly the intermediate and higher molecular mass bands to tetramers and hexamers, a concatenated cDNA construct was engineered for one of the transporters (ecgltP-ecgltP) by linking two ecgltP coding regions in a single open reading frame. By reducing SDS-PAGE, the (ecgltP-ecgltP) polypeptide was resolved as a 74 kDa protein (Fig. 21B, lane 2), i.e. twice the mass of the apparent molecular mass of 37 kDa for the ecgltP monomer (lane 4). In BN-PAGE two major bands were observed (Fig. 22, lane 1), and dissociating treatment with SDS led to the appearance of a third major non further dissociable band of ecgltP-ecgltP (lane 2), which migrated at approximately the same position as the non covalently associated ecgltP

dimer, $(ecgltP)_2$ (lane 10). These results show that the intermediate molecular mass band dissociated from the ecgltP protein indeed corresponds to the dimeric form and, accordingly, the lowest and higher molecular band to the monomer and trimer, respectively. The intermediate band of concatenated ecgltP-ecgltP (Fig. 22B, lane 2) migrated slightly higher than the trimer formed from ecgltP monomers (lane 9) and most likely corresponds to the association of two dimers $((ecgltP\text{-}ecgltP)_2)$. Likewise, the slowest migrating band corresponds to a trimer formed by three ecgltP-ecgltP concatamers $((ecgltP\text{-}ecgltP)_3)$. Under non-denaturing conditions (lane 1) these two bands are prominent indicating that both conformations are stable and occur with comparable probability.

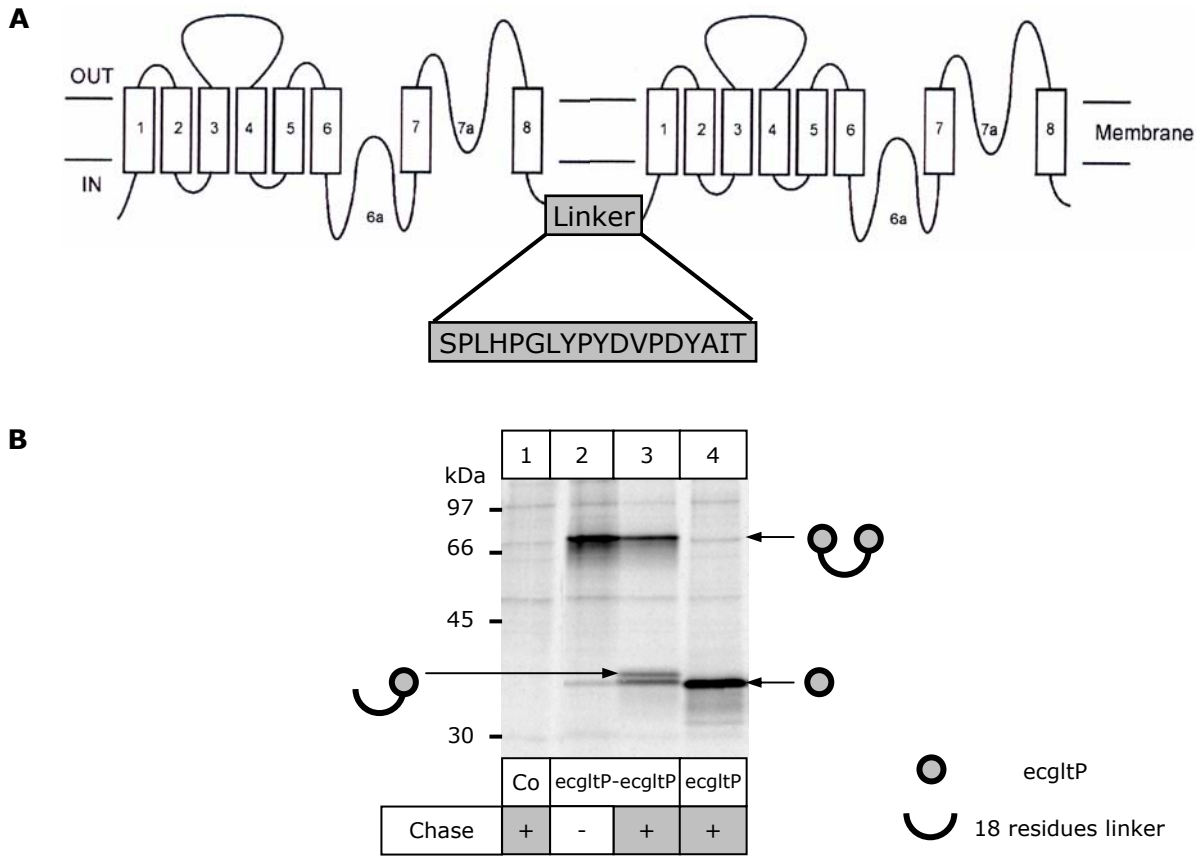


**Fig. 21: Biochemical analysis of an ecgltP-ecgltP concatamer expressed in *Xenopus* oocytes.** (A) Schematic representation of the ecgltP-ecgltP concatamer (the membrane topology of ecgltP is inspired from (Slotboom et al., 2001a)). Two ecgltP monomers were joined tail-to-head by a 18 residues linker sequence (gray box). (B) Reducing SDS-PAGE analysis of the isolated polypeptides. Proteins were resolved on a 10% SDS-polyacrylamide gel. During the chase interval two polypeptides appeared with masses corresponding to the ecgltP monomer that are barely detectable after the pulse. Co, non injected control oocytes.

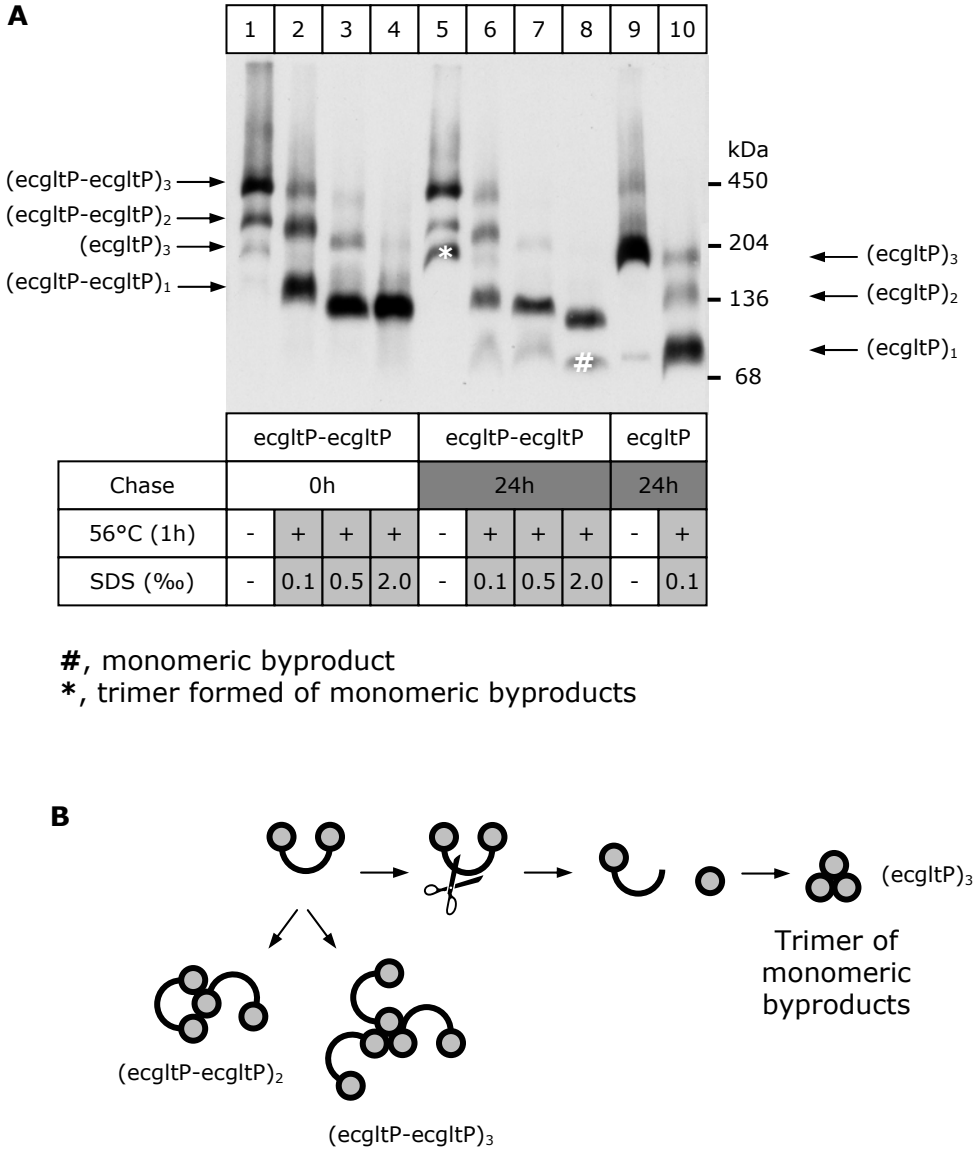


**Fig. 22: Oligomeric state of the concatenated ecgltP dimer determined by BN-PAGE.** (A) Autoradiography of the gel. The oligomeric state of the monomeric ecgltP form is shown for easier comparison. Dissociation into lower order intermediates was induced by partial denaturing with SDS as indicated. The monomeric byproducts (**#**) formed during the chase interval assemble into non-covalently linked trimeric ecgltP proteins (*****), that migrate at the same position as the ecgltP trimer assembled from expressed monomers. (B) Cartoon showing the assembly of full length concatenated ecgltP dimers and monomeric byproducts. The ecgltP concatamer consist of two ecgltP monomers (indicated by gray circles) joined tail-to-head by a 18 residues linker sequence. Concatenated dimers assemble predominantly to a trimer that comprises a total of six ecgltP copies. To a lower extent dimers of concatenated dimers with a total of four ecgltP copies are also formed. In addition, monomeric sides products that arise most likely from proteolytic cleavage of concatenated dimers assemble to trimers of three monomers.

This observation further supports a trimeric structure that predicts two oligomeric populations from dimeric concatamers (Fig. 22B): an assembly of two concatamers, one of them providing two subunits ((ecgltP-ecgltP)$_2$) or the association of three dimeric concatamers, each of them contributing one subunit ((ecgltP-ecgltP)$_3$) to the trimer interface.

An additional faint band (lane 1 of Fig. 22A) migrated at exactly the same position as the ecgltP trimer assembled from three ecgltP monomers, (ecgltP)$_3$ (lane 9). This band became more abundant after an additional chase period (Fig. 22A, lane 5). The occurrence of this oligomeric complex is most likely due to proteolytic formation (Nicke et al., 2003) of a single coding region of ecgltP. Upon treatment with SDS, this protein dissociated into a polypeptide migrating at virtually the same position as the ecgltP monomer (Fig. 22A, lanes 6-8). This is confirmed in SDS-PAGE analysis, where two byproducts were observed in addition to the full length concatamer, one migrating virtually at the same position as the ecgltP monomer (Fig. 21B, lane 4), and a second one with 1-2 kDa larger mass and probably corresponding to the ecgltP monomer plus the 18 residue linker (Fig. 21B, lane 3). The findings that two distinct concatameric constructs, the one used in this study, and the one of Nicke et al. (Nicke et al., 2003) are both subjected to proteolytic digestion (Fig. 22B) demonstrates the limitations of using tandem constructs to study heteromultimeric proteins in *Xenopus* oocytes.

## 2.3 Cross-linking of hEAAT2 or ecgltP generates covalently bound dimers and trimers

To confirm the trimeric structure of hEAAT2 and ecgltP resolved with the BN-PAGE technique, protein cross-linking was used to study intermolecular interactions within glutamate transporters subunits. Two homobifunctional imidoesters reagents, DMA (dimethyl adipimidate) and DMS (Dimethyl suberimidate) were tested for their ability to covalently

link transporter molecules extracted from *Xenopus* oocytes. The cross-linking reagents were incubated with purified proteins still bound to the $Ni^{2+}$-NTA beads just before elution. The cross-linked proteins were then eluted once with 250 mM imidazole 0.5% (w/v) digitonin.

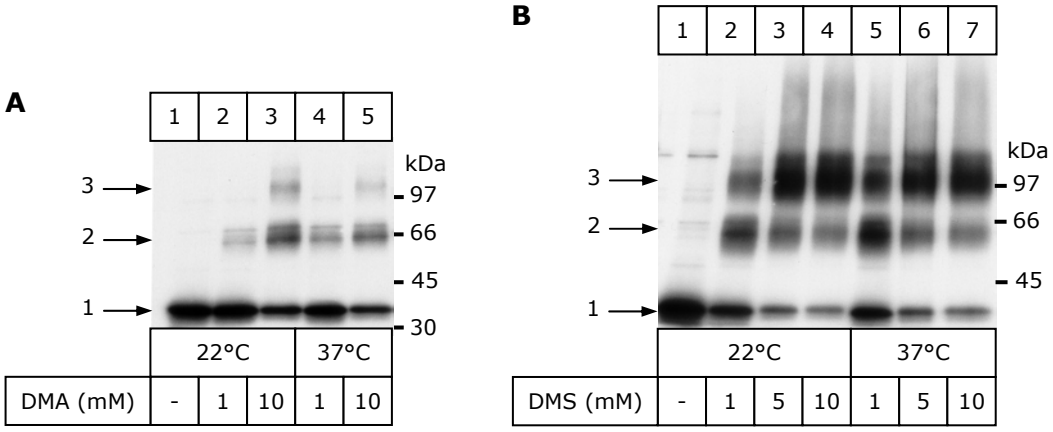


**Fig. 23: Cross-linking of digitonin-solubilized, purified ecgltP.** EcgltP transporter (A, B) was purified from [$^{35}$S]methionine labeled oocytes and incubated with cross-linkers as indicated while still bound to beads. After elution with non-denaturing elution buffer, samples were supplemented with SDS sample buffer containing 20 mM DTT and resolved by SDS-PAGE (4-10% acrylamide gradient gel) followed by autoradiography. Numbered arrows indicate the positions of monomers, dimers, and trimers.

DMS differs from DMA by a slightly longer spacer arm (11 Å *vs.* 8.6 Å) and was more efficient in cross-linking ecgltP to dimers and trimers at both 22°C (Fig. 23B, lanes 2-4) and 37°C (Fig. 23B, lanes 5-7).

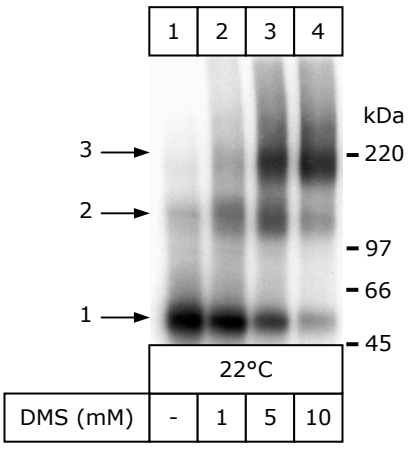


**Fig. 24: Cross-linking of digitonin-solubilized, purified hEAAT2.** hEAAT2 transporter was purified from [$^{35}$S]methionine labeled oocytes and incubated with cross-linkers as indicated while still bound to beads. After elution with non-denaturing elution buffer, samples were supplemented with SDS sample buffer containing 20 mM DTT and resolved by SDS-PAGE (4-10% acrylamide gradient gel) followed by autoradiography. Numbered arrows indicate the positions of monomers, dimers and trimers.

DMS also cross-linked hEAAT2 transporter subunits to dimers and to trimers preferentially at higher concentrations (Fig. 24). Adducts larger than trimers were neither observed with ecgltP nor with hEAAT2 transporters, corroborating the results obtained by BN-PAGE analysis that the natively purified glutamate transporters possess a trimeric architecture.

## 2.4 hEAAT2 is complex-glycosylated

Membrane proteins are often *N*-glycosylated when expressed in eukaryotic cells. Glycosylation alters the molecular mass of proteins and thus has to be taken into consideration in gel electrophoresis analysis. Moreover, oligosaccharide side chains are sequentially processed in the Golgi apparatus from a high mannose to the complex-glycosylated form, and this process can be used to monitor the efficiency of ER exit of the protein.

The hEAAT2 sequence shows two glycosylation sequences, $^{206}$NATS and $^{216}$NETV, which are both located on the predicted large ectodomain (residues 143-239) between transmembrane regions TM3 and TM4 (Danbolt, 2001). Complete deglycosylation of newly synthesized hEAAT2 polypeptide produced in *Xenopus* oocytes during a 4 h pulse period resulted in a 3 kDa decrease of the molecular mass (Fig. 25A, lanes 1-2), corresponding to the mass of one single N-glycan, suggesting that only one of the two possible glycosylation sites is used. No mass shift by PNGase F was observed when the asparagines residues of both N-glycosylation sequons were replaced by glutamine (Fig. 25A, lanes 7 & 8). Glutamine substitution of only one of the two asparagine residues resulted in polypeptides migrating at the same position as the wild-type hEAAT2 (Fig. 25A, lanes 3 & 5), thus indicating that $^{206}$N and $^{216}$N can substitute for each other to carry the N-glycan. If both *N*-glycosylation acceptor sites were present as on the parent hEAAT2 polypeptide, one of

the two remained unused presumably because of the small distance of only 10 amino acids between the two sites.

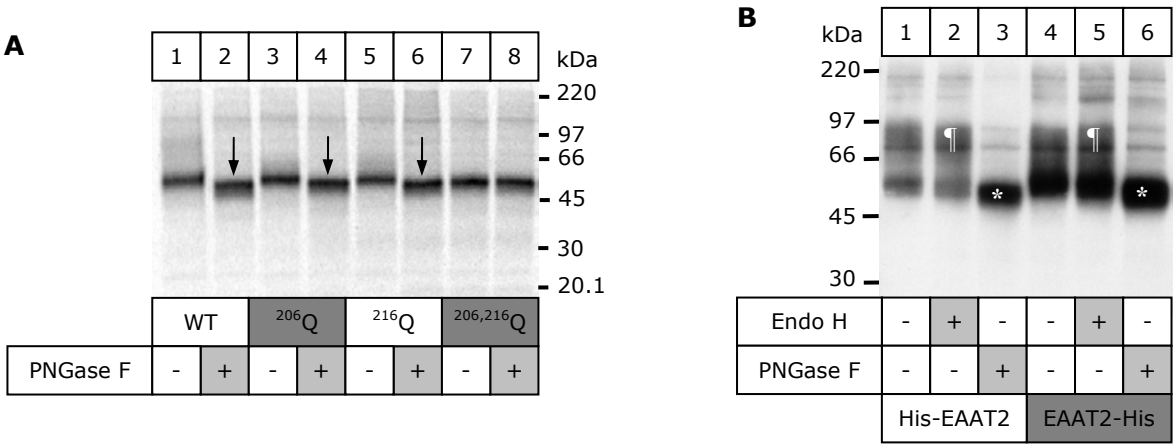


**Fig. 25: Comparison of the deglycosylation of wild-type $(His)_6$-hEAAT2 and single $(His)_6$-hEAAT2 mutants (A), and deglycosylation of $(His)_6$-EAAT2 and EAAT2-$(His)_6$ after a chase period (B).** (A) SDS-PAGE analysis (Tricine-SDS-Gel, 8% acrylamide) of the parent hEAAT2 polypeptide and N-glycan minus mutants purified from *Xenopus* oocytes after 4h [$^{35}$S]methionine pulse. Both possible glycosyl acceptor sites, Asn206 and Asn216 had to be replaced by Gln, to prevent addition of a single N-glycan to the hEAAT2 polypeptide. Proteins were deglycosylated by PNGase F as indicated. (B) SDS-PAGE analysis (Tricine-SDS-Gel, 8% acrylamide) of the $(His)_6$-hEAAT2 and hEAAT2-$(His)_6$ polypeptides. Both proteins were purified from *Xenopus* oocytes after 4h [$^{35}$S]methionine pulse and a subsequent 36h chase. After 36h chase an Endo H resistant EAAT2 polypeptide (¶) appeared on the gel, which can be reduced to the protein core (*) by PNGase F.

After a 36h chase interval, most of the $(His)_6$-hEAAT2 or hEAAT2-$(His)_6$ polypeptides migrated as a broad band (75-95 kDa) well above that of the core-glycosylated hEAAT2 polypeptide (~60 kDa in Fig. 25B, lanes 1 and 4 respectively). These broad bands could be reduced to the hEAAT2 apoprotein by incubation with PNGase F (~57 kDa in Fig. 25B, lanes 3 and 6), but was resistant to Endo H (Fig. 25B, lanes 2 and 5). Resistance to cleavage by Endo H occurs if high mannose type *N*-linked glycans are processed to complex type oligosaccharides in the Golgi apparatus. These results showed that the broad bands correspond to the mature complex-glycosylated hEAAT2 polypeptides. Quantification by phosphorimage analysis suggested that 66% of the total hEAAT2 protein had left the ER within the 36h chase interval. The conclusion of these results is that the

majority of hEAAT2 subunits are in a mature state located in post-ER compartment including the plasma membrane.

After an additional chase period to allow for post-translational modifications, two native forms of the hEAAT2 transporter (His-tag in N-terminal or C-terminal) were observed on BN-polyacrylamide gels (Fig. 26A), one migrating at the same position as described in 2.1.b and a second slower migrating band with an apparent mass larger than that of the 260 kDa homopentameric GlyR (Fig. 26A, lanes 2 and 5). This slower migrating band was not observed with the non-glycosylated $N^{206,216}$Q-hEAAT2 mutant (Fig. 26A, lane 7-8), implying that the additional band originates from the post-translational processing of N-glycans (cf. ¶ in Fig. 25B) and represents a homotrimer of the complex-glycosylated hEAAT2 form. The analysis of the quantitative profiles presented in Fig. 26B leads to the conclusions that for both $(His)_6$-hEAAT2 and hEAAT2-$(His)_6$ the proportion of the trimer composed of complex-glycosylated EAAT2 raised with the duration of the chase period. Moreover, hEAAT2-$(His)_6$ seemed to acquire the complex-glycosylated state faster than $(His)_6$-hEAAT2 (Fig. 26C).

The ability to assembly into trimers of each of the various EAAT2 N-glycan mutants presented in Fig. 25A was investigated by BN-PAGE analysis (Fig. 26D). Both the single mutants ($N^{206}$Q-hEAAT2 and $N^{216}$Q-hEAAT2) and the double mutant ($N^{206,216}$Q-hEAAT2) were able to assemble into trimers as efficiently as the wild-type $(His)_6$-EAAT2. Apparently, the lack of core and complex glycosylation does not disturb the assembly of the transporter.

The prokaryotic ecgltP polypeptide does not possess any glycosylation sites precluding such an analysis for this particular transporter. When ecgltP was expressed in *Xenopus* oocytes it did not exhibit any electrophysiological activity (see 2.1). This may either signify that the ecgltP transporter does not acquire a functional conformation in *Xenopus* oocytes or that it is not exported to the plasma membrane. To discriminate between these possibilities, a consensus site for

N-glycosylation was incorporated into the ecgltP sequence. A glutamine (Q) residue located at the position 133 ($^{133}$QSS) in the ecgltP protein sequence was replaced by an asparagine (N) by site-directed mutagenesis ($^{133}$NSS).

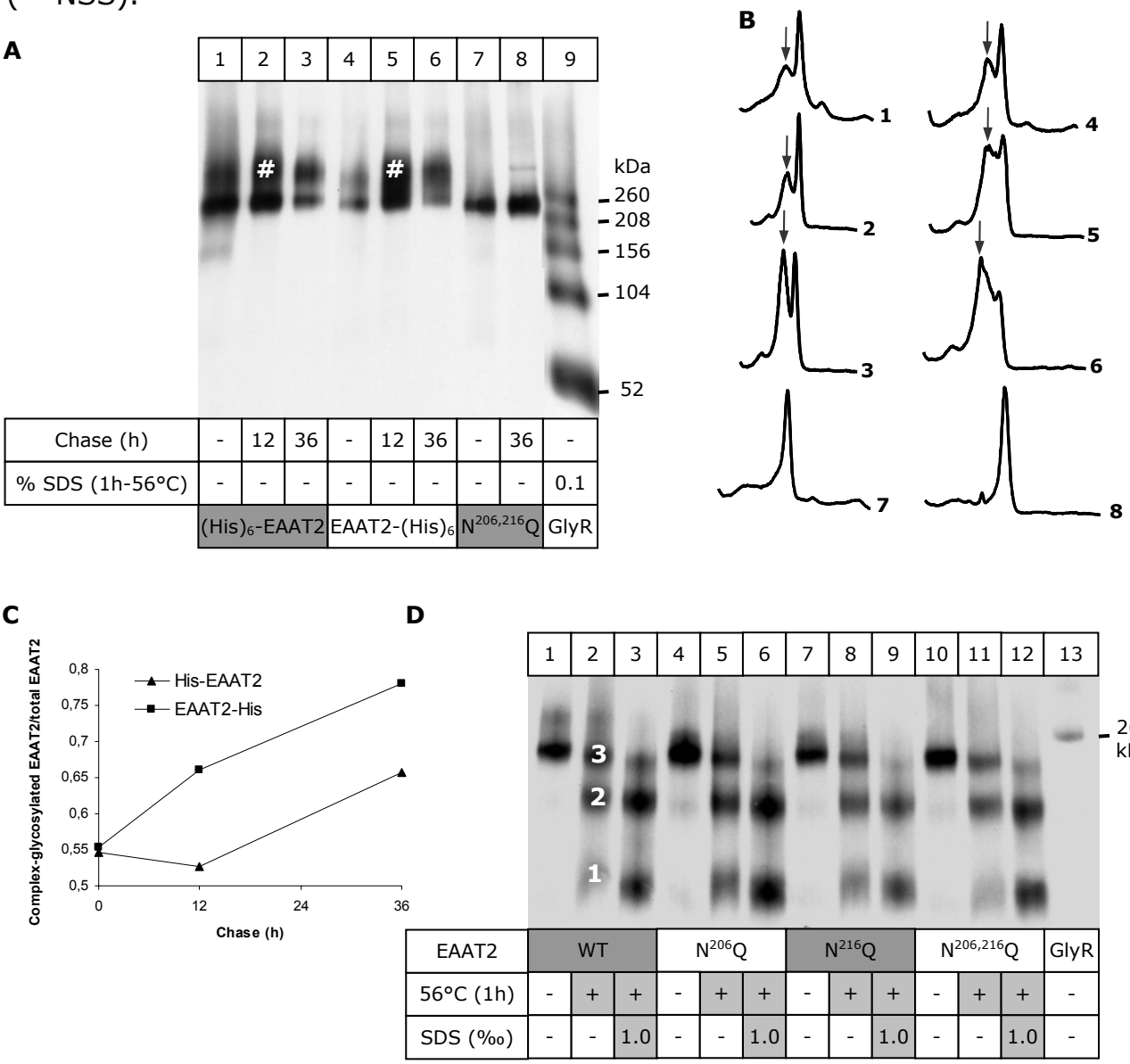


**Fig. 26: BN-PAGE analysis of $(His)_6$-hEAAT2 and hEAAT2-$(His)_6$ after different chase periods (A) and comparison of the oligomerization state of wild-type (WT) $(His)_6$-hEAAT2, $N^{206}$-, $N^{216}$-, and $N^{206,216}$ hEAAT2 mutants after a chase period (D).** (A), (D) Autography of the BN-polyacrylamide gels, (B) quantitative profiles of the gel lanes shown in (A), arrows show the peaks corresponding to trimers composed of complex-glycosylated hEAAT2 (# in A). (C), Graph representing the ratio of the complex-glycosylated form of $(His)_6$-hEAAT2 or hEAAT2-$(His)_6$ versus the duration of the chase period. The values were obtained from the areas under the peaks represented in (B). (A) Proteins were purified from *Xenopus* oocytes by Ni-NTA chromatography after a 4h [$^{35}$S]methionine pulse and the indicated chase period, then resolved by BN-PAGE (4-16% acrylamide). (D) Proteins were purified from *Xenopus* oocytes after a 12h [$^{35}$S]methionine pulse and then resolved by BN-PAGE (4-16% acrylamide). (A,D) Samples were treated as indicated to induce dissociation into lower order intermediates including monomers.

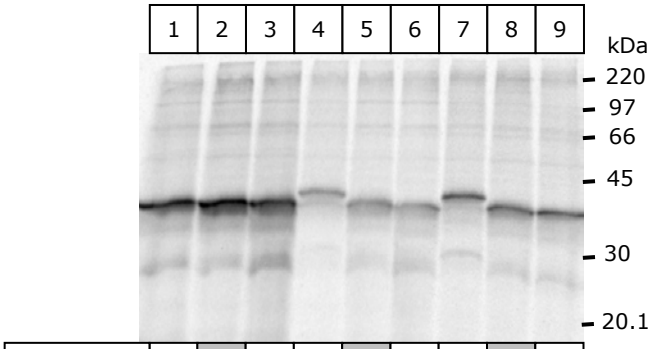


| | | | | | | | | | |
|---|---|---|---|---|---|---|---|---|---|
| EndoH | - | + | - | - | + | - | - | + | - |
| PNGase F | - | - | + | - | - | + | - | - | + |
| Chase (h) | - | - | - | - | - | - | 36 | 36 | 36 |
| ecgltP-His | $^{133}$QSS | | | $^{133}$NSS | | | $^{133}$NSS | | |

**Fig. 27: Deglycosylation of the wild-type ecgltP-$(His)_6$ and the $^{133}$NSS ecgltP-$(His)_6$ mutant.** Proteins were purified from *Xenopus* oocytes by Ni-NTA chromatography after a 12h [$^{35}$S]methionine pulse and the indicated chase period. Proteins were then digested by EndoH or PNGase F and resolved by SDS-PAGE (10% acrylamide).

The $^{133}$NSS-ecgltP mutant was expressed in *Xenopus laevis* oocytes and its glycosylation state was analyzed by deglycosylation with EndoH and PNGase F. As expected, the wild-type ecgltP was not glycosylated as no shift was observed after treatment with EndoH or PNGase F (Fig. 27, lanes 2 and 3 respectively). On the other hand, the $^{133}$NSS-ecgltP mutant migrated at a 2-3 kDa higher mass consistent with the presence of one oligosaccharide side chain. Indeed, deglycosylation by EndoH decreased the mass of the $^{133}$NSS-ecgltP mutant to that of the non-glycosylated parental ecgltP protein (Fig. 27, lanes 5 and 6). After an additional 36h chase period, it was however not possible to observe any complex-glycosylation, indicating that the ecgltP mutant resisted in the EndoH-sensitive form (Fig. 27, lane 8).

The acquisition of an N-glycan at position 133 indicates that the underlying consensus sequence assumed the predicted extracellular location, thus implying that the ecgltP mutant is capable of adopting a correct transmembrane disposition in the ER. The question whether egltP can leave the ER or not cannot be definitively answered from these data,

since it cannot be completely ruled out that the egltP mutant is exported from the ER, yet the N-glycan at Asn133 is not accessible to Golgi enzymes for sterical reasons. However, given that the hEAAT2 transporter acquires complex-type carbohydrates at a corresponding position and that the egltP transporter is non-functional in Xenopus oocytes, it appears more likely that ER export does not take place.

## 2.5 Does hEAAT2 form hetero-oligomers with hEAAT3 or ecgltP?

An interesting question concerning the oligomerization of glutamate transporters is to know if they are able to form hetero-oligomers by co-assembly with other members of the family.

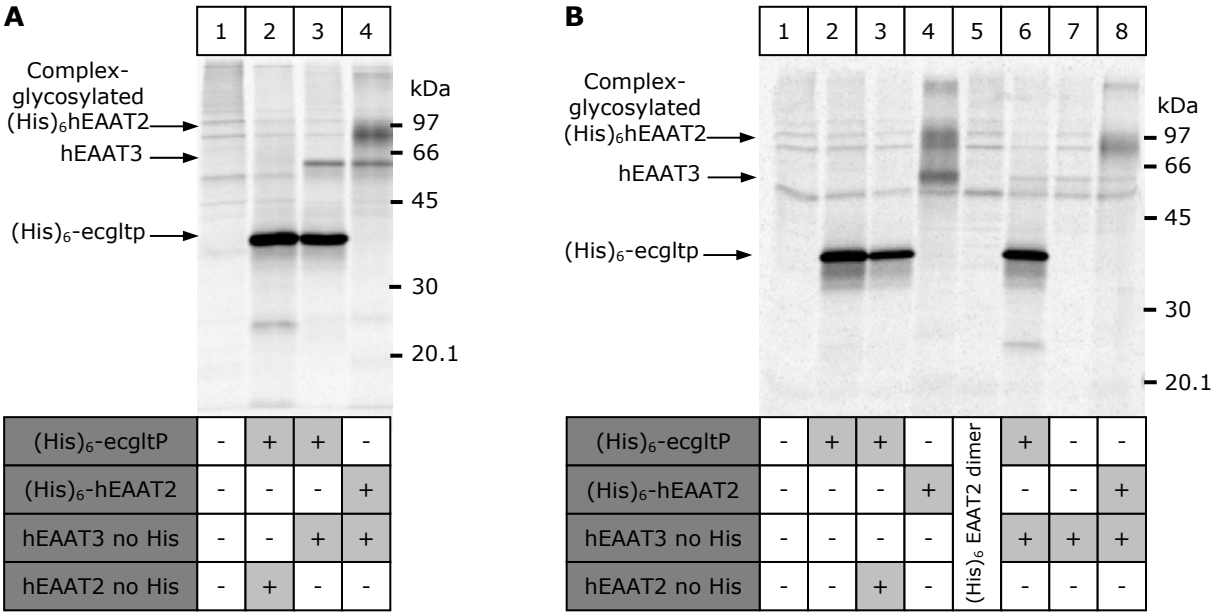


**Fig. 28: Co-expression of $(His)_6$-hEAAT2 and $(His)_6$-ecgltP with hEAAT2 or hEAAT3 in *Xenopus laevis* oocytes.** (A) His-tagged proteins were purified from *Xenopus* oocytes by Ni-NTA chromatography after a 12h [$^{35}$S]methionine pulse and were resolved by reducing SDS-PAGE (10% acrylamide) in parallel with [$^{14}$C]-labeled molecular mass markers. Oocytes were injected with a combination of two cRNAs (ratio 1:1) as indicated. (B) Same experiment as in (A), in which some control injections were performed: cRNAs coding for hEAAT2 and hEAAT3 without His-tag were injected alone, cRNA coding for $(His)_6$-hEAAT2 too.

To explore this possibility, protein co-expression experiments were performed in *Xenopus laevis* oocytes. Two cRNAs, one coding for an hexahistidyl tagged protein, and another one coding for a non-tagged protein were mixed in a 1:1 ratio and injected into oocytes. The oocytes were metabolically labeled by overnight incubation with [$^{35}$S]methionine. If both proteins are purified through the $Ni^{2+}$-NTA column, this may signify that they existed as hetero-oligomers and that their interaction was strong enough to preserve the oligomeric nature along the purification steps. The results of these experiments are presented in Fig. 28. Fig. 28A shows the proteins isolated after co-expression of $(His)_6$-ecgltP or $(His)_6$-hEAAT2 with hEAAT3. The comparison between lane 2 and lane 3 (hEAAT3 co-injected with $(His)_6$-ecgltP) reveals an additional protein band migrating at about 60 kDa. This band might represent EAAT3. The hEAAT3 core protein has a calculated molecular mass of 57 kDa. The protein sequence contains four N-glycosylation consensus sequences at positions $^{43}$NLST, $^{85}$NVSG, $^{178}$NMTE and $^{195}$NKTK. $^{43}$NLST is located between the transmembrane domains 1 and 2 at the extracellular side of the plasma membrane and should be glycosylated. $^{85}$NVSG, on the other hand, is located between the transmembrane domains 2 and 3 in an intracellular domain, it is therefore unlikely to become glycosylated. The two last positions are homologues to the $^{206}$NATS and $^{216}$NETV consensus sequences in hEAAT2. It was shown in paragraph 2.4 that hEAAT2 is glycosylated at only one of its two consensus sites, probably because they are too close to each other to be occupied simultaneously by a bulky N-glycan. Given that the same phenomenon holds true with hEAAT3, it should carry 2 N-glycans and thus posses a calculated molecular mass of 63 kDa, assuming that the two N-glycans have a mass of 3 kDa each. It was further observed in 2.1.b that glutamate transporters migrate at 10-20% lower masses than calculated from their amino acid sequences. If this characteristic is also taken into consideration, the 60 kDa protein detected in Fig. 28A, lane 3 can be judged to represent the core-glycosylated form of hEAAT3.

An important control in co-injection/co-purification experiments is to verify that the protein, which does not posses a $(His)_6$-tag, does not bind non-specifically to the $Ni^{2+}$-NTA beads when it is expressed alone. Fig. 28B shows a control experiment, in which single cRNAs coding for hEAAT2, hEAAT3, or $(His)_6$-hEAAT2 were expressed in Xenopus oocytes. [$^{35}$S]-labeled proteins were purified by affinity chromatography with $Ni^{2+}$-NTA agarose beads. The comparison between lanes 2 and 3 (Fig. 28B) leads to the conclusion that $(His)_6$-ecgltP did not interact with hEAAT2. In this experiment $(His)_6$-ecgltP seemed once again to interact with hEAAT3 (Fig. 28B, lane 6), but the hEAAT3 band was also observed when EAAT3 was expressed alone (Fig. 28B, lane 7), i.e. without His-tagged partner protein. Accordingly, the non-tagged form of hEAAT3 seemed to interact non-specifically with the $Ni^{2+}$-NTA beads.

The core-glycosylated hEAAT2 has a calculated molecular mass of 66 kDa, which is unfortunately identical with the molecular mass of core-glycosylated hEAAT3. Because the bands corresponding to the core-glycosylated proteins overlap on SDS-polyacrylamide gels, it is not possible with the SDS-PAGE technique to determine if hEAAT2 and hEAAT3 interact together.

The conclusions of these experiments are that ecgltP neither interacts with hEAAT2 nor with hEAAT3. It was also not possible with these methods to demonstrate that hEAAT2 interacts with hEAAT3 to form hetero-oligomers.

## 2.6 Study on the assembly motif of ecgltP using deletion mutants

In attempt to identify the motif responsible for the oligomerization of ecgltP, a series of deletion mutants was engineered. Incrementally larger pieces of the C-terminal part of the protein were removed. An additional construct (ecgltP$^{83-443}$) lacked the uttermost 82 N-terminal amino acids. Each construct was expressed by cRNA injection in oocytes, which were subsequently labeled with [$^{35}$S]methionine overnight. Proteins were

purified by $Ni^{2+}$-affinity chromatography. The oligomeric state of each deletion mutant was analyzed by the blue-native PAGE technique and each was tested for its resistance to dissociate into lower order oligomers. Fig. 29 shows the proposed membrane topology of ecgltP and the position of the various truncations.

Fig. 30A represents an autoradiography of an SDS-polyacrylamide gel, which shows the expression level and the apparent masses of wild-type ecgltP and its seven mutants expressed in *Xenopus* oocytes. All proteins were expressed at a high level, and all (including the wild-type ecgltP) migrated much faster than expected from their calculated molecular masses (Fig. 30B). A faster migration was already described for the ecgltP wild-type in 2.1.b. The protein bands of the mutants F and G (Fig. 30A) were particularly broad. This anomalous migration is likely caused by the hydrophobic character of the proteins.

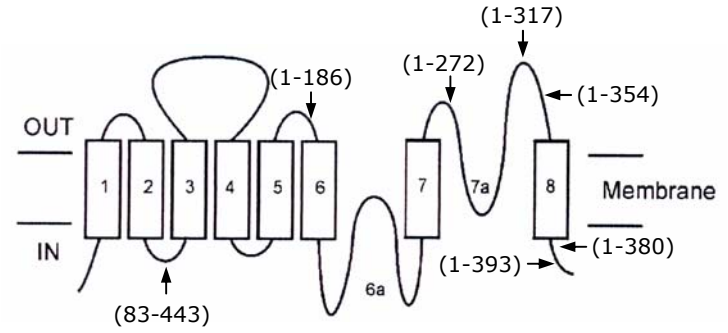


**Fig. 29: Model for the membrane topology of glutamate transporters (Slotboom et al., 2001a) and positions of the different deletions engineered for the assembly study of ecgltP.** Numbered rectangles indicate membrane-spanning segments, the reentrant loops are numbered 6a and 7a. Arrows show the position of the deleted fragments in ecgltP, brackets indicate the corresponding amino acids positions.

Deletion of up to 169 amino acid at the C-terminal side of the protein (mutant E: ecgltP$^{1-272}$) did not prevent the formation of a trimer (Fig. 31, panel C, first column). However, mutants shorter than mutant B (ecgltP$^{1-380}$) had a tendency to dissociate more easily into monomers when incubated in the presence of 0.1% SDS. Mutants F (ecgltP$^{1-186}$) and G (ecgltP$^{83-443}$) were not able anymore to assemble correctly (Fig. 31B).

Mutant F (ecgltP$^{1-186}$) formed only dimers (Fig. 31B, lanes 7-9), while mutant G (ecgltP$^{83-443}$) existed almost entirely in the form of aggregates (Fig. 31B, lanes 4-6), which represent a non-organized association of proteins.

**A**

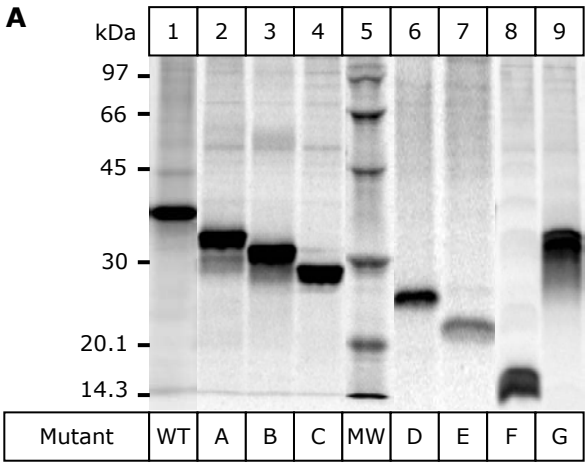


**B**

| Mutant | Amino acid position | MW (kDa) |
|---|---|---|
| A | 1-393 | 46 |
| B | 1-380 | 41.6 |
| C | 1-354 | 39.2 |
| D | 1-317 | 35.1 |
| E | 1-272 | 30.3 |
| F | 1-186 | 20.7 |
| G | 83-443 | 43.2 |

**Fig. 30: Expression of ecgltP deletion mutants in *Xenopus laevis* oocytes.** (A) His-ecgltP and many deletion mutants were expressed in *Xenopus* oocytes and purified by Ni-NTA chromatography after a 12h [$^{35}$S]methionine pulse. Proteins were resolved by reducing SDS-PAGE (10% acrylamide) in parallel with [$^{14}$C]-labeled molecular mass markers. A letter was assigned to the different mutants. The table represented in (B) indicates the amino acid portion contained in each mutant and the corresponding calculated molecular masses of the protein including the His-tag.

Taken together, an assembly motif in the ecgltP protein is probably located in the first 83 amino acids of the protein, but it seems that a protein domain located between amino acids 186 and 272 also plays an important role.

## 2.7 BN-PAGE analysis of TetA(B), a tetracycline cation/proton antiporter

In an additional attempt to validate the blue-native PAGE technique as a convenient method for the determination of the oligomeric state of proteins, we expressed TetA(B) in *Xenopus laevis* oocytes and analyzed its oligomeric state by BN-PAGE. TetA(B) is a tetracycline cation/proton inner membrane antiporter, which mediates tetracycline resistance in Gram-

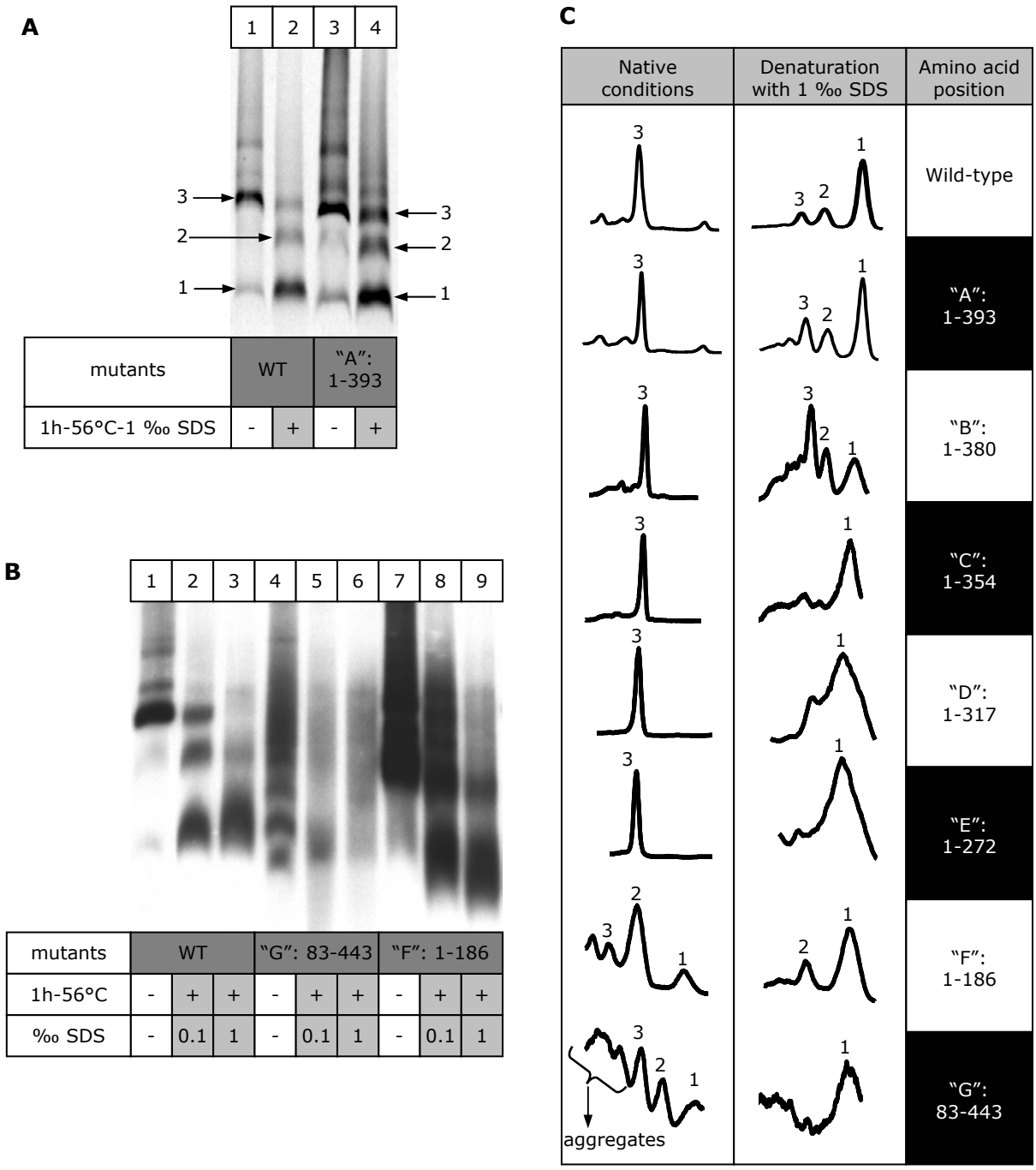


**Fig. 31: Expression of ecgltP deletion mutants in *Xenopus laevis* oocytes and analysis of their oligomeric state by blue-native PAGE.** His-ecgltP and the deletion mutants were expressed in *Xenopus* oocytes and purified by $Ni^{2+}$-NTA affinity chromatography after an overnight pulse with [$^{35}$S]methionine. Proteins were resolved by BN-PAGE (4-16% of acrylamide). (A, B) Examples of BN-PAGE analyses of the wild-type ecgltP and the ecgltP$^{1-393}$, ecgltP$^{83-443}$, ecgltP$^{1-186}$ deletion mutants. (c) Quantitative profiles determined by PhosphorImager analysis of the BN-polyacrylamide gels obtained with the indicated mutants and the wild-type ecgltP. The oligomeric structure of each protein was analyzed in native conditions and after denaturating with 0.1 ‰ SDS for 1h at 56°C.

negative bacteria. It has already been shown by the analysis of two-dimensional crystals that TetA(B) displays a trimeric architecture (Yin et al., 2000). TetA(B) was used in our study as a positive control to confirm that BN-PAGE analyses and crystallography lead to the same conclusions concerning the oligomeric structure of membrane proteins.

A plasmide containing the cDNA coding for TetA(B) was kindly provided by Dr. Stuart B. Levy from the Center for Adaptation Genetics and Drug Resistance at the Tufts University School of Medicine (Boston, USA). This cDNA was subcloned into a pNKS vector, and a hexahistidyl tag was added in N-terminal of the open reading frame by site-directed mutagenesis. The cRNA coding for TetA(B) was then injected into *Xenopus laevis* oocytes, and proteins were purified by $Ni^{2+}$-NTA affinity chromatography. The autoradiographies of the SDS- and BN-polyacrylamide gels are presented in Fig. 32A and 32B, respectively. The SDS-PAGE analyze of TetA(B) (Fig. 32A) shows that the protein was well expressed by oocytes and migrated at its expected molecular mass of 43 kDa (Yin et al., 2000).

The BN-PAGE analysis revealed that TetA(B) failed to assemble into trimers in oocytes (Fig. 32B) or partially dissociated during the purification steps. In native conditions, TetA(B) run as dimers and predominantly as monomers (Fig. 32B, lane 2). The dimeric form was particularly resistant to denaturing treatment with SDS (Fig. 32B, lanes 4 and 5) and incubation in the presence of 1% SDS was required to produce a complete dissociation of the dimer into monomers (Fig. 32D, lanes 5 and 6).

These results suggest that either the TetA(B)-trimer is not stable enough to survive the experimental conditions used or that the oocytes are not able to fold and assembly this protein properly. Alternatively, it is also possible that the trimeric structure deduced from 2-D-crystals is incorrect. Caveats to structural prediction from 2D-crystals come from studies about the bacterial mechanosensitive ion channel MscL, which was first reported to form a hexamer (Saint et al., 1998) and later shown to be organized as

a pentamer (Chang et al., 1998). It is therefore not excluded that TetA(B) assembles as a dimer.

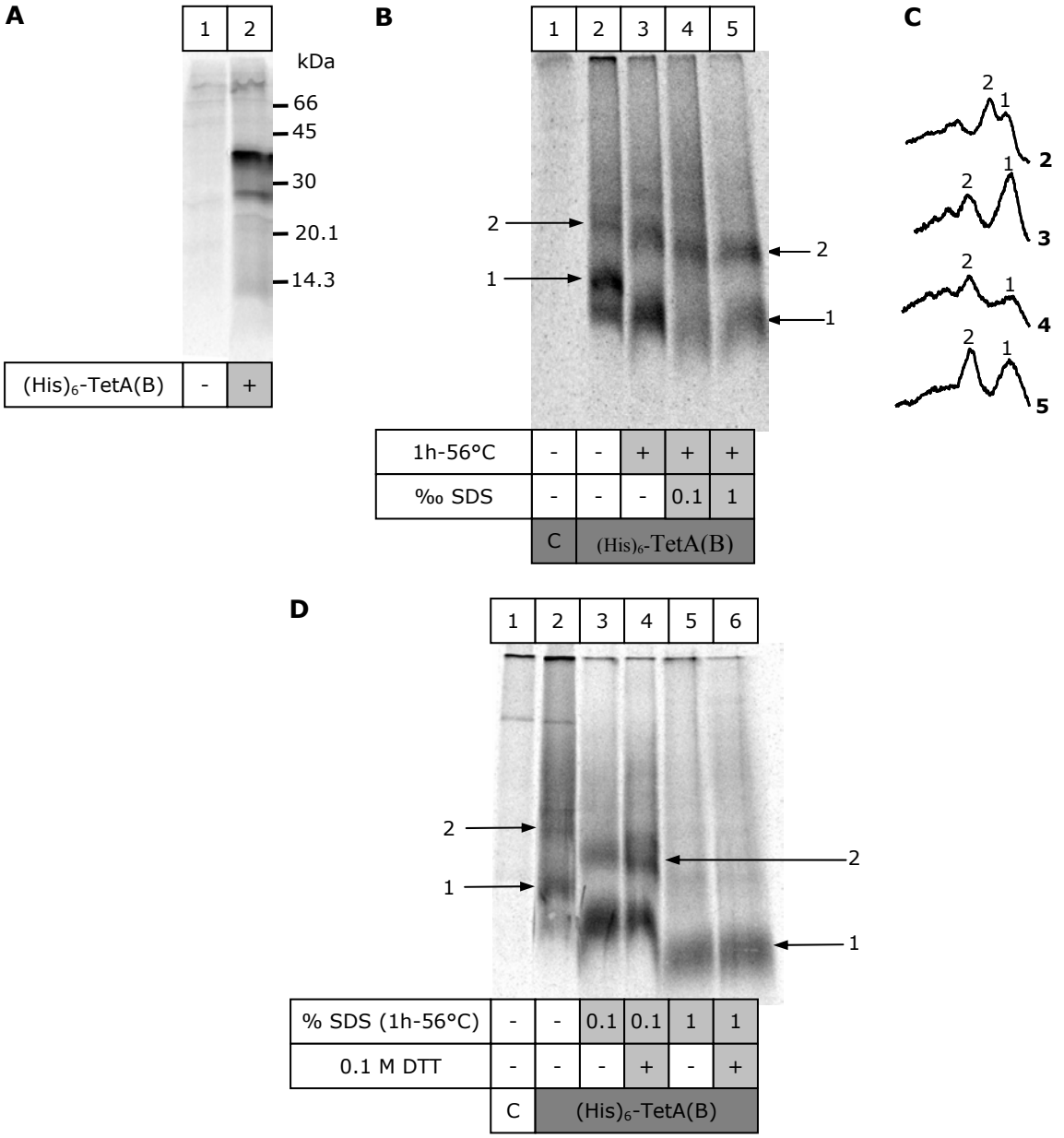


**Fig. 32: Expression of $(His)_6$-TetA(B) in *Xenopus laevis* oocytes and analysis of its oligomeric state by blue-native PAGE.** His-TetA(B) was expressed in *Xenopus* oocytes and purified by $Ni^{2+}$-NTA affinity chromatography after an overnight pulse with [$^{35}$S]methionine (1% digitonin in homogenizing buffer). Proteins were resolved on a 12.5% SDS-polyacrylamide gel (A) and on 4-16% BN-polyacrylamide gels (B, D). TetA(B) was analyzed in native conditions and after denaturation as indicated (B, D). (C) Quantitative profiles determined by PhosphorImager analysis of the BN-polyacrylamide gel represented in Fig. (B).

# IV/ Discussion

## IV-1. Identification of proteins interacting with P2X receptors

### 1.1 ßIII tubulin and MBP as binding partners of the rP2X$_2$ subunit

#### a- *The rP2X$_2$ subunit interacts directly with the cytoskeleton*

Anchoring neurotransmitter receptors at appropriate locations on the cell surface is critical for the formation and functioning of chemical synapses. In the present study the direct, stable and specific interaction between ßIII tubulin (isoform of tubulin which is reported to be restricted to neuronal tissue) and the rP2X$_2$ subunit was revealed. Tubulin exists as a heterodimer consisting of two tightly linked $\alpha$ and ß isoforms, and both subunits polymerize to form microtubules that provide a cytoskeletal network (Fig. 1). It can not be excluded that rP2X$_2$ interacts with $\alpha$ tubulin. To verify this possibility, proteins eluted after pull-down with GST-rP2X$_2$ have to be probed with a specific antibody to $\alpha$ tubulin. It is unlikely that $\gamma$ tubulin interacts with P2X$_2$ because the two proteins are not located in the same region of the neuron. $\gamma$ tubulin is a specialized minor form of tubulin and is one of the centrosome-specific proteins.

Many neurotransmitter receptors have been shown to interact directly or indirectly with tubulin. The GABA$_A$ receptor is linked to the microtubule network by the 13.9 kDa protein GABARAP (Wang et al., 1999), whereas gephyrin, a 93 kDa protein anchors the inhibitory glycine receptor at postsynaptic sites via binding to subsynaptic tubulin (Kirsch et al., 1991). On the other hand two types of glutamate receptors have been shown to interact directly with tubulin. van Rossum D. et al. found out that the NMDA receptors NR1 and NR2, which are ligand-gated ion channels, are able to interact directly with soluble tubulin (van Rossum et al., 1999a). The metabotropic glutamate receptor type 1$\alpha$ is also able to bind to

tubulin directly (Ciruela et al., 1999). The $P2X_2$ receptors can be now added to this list of receptors which are in tight relationship with the microtubule cytoskeleton. These results suggest that interactions with the cytoskeleton could tether the $P2X_{2A}$ receptors to specific locations. Alternatively, the interaction with tubulin may play a role in the transport of the $P2X_2$ receptors to the synapse.

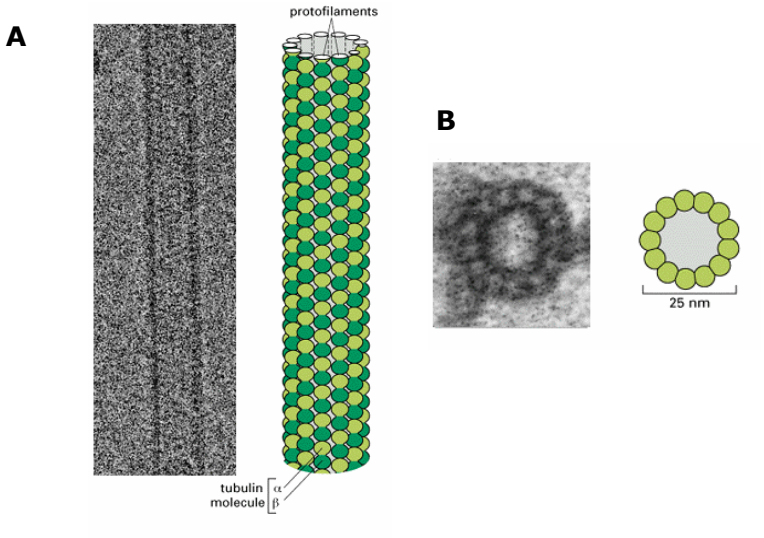


**Fig. 1: Microtubule structure.** (A) longitudinal view, (B) cross-section (Alberts et al., 1994). (A,B) The right picture is a schematic representation of the microtubules and the left picture, a photo taken with an electronic microscope.

The C terminal tails of the $rP2X_5$ and $rP2X_7$ subunits do not interact with tubulin. This result underlines the fact that the different P2X receptors possess unique features and distinct functions. Kim and al. showed that the $P2X_7$ receptor is in the center of an elaborated signalling complex (Kim et al., 2001). By co-immunoprecipitation followed by MALDI-TOF mass spectrometry the authors were able to identify 11 proteins that interact with the rat $P2X_7$ receptor (Fig. 2). Among the interacting partners were $\alpha$-actinin 4 and ß-actin. These results suggest that the $P2X_7$ receptor is also anchored by the cytoskeleton at locations where it can efficiently play its role. Moreover, the high number of interacting partners may reflect the multiple roles of the $P2X_7$ receptor in the nervous system as well as in the immune system.

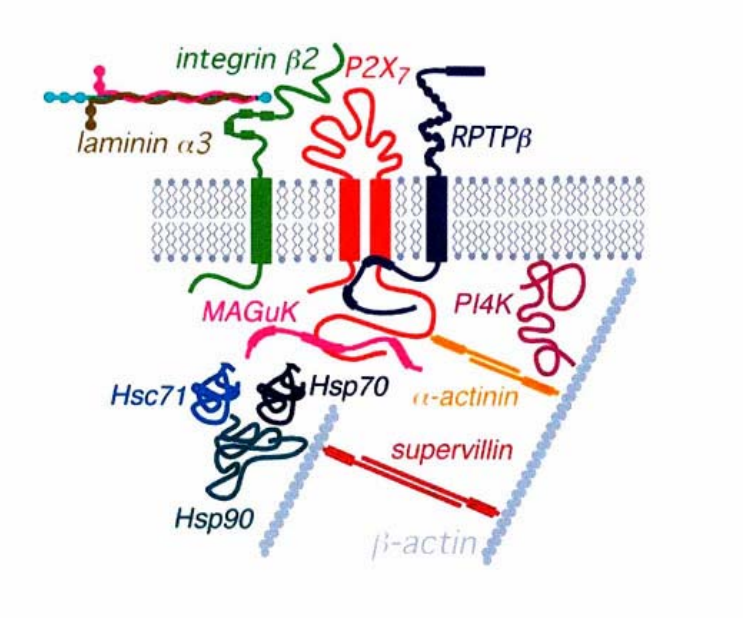


**Fig. 2: Schematic summary of $P2X_7$ receptor signalling complex (Kim et al., 2001).**

b- *All three GST-P2X fusion proteins bind MBP*

Myelin basic protein (MBP) binds to negatively charged lipids on the cytosolic surface of oligodendrocytes and is believed to be responsible for adhesion of these surfaces in the multilayered myelin sheath. In the present work MBP was one of the proteins purified by affinity chromatography with GST-$P2X_2$, GST-$P2X_5$ and GST-$P2X_7$. The significance of this binding is difficult to interpret because myelin and/or MBP have functions and locations which are incompatible with those of P2X receptors. Recently, Boggs et al. suggested that another function of MBP may be to interact with the cytoskeleton (Boggs and Rangaraj, 2000). Indeed, this group demonstrated that MBP interacts with actin and induces its polymerization. It was suggested that MBP and actin are bound by an electrostatic interaction, positively charged residues of MBP would interact with negatively charged residues of actin.

The C-terminal tail of tubulin is known to be acidic and promotes the interaction with highly positively charged regions in MAPs (Microtubules associates proteins) (Maccioni and Cambiazo, 1995). Moreover, immunohistochemical colocalization studies in immature cultured

oligodendrocytes indicate that MBP is closely associated with microtubules and actin microfilaments (Wilson and Brophy, 1989). All these data together strongly suggest that MBP and tubulin could interact together through electrostatic binding. Our results did not answer the question of a direct binding between MBP and the different fusion proteins.

It is likely that MBP co-purified with tubulin bound to GST-$P2X_2$ or with actin indirectly bound to GST-$P2X_7$ (Kim et al., 2001). Almost the same observation was made with GAPDH (glyceraldehydes-3-phosphate dehydrogenase) and the mGluR 1$\alpha$ glutamate receptor. The mGluR 1$\alpha$ receptor interacts directly with tubulin and GAPDH was co-purified in pull-down experiments with the C-terminal domain of the mGluR 1$\alpha$ receptor because it was able to interact with tubulin (Ciruela et al., 1999).

## 1.2 Localization of the tubulin binding motif on the $rP2X_2$ subunit

By using GST fusion proteins that include various portions of the C-terminal tail of the $P2X_2$ subunit, we were able to confine the binding domain of $P2X_2$ for tubulin to a 42 amino acid long region, ranging from amino acid 371 to 412.

Interestingly, the tubulin binding sequence identified in the present study overlaps to a significant extent with a 69 amino acid long sequence ($V^{370}$-$Q^{438}$) which is lacking in a splice variant isoform (designated $P2X_{2B}$) of the $P2X_2$ subunit (Simon et al., 1997). In contrast to the nondesensitizing $rP2X_{2A}$ receptor, a more rapid desensitization in the continued presence of ATP was observed for the $rP2X_{2B}$ receptor. Simon et al. suggested that the channel formed of $rP2X_{2B}$ subunits is less tightly anchored to certain cytoskeletal or membrane proteins than $P2X_{2A}$ channels (Simon et al., 1997). This would influence conformational changes in the receptor. Using mutational analysis, Smith et al. identified amino acids within the $P2X_2$ receptor C-terminus that regulate desensitization (Smith et al., 1999). They found that truncating the

receptor at the lysine 369 splice site dramatically increased the rate of desensitization. They identified two structural features, which are important in producing the slowly desensitizing phenotype that is characteristic of the $P2X_{2A}$ subtype. One is the presence of a hydrophobic amino acid at position 370 (V370) immediately adjacent to the splice site, and the other is the presence of several lysines within the 20 amino acid region that lies proximal to TM2 (Smith et al., 1999). Also in this study the authors considered the possibility that another associated protein is involved in regulating desensitizing.

It was observed many times that the $P2X_2$ splice variants desensitized more rapidly when expressed in human kidney HEK 293 cells than in oocytes (Simon et al., 1997). Zhou & Hume also reported that in outside-out membrane patches, $P2X_2$ receptors desensitize considerably faster than in cell-attached patches (Zhou and Hume, 1998). This could be a consequence of the disruption of the cytoskeleton. When $P2X_1$ receptors are stably expressed in HEK 293 cells and assayed by patch-clamp on the first day after passage of the culture, they are found to have whole-cell current kinetics which desensitize faster than those found in the native vas deferens tissue (Parker, 1998). By the second day after passage of the culture, however, the whole-cell current kinetics of the expressed receptors shifted, slowing in both activation and desensitization. Treatment of cells three days after passage with cytochalasine B or D caused a reversion to the rapid kinetic phenotype, implicating the actin cytoskeleton in the development of the native kinetic. $P2X_1$ receptors may therefore require interaction with an intact actin cytoskeleton for native kinetics (Parker, 1998).

All these information together strongly suggest that the interaction between ßIII tubulin and $P2X_2$ receptors may modulate the functions of the channel. Tubulin may protect the receptor from a rapid desensitization by an allosteric mechanism or by protecting the receptor against internalization. The faster desensitization of the $P2X_{2B}$ subunit may be attributed to the failure of this receptor to interact with tubulin due to the

lack of the tubulin binding domain. To test this hypothesis Dr. J. Rettinger performed electrophysiological studies in *Xenopus* oocytes of the $P2X_{2A}$ receptor in the presence of taxol as a tubulin depolymerizing agent. Unfortunately, he failed to show a difference in the currents of $P2X_{2A}$ in the presence or in the absence of taxol.

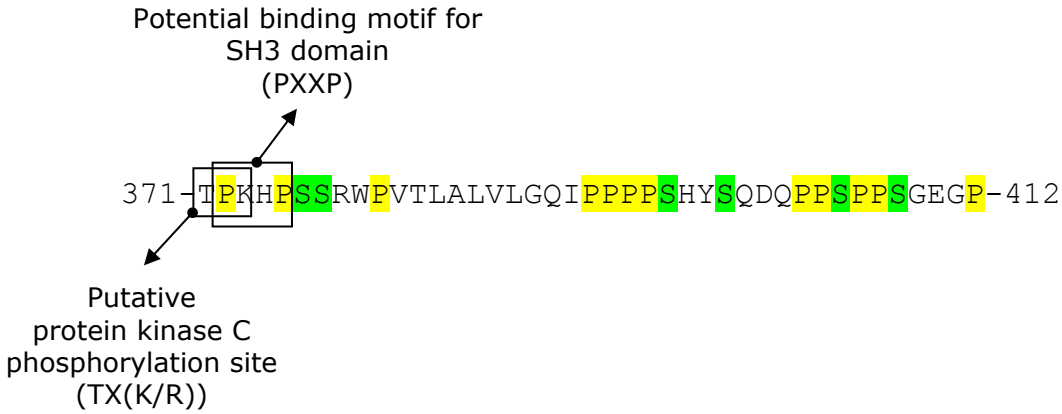


**Fig. 3: Binding motif of rP2X$_2$ for ßIII tubulin.** The amino acid sequence of the identified binding motif of $P2X_2$ for ßIII tubulin is represented, proline residues are highlighted in yellow and serine residues in green. Putative PKC phosphorylation site and SH3 binding motif are indicated.

The tubulin binding domain identified in this study contains a total of six serine residues and twelve proline residues (Fig. 3). In contrast, both the $P2X_5$ and $P2X_7$ subunits do not possess domains rich in proline and serine residues, which may explain their inability to interact with tubulin (Fig. 4).

Proline residues $^{372}$P and $^{375}$P may be interpreted to constitute a binding motif for SH3 domains, at least when based on the minimal consensus motif, PXXP (Mayer, 2001). SH3 domains bind with moderate affinity and selectively to proline-rich ligands. These domains play critical roles in a wide variety of biological process ranging from regulation of enzymes by intramolecular interactions, increasing the local concentration or altering the subcellular localization of components of signalling pathways, and mediating the assembly of large multiprotein complexes (Mayer, 2001). SH3 domains provide the cell with an especially handy and adaptable means of bringing proteins together. The epithelial $Na^+$ channel ENaC, for example, is located at the apical membrane by binding to $\alpha$-spectrin. The

putative pore forming subunit of the rat ENaC (α-ENaC) binds through a unique proline-rich sequence located in its C-terminal region to the SH3 domain of α-spectrin (Rotin et al., 1994). It could be speculated that $P2X_{2A}$ and ßIII tubulin interact through such an interaction. However the analyze of the ßIII tubulin protein sequence with the scanprosite program available in the Internet (http://us.expasy.org/cgi-bin/scanprosite) did not reveal the presence of SH3 domains in ßIII tubulin.

The mGluR1α, the NR1 and NR2 glutamate receptors interact directly with tubulin through their C-terminal domains. The sequence alignment of the C-termini of these receptors with the tubulin binding motif of $P2X_2$ did not show any analogy. Nevertheless microtubule-associated proteins (MAPs) such as MAP2, MAP4, and Tau also have a proline-rich region in their microtubule binding domain, which stimulate tubulin polymerization and stabilize microtubules inside cells (Aizawa et al., 1991). The proline-rich domain of $P2X_2$ may play a role in the interaction between $P2X_2$ and tubulin.

```
|P2X2|     T------------------FMNKNKLYSHKKFDKVRTPKHPSSRWPVTLALVLGQIPPPP  395
|P2X5|     Y------------------LIRKSEFYRDKKFEKVRGQKEDANVEVEANEMEQERPEDEP  401
|P2X7|     TYASTCCRSRVYPSCKCCEPCAVNEYYYRKKCEPIVEPKPTLKYVSFVDEPHIWMVDQQL  416

|P2X2|      SHYSQDQPPSPPSGEGPTLGEGAELPLAVQSPRPCSISALTEQVVDTLGQHMGQRPPVP  454
|P2X5|      LERVRQDEQSQELAQSGRKQNSNCQVLLEPARFGLRENAIVNVKQSQILHPVKT       455
|P2X7|      LGKSLQDVKGQEVPRPQTDFLELSRLSLSLHHSPPIPGQPEEMQLLQIEAVPRSRDSPD  475

|P2X2|      EPSQQDSTSTDPKGLAQL                                           472
|P2X7|      WCQCGNCLPSQLPENRRALEELCCRRKPGQCITTSELFSKIVLSREALQLLLLYQEPLL  534

|P2X7|      ALEGEAINSKLRHCAYRSYATWRFVSQDMADFAILPSCCRWKIRKEFPKTQGQYSGFKY  593

|P2X7|      PY                                                           595
```

**Fig. 4: Sequence comparison of the C-terminal part of $rP2X_2$, $rP2X_5$ and $rP2X_7$.** The amino acid sequences of the C-terminal part of $rP2X_2$, $rP2X_5$ and $rP2X_7$ are represented. The sequence of the identified binding motif of $P2X_2$ for ßIII tubulin is showed by a rectangular box. Proline residues are highlighted in yellow and serine residues in green. Identical amino acids are highlighted by shaded boxes.

As shown in Fig.3, the binding motif of $rP2X_2$ for ßIII tubulin contains a putative PKC phosphorylation site ($^{372}$TPK). The $rP2X_2$ receptor contains two other potential protein kinase C sites, $Thr^{18}$ ($^{18}$TPK) located in the N-terminal domain, and $Thr^{464}$ ($^{464}$TDPK) located in the C-terminal domain. Boué-Grabot et al. showed that the $Thr^{18}$ is the only protein kinase C site, which is phosphorylated in Xenopus oocytes and that a mutant (K20T) that lacks this consensus site exhibited quickly desensitizing properties (Boue-Grabot et al., 2000). The PKC phosphorylation site at the position $Thr^{18}$ is highly conserved among the seven P2X receptors subunits (Boue-Grabot et al., 2000), which is not the case for the PKC phosphorylation site at the position $Thr^{372}$ (Fig. 3). However, when the two threonines in the C-terminal domain ($Thr^{372}$, $Thr^{464}$) are lacking, the mutated $P2X_2$ channels exhibited two phenotypes when expressed in oocytes. ATP responses were either slowly desensitizing or had a biphasic phenotype with a quickly desensitizing current followed by a sustained phase (Boue-Grabot et al., 2000). The authors suggested that the C-terminal domain plays an important role in the stabilization of the slowly desensitizing kinetic. Their hypothesis was that the C-terminus domain would promote phosphorylation of the subunit and/or protect phosphorylated subunits from phosphatase activity. It is possible that the binding between ßIII tubulin and the C-terminal of the $P2X_2$ receptor depends on the presence of the threonine at the position 372, and that ßIII tubulin plays a role of protection against phosphatase.

The tubulin binding domain does not contains any PKA phosphorylation consensus site (RXXS).

## 1.3 Co-expression of rP2X$_2$ and ßIII tubulin in heterologous expression systems

### a- *Expression in Xenopus laevis oocytes*

In a second part of the study on the interaction tubulin/P2X$_2$, both proteins were expressed in *Xenopus laevis* oocytes in attempt to demonstrate that this interaction occurs in other expression systems. Unfortunately, it was not possible to prove by $Ni^{2+}$-NTA affinity chromatography that ßIII tubulin and rP2X$_2$ interact with each other in *Xenopus* oocytes. This result can be explained by the existence of endogenous ß tubulin in Xenopus oocytes (Bieker and Yazdani-Buicky, 1992). Indeed, this ß tubulin isoform (accession number AAA49977) is ~90% homologous to the rat ßIII tubulin (see Fig.5).

```
Rat       MREIVHIQAGQCGNQIGAKFWEVISDEHGIDPSGNYVGDSDLQLERISVYYNEASSHKYV
Xenopus   MREIVHLQAGQCGNQIGAKFWEVISDEHGIDPTGAYHGDSDLQLERINVYYNEATGGKYV
          ******:*************************:* * **********.******:. ***

Rat       PRAILVDLEPGTMDSVRSGAFGHLFRPDNFIFGQSGAGNNWAKGHYTEGAELVDSVLDVV
Xenopus   PRAVLVDLEPGTMDSVRSGPFGQIFRPDNFVFGQSGAGNNWAKGHYTEGAELVDSVLDVV
          ***:***************.**::******:*****************************

Rat       RKECENCDCLQGFQLTHSLGGGTGSGMGTLLISKVREEYPDRIMNTFSVVPSPKVSDTVV
Xenopus   RKEAESCDCLQGFQLTHSLGGGTGSGMGTLLISKIREEYPDRIMNTFSVVPSPKVSDTVV
          ***.*.*****************************:************************

Rat       EPYNATLSIHQLVENTDETYCIDNEALYDICFRTLKLATPTYGDLNHLVSATMSGVTTSL
Xenopus   EPYNATLSVHQLVENTDETYCIDNEALYDICFRTLKLTTPTYGDLNHLVSATMSGVTTCL
          ********:*****************************:*******************.*

Rat       RFPGQLNAHLRKLAVNMVPFPRLHFFMPGFAPLTARGSQQYRALTVPELTQQMFDAKNMM
Xenopus   RFPGQLNADLRKLAVNMVPFPRLHFFMPGFAPLTSRGSQQYRALTVPELTQQMFDAKNMM
          ********.************************:************************

Rat       AACDPRHGRYLTVATVFRGRMSMKEVDEQMLAIQSKNSSYFVEWIPNNVKVAVCDIPPRG
Xenopus   AACDPRHGRYLTVAAIFRGRMSMKEVDEQMLNVQNKNSSYFVEWIPNNVKTAVCDIPPRG
          **************::*************** :*.***************.*********

Rat       LKMSSTFIGNSTAIQELFKRISEQFTAMXX-KAFLHWYTGQGMDEMEFTEAESNMNDLVS
Xenopus   LKMSATFIGNSTAIQELFKRISEQFTAMFRRKAFLHWYTGEGMDEMEFTEAESNMNDLVS
          ****:************************   *********:*******************

Rat       EYQQYQDATAEEEGEMYEDDDEESERQGPK
Xenopus   EYQQYQDATAEEEGEFEEGEEEENA-----
          ***************: *.::**.
```

**Fig. 5: Amino acid sequence alignment of oocyte ß tubulin and rat ßIII tubulin.** Sequences are deduced from NCBI accession numbers AAA49977 (oocyte ß tubulin) and P04691 (rat ßIII tubulin). The alignment was made using the ClustalW program available in the Internet (http://clustalw.genome.ad.jp/).

It is therefore likely that the oocyte ß tubulin compete with the expressed ßIII tubulin for the binding to $P2X_2$. The presence of an excess of endogenous non labeled ß tubulin may be an explanation why it was not possible to co-purify radioactive ßIII tubulin with the co-expressed rat $P2X_2$ receptor in Xenopus laevis oocytes.

To bypass this problem, oocytes were injected with a cRNA coding for the $rP2X_2$ receptor and the whole oocyte microtubules were purified after polymerization with GTP and taxol (Vallee, 1986). The aim of this experiment was to co-purify $rP2X_2$ with the endogenous microtubules. This attempt was also unsuccessfull. van Rossum et al. showed that the NR1 and NR2 glutamate receptors bind directly to tubulin but were also not able to isolate these two receptors with polymerized tubulin (van Rossum et al., 1999b). The authors suggested that the NR1 and NR2 receptors preferentially interact with soluble form of tubulin rather than with polymerized tubulin. Interaction of the $rP2X_2$ receptor with soluble tubulin may also explain the impossibility to co-purify this receptor with endogenous tubulin.

b- *Expression of $rP2X_2$-GFP in COS-7 cells*

To visualize the subcellular localization of the $P2X_2$ receptor in mammalian cells, the fusion protein $rP2X_2$-GFP was expressed in COS-7 cells.

Other groups already expressed $rP2X_2$-GFP in mammalian cell lines. Fig. 6 shows the comparison of the pattern of expression obtained in COS-7 cells in the present study with the pattern of expression in HEK293 cells or in hippocampal neurons (Bobanovic et al., 2002; Khakh et al., 2001). Khakh et al. observed that the expression of $rP2X_2$-GFP in neurons resulted in green fluorescence that localized to the plasma membrane and the cell interior (Fig. 6C right picture). They were able to measure the somatic $rP2X_2$-GFP receptor pool size and found that most $rP2X_2$-GFP

receptors are located inside the cell. They suggested that this pool may be a source for delivery to the plasma membrane.

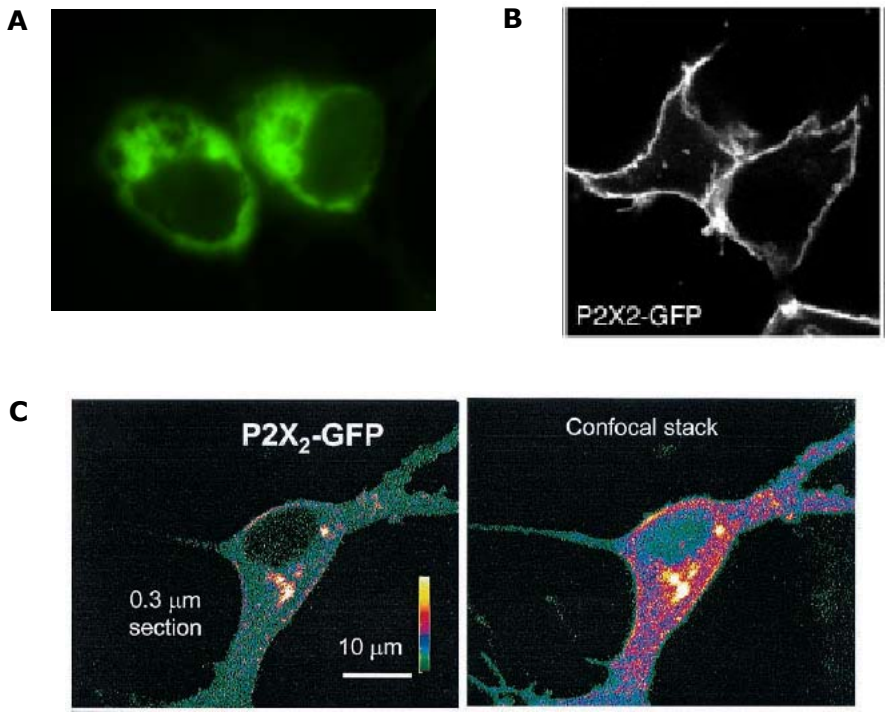


**Fig. 6: Subcellular distribution of $P2X_2$-GFP constructs in different cell types.** (A) Expression of $rP2X_2$-GFP in COS-7 cells. The cells were observed using a fluorescence microscope. (B) Expression of $rP2X_2$-GFP in HEK293 cells (Bobanovic et al., 2002). The cells were observed using a confocal microscope. (C) Expression of $rP2X_2$-GFP in embryonic hippocampal neurons (Khakh et al., 2001). The cells were observed using a confocal microscope. (Left) An image through the soma of a neuron expressing $P2X_2$-GFP receptors. (Right) A confocal stack of 25 optical sections of the same neuron spaced at 0.3 μm.

In contrast Bobanovic et al. observed that $rP2X_2$-GFP in HEK293 cells were uniformly distributed and predominantly at the periphery of the cell (Fig. 6B). Observations in neurons and in HEK293 cells therefore suggest that $P2X_2$ receptors localize as well at the plasma membrane as inside the cell. In COS-7 cells both localizations were observed simultaneously.

Interestingly, Khakh et al. reported that ATP application to dendrites caused receptor redistribution and the formation of varicose hot spots of higher $P2X_2$-GFP receptor density (Khakh et al., 2001). Activation of glutamate receptors also results in the formation of varicosities in neuronal processes (Emery and Lucas, 1995), and the glutamate receptor subunit, mGluR1, moves from a cytosolic pool to the plasma membrane

during activity in hippocampal neurons (Shi et al., 1999). These results show that the mGluR1 glutamate receptor and the $P2X_2$ receptors share two important features. Both directly bind to tubulin and both move in the cell under activation by their respective ligands. Altogether these data strongly suggest an important role of tubulin in the anchoring and/or the dynamic of the $P2X_2$ receptors.

## IV-2. Bacterial and human glutamate transporters share a trimeric quaternary structure

### 2.1 Evidences for multimeric glutamate transporters

Excitatory amino acid transporters (EAATs) buffer and remove synaptically released L-glutamate and maintain its concentrations below neurotoxic levels. EAAT also mediate a thermodynamically uncoupled substrate-gated anion conductance that may modulate cell excitability (Fairman et al., 1995).

The quaternary structure of two distantly related sodium-coupled glutamate transporters, the bacterial ecgltP and the human EAAT2 was investigated in the present study. Prokaryotic and eukaryotic glutamate transporters both exhibit a single oligomeric state formed by the assembly of three subunits. BN-PAGE analysis as well as chemical cross-linking demonstrated that both glutamate transporters exist in *Xenopus* oocytes primarily as multimers composed of three identical units. EcgltP purified as a recombinant protein from its natural host *E.coli* migrated also as a homotrimer in BN-PAGE (results obtained in our laboratory by N. Lang) and behaved in size exclusion chromatography as a homogenous protein of a single oligomeric state (experiments realized by the group of Prof. C. Fahlke).

When cRNA coding for $(His)_6$-tagged ecgltP was injected in *Xenopus* oocytes, neither glutamate-induced inward current nor glutamate-induced

increase of anion currents were observed. As ecgltP is effectively translated in oocytes, this may either signify that the ecgltP transporter does not acquire a functional conformation in *Xenopus* oocytes or that it is not exported to the plasma membrane. Nevertheless the purified ecgltP trimer can mediate radioactive glutamate uptake after reconstitution in lipid vesicles and is therefore functional (experiments realized by the group of Prof. C.Fahlke).

A few years ago, the group of N.C. Danbold observed that the purified EAAT2 protein from fresh rat brain tissue presented different electrophoretic behaviors on SDS-PAGE if the protein was immediately resolved after solubilization or if the protein was resolved after six month storage at –75°C (Haugeto et al., 1996). In both cases no reducing agent was used for the preparation of the probes. Without storage EAAT2 migrated as a single band corresponding to the monomeric form of the protein. During storage the proteins oxidized and higher molecular mass bands appeared on the gel. The authors suggested that during the oxidation monomers have been connected to each other by disulfide bridges and that the higher molecular mass bands corresponded to oligomers. They confirmed the oligomerization of EAAT2 and EAAT1 by performing cross-linking experiments in intact membranes purified from fresh rat forebrain or from transfected HeLa cells. These cross-linking experiments led to the conclusions that EAAT2 assembles predominantly as a trimer but that EAAT1 may also exist as dimers. However, as the authors observed in their cross-linking experiments also adducts larger than trimers, they were unable to come to a clear conclusion about the oligomeric structures of glutamate transporters. My results provide for the first time clear evidence that EAAT2 assembles as a trimer. Concerning EAAT1 or other EAAT subtypes further experiments are necessary to resolve the question of their stoichiometry. The SDS-induced dissociation of the EAAT2 trimers into monomers in the absence of reducing agents clearly indicates that the trimers are held together by non-covalent forces.

Another study about the assembly of glutamate transporters was done by Eskandari et al. using the freeze-fracture electron microscopy technique (Eskandari et al., 2000). In this work EAAT3 was also expressed in *Xenopus* oocytes. By comparison with non-injected oocytes, the authors were able to identify particles which correspond to EAAT3 multimers. They used the principle that the cross-sectional area of freeze fracture particles of integral membrane proteins is proportional to the number of membrane-spanning $\alpha$-helices (1.4 $nm^2/\alpha$-helix). By microscopical analysis, an area was determined which corresponded to a complex containing $35 \pm 3$ transmembrane $\alpha$-helices. The membrane topology of glutamate transporters is not completely elucidated so far. The presence of 6 transmembrane $\alpha$-helix in the N-terminal part of the protein is clearly indicated by hydropathy plots, but the topology of the C-terminal part of the protein is still debated (Danbolt, 2001). Nevertheless many studies investigating the extracellular accessibility of substituted cysteines suggested that the C-terminal domain is composed of two additional transmembrane $\alpha$-helices and two reentrant loop domains which could form a pore in the lipid bilayer (Grunewald and Kanner, 2000; Seal et al., 2000; Slotboom et al., 2001b). Eskandari et al. deduced from their study that the EAAT3 glutamate transporter assembles as a pentamer in *Xenopus* laevis oocytes. These results are incompatible with the trimeric model deduced from our experiments. It is already known that the use of the freeze-fracture technique could be limited when the topology of the investigated proteins is not exactly known. Secondary structure like reentrant loops are also source of problems for the accuracy of the results. For all these reasons the results coming from the low-resolution freeze-fracture study of EAAT3 have to be considered with caution.

Recently Yernool D. et al. investigated the stoichiometry of two bacterial glutamate transporters, $GltT_{Bs}$ from *Bacillus caldotenax* and $GltT_{Bc}$ from *Bacillus stearothermophilus* (Yernool et al., 2003). By size exclusion chromatography and cross-linking experiments the authors were able to show that both proteins expressed in *E.coli* possess a trimeric

stoichiometry. These results agree with my own results obtained with ecgltP. In their cross-linking experiments Yernool D. et al observed the appearance of a faint high molecular weight band and suggested that this band may correspond to a dimer of trimers. By BN-PAGE analysis of ecgltP I also observed a slower migrating distinct band, most likely a ecgltP hexamer. In the case of EAAT2, no band with higher molecular mass than the trimer was detected excepted of a band corresponding to a trimer composed of complex-glycosylated EAAT2 subunits. For ecgltP I cannot entirely exclude that the hexamer represents the functional form of the protein. However, because of its stability, the trimer must be an essential element of the ecgltP architecture *in vivo*.

## 2.2 What is the impact of the trimeric structure on the function of the EAAT glutamate transporters? Putative relationship between oligomerization and the chloride channel activity of EAAT transporters

For neurotransmitter transporters, monomeric as well as multimeric assemblies have been reported. The GAT/NET transporter family encodes carriers for neurotransmitters including GABA, dopamine, serotonin, norepinephrine, solutes and amino acids (Masson et al., 1999). Within this family separate subunit stoichiometries were observed. A prokaryotic GABA transporter (Li et al., 2001) and a mammalian glycine transporter were shown to form monomers (Horiuchi et al., 2001). There is evidence for the formation of tetrameric dopamine transporters (Hastrup et al., 2003; Norgaard-Nielsen et al., 2002), and serotonin transporters were shown to be dimers and tetramers (Jess et al., 1996; Kilic and Rudnick, 2000; Schmid et al., 2001).

In contrast to the different stoichiometry presented by the GAT/NET family members, the trimeric stoichiometry of glutamate transporters is conserved through evolution. This raise the important question concerning

the physiological significance of this oligomerization: does the trimeric structure have an importance for the transport process and/or for the associated ion channel activity? Results from radiation inactivation studies suggest that the neuronal (EAAT1-3) and the intestinal glutamate transporters function as oligomeric assemblies (Haugeto et al., 1996; Beliveau et al., 1990). However, evidence from other ion driven transporters indicate that assembly *per se* is not necessary for secondary active transport. Both mammalian $Na^+$/glucose co-transporter and *E.coli* lactose permease function as monomeric units (Eskandari et al., 1998; Sahin-Toth et al., 1994).

It has been shown that in addition to their function as secondary active transporters of glutamate, glutamate transporters behave as glutamate-activated chloride channels (Fairman et al., 1995). Chloride flux through the channel is not thermodynamically coupled to glutamate transport (Masson et al., 1999; Seal and Amara, 1999). Moreover, it is possible by mutation and sulfhydryl modification of the glutamate transporter EAAT1 to abolish the substrate transport, but not the substrate-gated anion conductance (Seal et al., 2001). Therefore, the two transporter-mediated activities are structurally separable. Anion conductance occurs in the absence of substrate transport, which imply that the pathway(s) for substrate and cotransported ions is to some degree structurally distinct from that for anions. Our data demonstrate that EAAT2 forms multimers in *Xenopus laevis* oocytes. It is possible that the trimer assembles in a manner that leads to the formation of a central pore constituting the ion conducting pathway lined by all three subunits. Many ligand-gated ion channels and voltage-gated cation channels form multimeric assemblies. The ion conduction pathway is formed by multiple subunits resulting in a symmetrical aqueous pore that allows coordinative binding of permeative anions by distinct subunits (Hille, 1992). For all these reasons it is tempting to speculate that the EAAT2 monomer performs secondary active glutamate transport, whereas the chloride channel mode seen in these transporters is a consequence of the oligomeric assembly. An attractive

hypothesis is that each of the subunits binds one sodium ion thus accounting for the three sodium ions binding steps involved in the glutamate transport cycle (Zerangue and Kavanaugh, 1996).

Similar to EAAT transporters, GAT/NET transporters not only exhibit a stoichiometric cotransport (Galli et al., 1999; Hilgemann and Lu, 1999), but also current components that appear to be conducted by permeation pathways similar to that of ion channels (Cammack and Schwartz, 1996; Galli et al., 1997; Lin et al., 1996; Mager et al., 1994). For rat and human SERT, this channel-like activity is becoming more prominent with increasing expression levels. This might suggest the existence of an endogenous regulatory protein that may interact with SERT in a variable stoichiometry and led to the generation of different protein complexes acting as channels in one stoichiometry and as carrier in another (Ramsey and DeFelice, 2002). Another possible explanation for this experimental finding is the existence of distinct oligomerization states (Ramsey and DeFelice, 2002), and this hypothesis could also account for the various experimentally determined subunit stoichiometries within the GAT/NET family.

In the case of EAAT transporters it was suggested many times that putative interacting proteins could be involved in the anion channel activity of these transporters (Danbolt, 2001). There are, however, also many arguments against this hypothesis. First, EAAT glutamate transporters function as anion channel when expressed in different expression systems like oocytes, CHO cells, HEK cells, and COS cells for example. This would imply that these putative interacting proteins are expressed in all these different cell types, which is pretty unlikely. Second, no additional protein was co-purified by affinity chromatography in my own experiments after expression of hEAAT2 and ecgltP in *Xenopus* oocytes and purification by affinity chromatography. Many proteins were reported to interact with the C-termini of EAAT2, EAAT3 and EAAT4 (Marie et al., 2000; Lin et al., 2001; Jackson et al., 2001). In the case of EAAT4, one of the two identified proteins (GTRAP48) is a guanine nucleotide

exchange factor, and the other (GTRAP41) possesses 87% homology with β-spectrin III, an actin interacting protein (Jackson et al., 2001). The authors suggested that both proteins stabilize and/or anchor EAAT4 at the cell membrane, making it less likely to be internalized and subsequently degraded. This two interacting proteins do not seem to play a role in the modulation of the ion channel activity of the EAAT4 glutamate transporter. Taken together, these results indicate that one quaternary structure of glutamate transporters supports two distinct transport processes, glutamate uptake and chloride permeability.

## 2.3 Study of the assembly motif of ecgltP

It is well established that the three-dimensional structure of proteins is far better conserved than the amino acid sequences and that protein with sequence identities as low as 30% have identical global structure (Lolkema and Slotboom, 1998; Yang and Honig, 2000). The human EAAT2 and the ecgltP glutamate transporters share 38% sequence homology and 22% identity. All members of the glutamate transporter family have the same membrane topology. Multiple sequence alignment of the transporters reveals sequence similarity throughout the entire length of the proteins, but a stretch of about 150 residues in the C-terminal half is particularly well conserved (Slotboom et al., 1999). This part of the proteins contains several sequence motifs, which are involved in recognition and/or translocation of glutamate and cotransported cations (Slotboom et al., 2001b). Fig. 7 shows the amino acid sequence comparison of the intracellular C-termini of the different human EAAT isoforms and Fig. 8 shows the comparison of the same domains of hEAAT2 and ecgltP.

```
EAAT1       IVLTSVGLPTDDITLIIAVDWFLDRLRTTTNVLGDSLGAGIVEHLSRHELKNRDVEMGNSVIE
EAAT2       LILTAVGLPTEDISLLVAVDWLLDRMRTSVNVVGDSFGAGIVYHLSKSELDTIDSQHRVHEDI
EAAT3       --------------------WLLDRFRTMVNVLGDAFGTGIVEKLSKKELEQMDVSSEVNIVN
EAAT4       ------------------------RLRTMTNVLGDSIGAAVIEHLSQRELELQEAELTLPSLG
EAAT5       ------------------RKDFARDTGTEKLLPCETKPVSLQEIVAAQQNGCVKSVAEASELT
                                     *   :  ::  ..:   ::  :    .

EAAT1       ENEMKKPYQLIAQDNETEKP-IDSETKM
EAAT2       EMTKTQSIYDDMKNHRESNSNQCVYAAHNSVIVDECKVTLAANGKSADCSVEEEPWKREK
EAAT3       PFALESTILDNEDSDTKKSYVNGGFAVDKSDTISFTQTSQF
EAAT4       ----KPYKSLMAQEKGASRGRGGNESAM
EAAT5       LGPTCPHHVPVQVERDEELPAASLNHCTIQISELETNV
```

**Fig. 7: Amino acid sequence alignment of the intracellular C-termini of the five EAAT isoforms.** Sequences are deduced from NCBI accession numbers P43003, P43004, P43005, P48664, O00341 for EAAT1, EAAT2, EAAT3, EAAT4 and EAAT5 respectively. The alignment was made using the ClustalW program available in the Internet (http://clustalw.genome.ad.jp/). Residues which are identical in the different subtypes are highlighted in gray. The 22 amino acids underlined in the EAAT2 protein sequence form a leucine zipper motif (see explanations in the text).

As that the quaternary structure of hEAAT2 and ecgltP is conserved through the evolution and the C-terminal part is the most similar portion of these proteins, the presence of a putative assembly motif was first considered to be located in the intracellular C-terminal part of ecgltP. In addition, the C-terminal domain of hEAAT2 transporter includes a "leucine zipper motif" at amino acid positions 452-473. Leucine zipper motifs consist of a periodic repetition of leucine or isoleucine residues at every seventh position over a distance covering eight helical turns. This motif is frequently found in nuclear transcription factors, and its role in promoting the homo- and heterodimerization of these proteins has been well characterized (Busch and Sassone-Corsi, 1990; Blank and Andrews, 1997). The leucine side chains extending from one $\alpha$-helix interact with those from a similar $\alpha$-helix of a second polypeptide, facilitating dimerization; the structure formed by cooperation of these two regions forms a coiled coil. It has been recently shown by Scholze P. et al. that mutations within an intramembrane leucine heptad repeat disrupt oligomer formation of the rat GABA transporter 1 (Scholze et al., 2002).

**A**

```
EAAT2     469-LILTAVGLPTEDISLLVAVDWLLDRMRTSVNVVGDSFGAGIVYHLSKSELDTIDSQHRVH
ecgltP    366-ATLGSVGIPLEGLAFIAGVDRILDMARTALNVVGN---ALAVLVIAKWEHKFDRKKALAY
                * :**:* *.::::..** :**  **::****:   *  *  ::* * .   .:  .:
                          ↑              ↑
                         380            393
                      (ecgltP)       (ecgltP)

EAAT2          EDIEMTKTQSIYDDMKNHRESNSNQCVYAAHNSVIVDECKVTLAANGKSADCSVEEEPWK
ecgltP         EREVLGKFDKTADQ-437
               *   : * :.  *:

EAAT2          REK-574
```

**B**

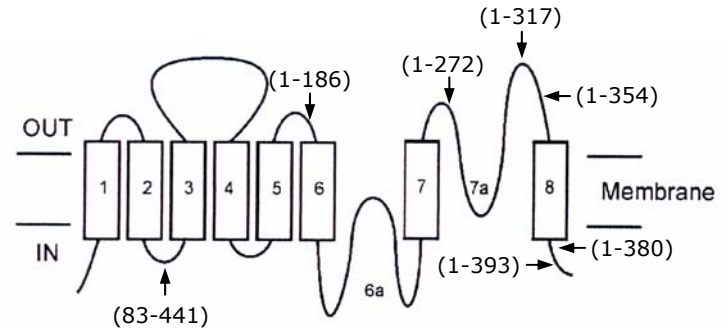


**Fig. 8: Amino acid sequence alignment of the intracellular C-termini of the human EAAT2 and the E.coli ecgltP proteins (A) and positions of the different deletions engineered for the assembly study of ecgltP (B).** (A) Sequences are deduced from NCBI accession numbers P43004 (hEAAT2) and P21345 (ecgltP). The alignment was made using the ClustalW program available in the Internet (http://clustalw.genome.ad.jp/). Residues which are identical in both sequences are highlighted in gray. The 22 amino acids underlined in the EAAT2 protein sequence form a leucine zipper motif (see explanations in the text). (B) Numbered rectangles indicate membrane-spanning segments. The two reentrant loops are numbered with 6a and 7a. Arrows indicate the position at which the ecgltP molecule was truncated. The numbers in parenthesis indicate the amino acid residues constituting the respective deletion mutants.

In attempt to identify a motif responsible for the oligomerization of ecgltP, a series of deletion mutants was engineered. Using the BN-PAGE technique, it was possible to show that a deletion of up to 169 amino acids of the C-terminal part of the protein (mutant: ecgltP$^{1-272}$) did not prevent the trimerization of ecgltP subunits. The involvement of a leucine zipper motive in the oligomerization of glutamate transporters can therefore be excluded. Retrospectively, this result may have been expected as the leucine zipper motif pattern found in the hEAAT2 subunit is neither conserved among other human EAAT isoforms nor present in ecgltP.

Two other deletion mutants: ecgltP$^{1-186}$ and ecgltP$^{83-443}$ were not able anymore to assemble correctly. Taken together these results suggest that an assembly motif in the ecgltP protein is probably located within the first 83 amino acids of the ecgltP subunit, but it seems that a protein domain located between amino acids 186 and 272 also plays an important role for assembly. It is possible that these two parts of the protein come close to each other when the protein is folded into the lipid bilayer, and that the domain responsible for the oligomerization is formed by the spatial association of two distinct amino acid sequences of ecgltP. It could also be possible that two different domains are necessary to achieve a complete assembly of ecgltP through two different interfaces, like it was suggested for the serotonin transporter SERT (Just et al., 2004). Further investigations are therefore needed to complete this study.

## 2.4 Perspectives

The next challenges of this exciting story would be to demonstrate that the functional glutamate transporters incorporated into the plasma membrane operated also as trimers, and to show the oligomeric organization of EAAT glutamate transporters in mammalian cell types and in native tissues. To answer the question of the stoichiometry of EAAT2 at the plasma membrane, experiments are in progress in our laboratory to radioiodinate the protein at the plasma membrane for subsequent visualization of its oligomeric state on BN-polyacrylamide gels.

After completing the experimental part of my thesis, I have evaluated the oligomeric state of hEAAT2 transporter stably expressed in tetracycline-induced HEK cells. The transporter was metabolically labeled with [$^{35}$S]Methionine, natively purified by nickel affinity chromatography and resolved by BN-PAGE. These recent experiments clearly showed that hEAAT2 subunits assemble efficiently into trimers also in a mammalian cell line. This observation strengthens the view that EAAT2 transporters are

trimers and that the information leading to trimer formation is inherent to the EAAT2 polypeptide itself and converted into structure independent of the expressing host cell.

# V/ Bibliography

Aizawa,H., Emori,Y., Mori,A., Murofushi,H., Sakai,H., and Suzuki,K. (1991). Functional analyses of the domain structure of microtubule-associated protein-4 (MAP-U). J. Biol. Chem. *266*, 9841-9846.

Alberts, B., Bray, D., Lewis, J., Raff, M., Roberts, K., and Watson, J. D. Molecular Biology of the Cell, 3rd edn. 1994.
Ref Type: Generic

Amersham Biosciences. The Recombinant Protein Handbook. 2001.
Ref Type: Generic

Attwell,D. and Laughlin,S.B. (2000). An energy budget for signalling in the grey matter of the brain. J. Physiol *525*, 61P.

Bauer,A. and Kuster,B. (2003). Affinity purification-mass spectrometry. Powerful tools for the characterization of protein complexes. European Journal of Biochemistry *270*, 570-578.

Beliveau,R., Demeule,M., Jette,M., and Potier,M. (1990). Molecular sizes of amino acid transporters in the luminal membrane from the kidney cortex, estimated by the radiation-inactivation method. Biochem. J. *268*, 195-200.

Berkelman, T. and Stenstedt, T. 2-D Electrophoresis using immobilized pH gradients, principles & methods. Amersham Biosciences . 1998.
Ref Type: Generic

Bieker,J.J. and Yazdani-Buicky,M. (1992). The multiple beta-tubulin genes of Xenopus: isolation and developmental expression of a germ-cell isotype beta-tubulin gene. Differentiation *50*, 15-23.

Blackman,S.M., Piston,D.W., and Beth,A.H. (1998). Oligomeric state of human erythrocyte band 3 measured by fluorescence resonance energy homotransfer. Biophys. J. *75*, 1117-1130.

Blank,V. and Andrews,N.C. (1997). The Maf transcription factors: regulators of differentiation. Trends Biochem. Sci. *22*, 437-441.

Blum,H., Beier,H., and Gross,H.J. (1987). Improved Silver Staining of Plant Proteins Rna and Dna in Polyacrylamide gels. Electrophoresis *8*, 93-99.

Bo,X., Schoepfer,R., and Burnstock,G. (2000). Molecular cloning and characterization of a novel ATP P2X receptor subtype from embryonic chick skeletal muscle. J. Biol. Chem. *275*, 14401-14407.

Bobanovic,L.K., Royle,S.J., and Murrell-Lagnado,R.D. (2002). P2X receptor trafficking in neurons is subunit specific. J. Neurosci. *22*, 4814-4824.

Boggs,J.M. and Rangaraj,G. (2000). Interaction of lipid-bound myelin basic protein with actin filaments and calmodulin. Biochemistry *39*, 7799-7806.

Boggs,J.M., Rangaraj,G., Koshy,K.M., and Mueller,J.P. (2000). Adhesion of acidic lipid vesicles by 21.5 kDa (recombinant) and 18.5 kDa isoforms of myelin basic protein. Biochim. Biophys. Acta *1463*, 81-87.

Boldt,W., Klapperstuck,M., Buttner,C., Sadtler,S., Schmalzing,G., and Markwardt,F. (2003). Glu496Ala polymorphism of human P2X7 receptor does not affect its electrophysiological phenotype. Am J Physiol Cell Physiol *284*, C749-C756.

Booth,R.F. and Clark,J.B. (1978). A rapid method for the preparation of relatively pure metabolically competent synaptosomes from rat brain. Biochem. J. *176*, 365-370.

Boue-Grabot,E., Archambault,V., and Seguela,P. (2000). A protein kinase C site highly conserved in P2X subunits controls the desensitization kinetics of P2X(2) ATP-gated channels. J. Biol. Chem. *275*, 10190-10195.

Brake,A.J., Wagenbach,M.J., and Julius,D. (1994). New structural motif for ligand-gated ion channels defined by an ionotropic ATP receptor. Nature *371*, 519-523.

Brändle,U., Spielmanns,P., Osteroth,R., Sim,J., Surprenant,A., Buell,G., Ruppersberg,J.P., Plinkert,P.K., Zenner,H.P., and Glowatzki,E. (1997). Desensitization of the P2X(2) receptor controlled by alternative splicing. FEBS Lett. *404*, 294-298.

Braun,K., Rettinger,J., Ganso,M., Kassack,M., Hildebrandt,C., Ullmann,H., Nickel,P., Schmalzing,G., and Lambrecht,G. (2001). NF449: a subnanomolar potency antagonist at recombinant rat P2X1 receptors. Naunyn Schmiedebergs Arch. Pharmacol. *364*, 285-290.

Busch,S.J. and Sassone-Corsi,P. (1990). Dimers, leucine zippers and DNA-binding domains. Trends Genet. *6*, 36-40.

Cammack,J.N. and Schwartz,E.A. (1996). Channel behavior in a gamma-aminobutyrate transporter. Proc. Natl. Acad. Sci. U. S. A *93*, 723-727.

Chang,G., Spencer,R.H., Lee,A.T., Barclay,M.T., and Rees,D.C. (1998). Structure of the MscL Homolog from Mycobacterium tuberculosis: A Gated Mechanosensitive Ion Channel. Science *282*, 2220-2226.

Chessell,I.P., Simon,J., Hibell,A.D., Michel,A.D., Barnard,E.A., and Humphrey,P.P. (1998). Cloning and functional characterisation of the mouse P2X7 receptor. FEBS Lett. *439*, 26-30.

Ciruela,F., Robbins,M.J., Willis,A.C., and McIlhinney,R.A. (1999). Interactions of the C terminus of metabotropic glutamate receptor type 1alpha with rat brain proteins: evidence for a direct interaction with tubulin. J. Neurochem. *72*, 346-354.

Collo,G., Neidhart,S., Kawashima,E., Kosco-Vilbois,M., North,R.A., and Buell,G. (1997). Tissue distribution of the P2X7 receptor. Neuropharmacology *36*, 1277-1283.

Collo,G., North,R.A., Kawashima,E., Merlo-Pich,E., Neidhart,S., Surprenant,A., and Buell,G. (1996). Cloning OF P2X5 and P2X6 receptors and the distribution and properties of an extended family of ATP-gated ion channels. J. Neurosci. *16*, 2495-2507.

Conradt,M. and Stoffel,W. (1995). Functional analysis of the high affinity, Na(+)-dependent glutamate transporter GLAST-1 by site-directed mutagenesis. J. Biol. Chem. *270*, 25207-25212.

Danbolt,N.C. (2001). Glutamate uptake. Prog. Neurobiol. *65*, 1-105.

Danbolt,N.C., Storm-Mathisen,J., and Kanner,B.I. (1992). An [Na+ + K+]coupled L-glutamate transporter purified from rat brain is located in glial cell processes. Neuroscience *51*, 295-310.

Deutsch,C. (2002). Potassium channel ontogeny. Annu. Rev. Physiol *64*, 19-46.

Ding,S. and Sachs,F. (1999). Single channel properties of P2X2 purinoceptors. J. Gen. Physiol *113*, 695-720.

Ding,S. and Sachs,F. (2000). Inactivation of P2X2 purinoceptors by divalent cations. J. Physiol *522 Pt 2*, 199-214.

Dunn,P.M. and Blakeley,A.G. (1988). Suramin: a reversible P2-purinoceptor antagonist in the mouse vas deferens. Br. J. Pharmacol. *93*, 243-245.

Emery,D.G. and Lucas,J.H. (1995). Ultrastructural damage and neuritic beading in cold-stressed spinal neurons with comparisons to NMDA and A23187 toxicity. Brain Res. *692*, 161-173.

Ennion,S.J. and Evans,R.J. (2002). Conserved cysteine residues in the extracellular loop of the human P2X(1) receptor form disulfide bonds and are involved in receptor trafficking to the cell surface. Mol. Pharmacol. *61*, 303-311.

Eskandari,S., Kreman,M., Kavanaugh,M.P., Wright,E.M., and Zampighi,G.A. (2000). Pentameric assembly of a neuronal glutamate transporter. Proc. Natl. Acad. Sci. U. S. A *97*, 8641-8646.

Eskandari,S., Wright,E.M., Kreman,M., Starace,D.M., and Zampighi,G.A. (1998). Structural analysis of cloned plasma membrane proteins by freeze-fracture electron microscopy. Proc. Natl. Acad. Sci. U. S. A *95*, 11235-11240.

Essrich,C., Lorez,M., Benson,J.A., Fritschy,J.M., and Luscher,B. (1998). Postsynaptic clustering of major GABAA receptor subtypes requires the gamma 2 subunit and gephyrin. Nat. Neurosci. *1*, 563-571.

Fairman,W.A., Vandenberg,R.J., Arriza,J.L., Kavanaugh,M.P., and Amara,S.G. (1995). An excitatory amino-acid transporter with properties of a ligand-gated chloride channel. Nature *375*, 599-603.

FERGUSON,K.A. (1964). STARCH-GEL ELECTROPHORESIS--APPLICATION TO THE CLASSIFICATION OF PITUITARY PROTEINS AND POLYPEPTIDES. Metabolism *13*, SUPPL-1002.

Galli,A., Jayanthi,L.D., Ramsey,I.S., Miller,J.W., Fremeau,R.T., Jr., and DeFelice,L.J. (1999). L-proline and L-pipecolate induce enkephalin-sensitive currents in human embryonic kidney 293 cells transfected with the high-affinity mammalian brain L-proline transporter. J. Neurosci. *19*, 6290-6297.

Galli,A., Petersen,C.I., deBlaquiere,M., Blakely,R.D., and DeFelice,L.J. (1997). Drosophila serotonin transporters have voltage-dependent uptake coupled to a serotonin-gated ion channel. J. Neurosci. *17*, 3401-3411.

Garcia-Guzman,M., Soto,F., Laube,B., and Stuhmer,W. (1996). Molecular cloning and functional expression of a novel rat heart P2X purinoceptor. FEBS Lett. *388*, 123-127.

Gloor,S., Pongs,O., and Schmalzing,G. (1995). A vector for the synthesis of cRNAs encoding Myc epitope-tagged proteins in Xenopus laevis oocytes. Gene *160*, 213-217.

Griffon,N., Buttner,C., Nicke,A., Kuhse,J., Schmalzing,G., and Betz,H. (1999). Molecular determinants of glycine receptor subunit assembly. EMBO J. *18*, 4711-4721.

Grunewald,M. and Kanner,B.I. (2000). The accessibility of a novel reentrant loop of the glutamate transporter GLT-1 is restricted by its substrate. J. Biol. Chem. *275*, 9684-9689.

Hastrup,H., Sen,N., and Javitch,J.A. (2003). The human dopamine transporter forms a tetramer in the plasma membrane: cross-linking of a

cysteine in the fourth transmembrane segment is sensitive to cocaine analogs. J. Biol. Chem. *C300349200*.

Haugeto,O., Ullensvang,K., Levy,L.M., Chaudhry,F.A., Honore,T., Nielsen,M., Lehre,K.P., and Danbolt,N.C. (1996). Brain glutamate transporter proteins form homomultimers. J. Biol. Chem. *271*, 27715-27722.

Hebert,D.N. and Carruthers,A. (1992). Glucose transporter oligomeric structure determines transporter function. Reversible redox-dependent interconversions of tetrameric and dimeric GLUT1. J. Biol. Chem. *267*, 23829-23838.

Hilgemann,D.W. and Lu,C.C. (1999). GAT1 (GABA:Na+:Cl-) cotransport function. Database reconstruction with an alternating access model. J. Gen. Physiol *114*, 459-475.

Hille,B. (1992). Ionic channels of excitable membranes. (Sunderland, MA: Sinauer Associates Inc. ).

Horiuchi,M., Nicke,A., Gomeza,J., Aschrafi,A., Schmalzing,G., and Betz,H. (2001). Surface-localized glycine transporters 1 and 2 function as monomeric proteins in Xenopus oocytes. Proc. Natl. Acad. Sci. U. S. A *98*, 1448-1453.

Hülsmann,M., Nickel,P., Kassack,M., Schmalzing,G., Lambrecht,G., and Markwardt,F. (2003). NF449, a novel picomolar potency antagonist at human P2X1 receptors. Eur J Pharmacol. *470*, 1-7.

Ikematsu,K., Tsuda,R., Kondo,T., and Nakasono,I. (2002). The expression of excitatory amino acid transporter 2 in traumatic brain injury. Forensic Sci. Int. *130*, 83-89.

Jackson,M., Song,W., Liu,M.Y., Jin,L., Dykes-Hoberg,M., Lin,C.I., Bowers,W.J., Federoff,H.J., Sternweis,P.C., and Rothstein,J.D. (2001). Modulation of the neuronal glutamate transporter EAAT4 by two interacting proteins. Nature *410*, 89-93.

Jess,U., Betz,H., and Schloss,P. (1996). The membrane-bound rat serotonin transporter, SERT1, is an oligomeric protein. FEBS Lett. *394*, 44-46.

Jiang,L.H., Kim,M., Spelta,V., Bo,X., Surprenant,A., and North,R.A. (2003). Subunit arrangement in P2X receptors. J. Neurosci. *23*, 8903-8910.

Jiang,L.H., Rassendren,F., Surprenant,A., and North,R.A. (2000). Identification of amino acid residues contributing to the ATP-binding site of a purinergic P2X receptor. J. Biol. Chem. *275*, 34190-34196.

Just,H., Sitte,H.H., Schmid,J.A., Freissmuth,M., and Kudlacek,O. (2004). Identification of an additional interaction domain in transmembrane domains 11 and 12 that supports oligomer formation in the human serotonin transporter. J. Biol. Chem. *279*, 6650-6657.

Kanai,Y. and Hediger,M.A. (1992). Primary structure and functional characterization of a high-affinity glutamate transporter. Nature *360*, 467-471.

Kanner,B.I., Kavanaugh,M.P., and Bendahan,A. (2001). Molecular characterization of substrate-binding sites in the glutamate transporter family. Biochem. Soc. Trans. *29*, 707-710.

Kanner,B.I. and Schuldiner,S. (1987). Mechanism of transport and storage of neurotransmitters. CRC Crit Rev. Biochem. *22*, 1-38.

Kassner,P.D., Conroy,W.G., and Berg,D.K. (1998). Organizing Effects of Rapsyn on Neuronal Nicotinic Acetylcholine Receptors. Mol. Cell Neurosci. *10*, 258-270.

Kavanaugh,M.P. (1999). Glutamate transporters in brain: new complexities in structure and function. J. Neurochem. *73*, S7B.

Khakh,B.S., Smith,W.B., Chiu,C.S., Ju,D., Davidson,N., and Lester,H.A. (2001). Activation-dependent changes in receptor distribution and dendritic morphology in hippocampal neurons expressing P2X2-green fluorescent protein receptors. Proc. Natl. Acad. Sci. U. S. A *98*, 5288-5293.

Kilic,F. and Rudnick,G. (2000). Oligomerization of serotonin transporter and its functional consequences. Proc. Natl. Acad. Sci. U. S. A *97*, 3106-3111.

Kim,M., Jiang,L.H., Wilson,H.L., North,R.A., and Surprenant,A. (2001). Proteomic and functional evidence for a P2X7 receptor signalling complex. EMBO J. *20*, 6347-6358.

Kim,M., Yoo,O.J., and Choe,S. (1997). Molecular assembly of the extracellular domain of P2X2, an ATP-gated ion channel. Biochem. Biophys. Res. Commun. *240*, 618-622.

King,B.F., Ziganshina,L.E., Pintor,J., and Burnstock,G. (1996). Full sensitivity of P2X2 purinoceptor to ATP revealed by changing extracellular pH. Br. J. Pharmacol. *117*, 1371-1373.

Kirsch,J. and Betz,H. (1993). Widespread expression of gephyrin, a putative glycine receptor-tubulin linker protein, in rat brain. Brain Res. *621*, 301-310.

Kirsch,J., Langosch,D., Prior,P., Littauer,U.Z., Schmitt,B., and Betz,H. (1991). The 93-kDa glycine receptor-associated protein binds to tubulin. J. Biol. Chem. *266*, 22242-22245.

Kittler,J.T., Rostaing,P., Schiavo,G., Fritschy,J.M., Olsen,R., Triller,A., and Moss,S.J. (2001). The subcellular distribution of GABARAP and its ability to interact with NSF suggest a role for this protein in the intracellular transport of GABA(A) receptors. Mol. Cell Neurosci. *18*, 13-25.

Klapperstuck,M., Buttner,C., Bohm,T., Schmalzing,G., and Markwardt,F. (2000). Characteristics of P2X7 receptors from human B lymphocytes expressed in Xenopus oocytes. Biochim. Biophys. Acta *1467*, 444-456.

Kneussel,M. and Betz,H. (2000). Clustering of inhibitory neurotransmitter receptors at developing postsynaptic sites: the membrane activation model. Trends Neurosci. *23*, 429-435.

Kneussel,M., Haverkamp,S., Fuhrmann,J.C., Wang,H., Wassle,H., Olsen,R.W., and Betz,H. (2000). The gamma-aminobutyric acid type A receptor (GABAAR)-associated protein GABARAP interacts with gephyrin but is not involved in receptor anchoring at the synapse. Proc. Natl. Acad. Sci. U. S. A *97*, 8594-8599.

Koshimizu,T., Tomic,M., Van Goor,F., and Stojilkovic,S.S. (1998). Functional role of alternative splicing in pituitary P2X2 receptor-channel activation and desensitization. Mol. Endocrinol. *12*, 901-913.

Lambrecht,G. (2000). Agonists and antagonists acting at P2X receptors: selectivity profiles and functional implications. Naunyn Schmiedebergs Arch. Pharmacol. *362*, 340-350.

Lambrecht,G., Friebe,T., Grimm,U., Windscheif,U., Bungardt,E., Hildebrandt,C., Baumert,H.G., Spatz-Kumbel,G., and Mutschler,E. (1992). PPADS, a novel functionally selective antagonist of P2 purinoceptor-mediated responses. Eur. J. Pharmacol. *217*, 217-219.

Laube,B., Kuhse,J., and Betz,H. (1998). Evidence for a tetrameric structure of recombinant NMDA receptors. J. Neurosci. *18*, 2954-2961.

Levy,L.M., Attwell,D., Hoover,F., Ash,J.F., Bjoras,M., and Danbolt,N.C. (1998). Inducible expression of the GLT-1 glutamate transporter in a CHO cell line selected for low endogenous glutamate uptake. FEBS Lett. *422*, 339-342.

Lewis,C., Neidhart,S., Holy,C., North,R.A., Buell,G., and Surprenant,A. (1995). Coexpression of P2X2 and P2X3 receptor subunits can account for ATP-gated currents in sensory neurons. Nature *377*, 432-435.

Li,C., Peoples,R.W., and Weight,F.F. (1997). Mg2+ inhibition of ATP-activated current in rat nodose ganglion neurons: evidence that Mg2+

decreases the agonist affinity of the receptor. J. Neurophysiol. *77*, 3391-3395.

Li,X.D., Villa,A., Gownley,C., Kim,M.J., Song,J., Auer,M., and Wang,D.N. (2001). Monomeric state and ligand binding of recombinant GABA transporter from Escherichia coli. FEBS Lett. *494*, 165-169.

Lin,C.I., Orlov,I., Ruggiero,A.M., Dykes-Hoberg,M., Lee,A., Jackson,M., and Rothstein,J.D. (2001). Modulation of the neuronal glutamate transporter EAAC1 by the interacting protein GTRAP3-18. Nature *410*, 84-88.

Lin,F., Lester,H.A., and Mager,S. (1996). Single-channel currents produced by the serotonin transporter and analysis of a mutation affecting ion permeation. Biophys. J. *71*, 3126-3135.

Lolkema,J.S. and Slotboom,D.J. (1998). Estimation of structural similarity of membrane proteins by hydropathy profile alignment. Mol. Membr. Biol. *15*, 33-42.

Lynch,K.J., Touma,E., Niforatos,W., Kage,K.L., Burgard,E.C., van Biesen,T., Kowaluk,E.A., and Jarvis,M.F. (1999). Molecular and functional characterization of human P2X(2) receptors. Mol. Pharmacol. *56*, 1171-1181.

Maccioni,R.B. and Cambiazo,V. (1995). Role of microtubule-associated proteins in the control of microtubule assembly. Physiol Rev. *75*, 835-864.

Mager,S., Min,C., Henry,D.J., Chavkin,C., Hoffman,B.J., Davidson,N., and Lester,H.A. (1994). Conducting states of a mammalian serotonin transporter. Neuron *12*, 845-859.

Marie,H., Billups,D., Bedford,F.K., Attwell,D., and Moss,S.J. (2000). Characterization of the interaction between the LIM protein Ajuba and the glial glutamate transporter GLT-1, in COS cells and bipolar cells in slices of rat retina. J. Physiol *525*, 61P.

Martinez-Lopez,I., Garcia,C., Barber,T., Vina,J.R., and Miralles,V.J. (1998). The L-glutamate transporters GLAST (EAAT1) and GLT-1 (EAAT2): expression and regulation in rat lactating mammary gland. Mol. Membr. Biol. *15*, 237-242.

Masson,J., Sagne,C., Hamon,M., and El Mestikawy,S. (1999). Neurotransmitter transporters in the central nervous system. Pharmacol. Rev. *51*, 439-464.

Matthews,J.C., Beveridge,M.J., Malandro,M.S., Rothstein,J.D., Campbell-Thompson,M., Verlander,J.W., Kilberg,M.S., and Novak,D.A. (1998). Activity and protein localization of multiple glutamate transporters in gestation day 14 vs. day 20 rat placenta. Am. J. Physiol *274*, C603-C614.

Mayer,B.J. (2001). SH3 domains: complexity in moderation. J. Cell Sci. *114*, 1253-1263.

McPherson,P.S., Czernik,A.J., Chilcote,T.J., Onofri,F., Benfenati,F., Greengard,P., Schlessinger,J., and De Camilli,P. (1994). Interaction of Grb2 via its Src homology 3 domains with synaptic proteins including synapsin I. Proc. Natl. Acad. Sci. U. S. A *91*, 6486-6490.

Nakazawa,K., Fujimori,K., Takanaka,A., and Inoue,K. (1990). An ATP-activated conductance in pheochromocytoma cells and its suppression by extracellular calcium. J. Physiol *428*, 257-272.

Newbolt,A., Stoop,R., Virginio,C., Surprenant,A., North,R.A., Buell,G., and Rassendren,F. (1998). Membrane topology of an ATP-gated ion channel (P2X receptor). J. Biol. Chem. *273*, 15177-15182.

Nicke,A., Baumert,H.G., Rettinger,J., Eichele,A., Lambrecht,G., Mutschler,E., and Schmalzing,G. (1998). P2X1 and P2X3 receptors form stable trimers: a novel structural motif of ligand-gated ion channels. EMBO J. *17*, 3016-3028.

Nicke,A., Rettinger,J., Buttner,C., Eichele,A., Lambrecht,G., and Schmalzing,G. (1999). Evolving view of quaternary structures of ligand-gated ion channels. Prog. Brain Res. *120*, 61-80.

Nicke,A., Rettinger,J., and Schmalzing,G. (2003). Monomeric and dimeric byproducts are the principal functional elements of higher order P2X1 concatamers. Mol. Pharmacol. *63*, 243-252.

Norgaard-Nielsen,K., Norregaard,L., Hastrup,H., Javitch,J.A., and Gether,U. (2002). Zn(2+) site engineering at the oligomeric interface of the dopamine transporter. FEBS Lett. *524*, 87-91.

North,R.A. (2002). Molecular physiology of P2X receptors. Physiol Rev. *82*, 1013-1067.

Parker,K.E. (1998). Modulation of ATP-gated non-selective cation channel (P2X1 receptor) activation and desensitization by the actin cytoskeleton. J. Physiol *510 ( Pt 1)*, 19-25.

Phizicky,E., Bastiaens,P.I., Zhu,H., Snyder,M., and Fields,S. (2003). Protein analysis on a proteomic scale. Nature *422*, 208-215.

Pines,G., Danbolt,N.C., Bjoras,M., Zhang,Y., Bendahan,A., Eide,L., Koepsell,H., Storm-Mathisen,J., Seeberg,E., and Kanner,B.I. (1992). Cloning and expression of a rat brain L-glutamate transporter. Nature *360*, 464-467.

Poduslo,J.F. (1981). Glycoprotein molecular-weight estimation using sodium dodecyl sulfate-pore gradient electrophoresis: comparison of tris-

glycine and tris-borate-EDTA buffer systems. Anal. Biochem. *114*, 131-139.

Ralevic,V. and Burnstock,G. (1998). Receptors for purines and pyrimidines. Pharmacol. Rev. *50*, 413-492.

Ramsey,I.S. and DeFelice,L.J. (2002). Serotonin transporter function and pharmacology are sensitive to expression level: evidence for an endogenous regulatory factor. J. Biol. Chem. *277*, 14475-14482.

Rassendren,F., Buell,G.N., Virginio,C., Collo,G., North,R.A., and Surprenant,A. (1997). The permeabilizing ATP receptor, P2X7. Cloning and expression of a human cDNA. J. Biol. Chem. *272*, 5482-5486.

Rauen,T. (2000). Diversity of glutamate transporter expression and function in the mammalian retina. Amino. Acids *19*, 53-62.

Rettinger,J., Aschrafi,A., and Schmalzing,G. (2000a). Roles of individual N-glycans for ATP potency and expression of the rat P2X1 receptor. J. Biol. Chem. *275*, 33542-33547.

Rettinger,J. and Schmalzing,G. (2003). Activation and desensitization of the recombinant P2X1 receptor at nanomolar ATP concentrations. J Gen. Physiol *121*, 451-461.

Rettinger,J. and Schmalzing,G. (2004). Desensitization Masks Nanomolar Potency of ATP for the P2X1 Receptor. J Biol. Chem. *279*, 6426-6433.

Rettinger,J., Schmalzing,G., Damer,S., Muller,G., Nickel,P., and Lambrecht,G. (2000b). The suramin analogue NF279 is a novel and potent antagonist selective for the P2X(1) receptor. Neuropharmacology *39*, 2044-2053.

Rothstein,J.D., Dykes-Hoberg,M., Pardo,C.A., Bristol,L.A., Jin,L., Kuncl,R.W., Kanai,Y., Hediger,M.A., Wang,Y., Schielke,J.P., and Welty,D.F. (1996). Knockout of glutamate transporters reveals a major role for astroglial transport in excitotoxicity and clearance of glutamate. Neuron *16*, 675-686.

Rothstein,J.D., Martin,L.J., and Kuncl,R.W. (1992). Decreased glutamate transport by the brain and spinal cord in amyotrophic lateral sclerosis. N. Engl. J. Med. *326*, 1464-1468.

Rothstein,J.D., Van Kammen,M., Levey,A.I., Martin,L.J., and Kuncl,R.W. (1995). Selective loss of glial glutamate transporter GLT-1 in amyotrophic lateral sclerosis. Ann. Neurol. *38*, 73-84.

Rotin,D., Bar-Sagi,D., O'Brodovich,H., Merilainen,J., Lehto,V.P., Canessa,C.M., Rossier,B.C., and Downey,G.P. (1994). An SH3 binding region in the epithelial Na+ channel (alpha rENaC) mediates its localization at the apical membrane. EMBO J. *13*, 4440-4450.

Ruppelt,A., Ma,W., Borchardt,K., Silberberg,S.D., and Soto,F. (2001). Genomic structure, developmental distribution and functional properties of the chicken P2X(5) receptor. J. Neurochem. *77*, 1256-1265.

Sahin-Toth,M., Lawrence,M.C., and Kaback,H.R. (1994). Properties of permease dimer, a fusion protein containing two lactose permease molecules from Escherichia coli. Proc. Natl. Acad. Sci. U. S. A *91*, 5421-5425.

Saint,N., Lacapere,J.J., Gu,L.Q., Ghazi,A., Martinac,B., and Rigaud,J.L. (1998). A Hexameric Transmembrane Pore Revealed by Two-dimensional Crystallization of the Large Mechanosensitive Ion Channel (MscL) of Escherichia coli. J. Biol. Chem. *273*, 14667-14670.

Schägger,H., Cramer,W.A., and von Jagow,G. (1994). Analysis of molecular masses and oligomeric states of protein complexes by blue native electrophoresis and isolation of membrane protein complexes by two-dimensional native electrophoresis. Anal. Biochem. *217*, 220-230.

Schägger,H. and von Jagow,G. (1987). Tricine-sodium dodecyl sulfate-polyacrylamide gel electrophoresis for the separation of proteins in the range from 1 to 100 kDa. Anal. Biochem. *166*, 368-379.

Schägger,H. and von Jagow,G. (1991). Blue native electrophoresis for isolation of membrane protein complexes in enzymatically active form. Anal. Biochem. *199*, 223-231.

Schmalzing,G. (1985). Mechanism of depolarization of rat cortical synaptosomes at submicromolar external Ca2+ activity. The use of Ca2+ buffers to control the synaptosomal membrane potential. Biochem. J. *225*, 671-680.

Schmid,J.A., Scholze,P., Kudlacek,O., Freissmuth,M., Singer,E.A., and Sitte,H.H. (2001). Oligomerization of the human serotonin transporter and of the rat GABA transporter 1 visualized by fluorescence resonance energy transfer microscopy in living cells. J. Biol. Chem. *276*, 3805-3810.

Schmidt,G., Goehring,U.M., Schirmer,J., Lerm,M., and Aktories,K. (1999). Identification of the C-terminal part of Bordetella dermonecrotic toxin as a transglutaminase for rho GTPases. J. Biol. Chem. *274*, 31875-31881.

Scholze,P., Freissmuth,M., and Sitte,H.H. (2002). Mutations within an intramembrane leucine heptad repeat disrupt oligomer formation of the rat GABA transporter 1. J. Biol. Chem. *277*, 43682-43690.

Scott,H.L., Tannenberg,A.E., and Dodd,P.R. (1995). Variant forms of neuronal glutamate transporter sites in Alzheimer's disease cerebral cortex. J. Neurochem. *64*, 2193-2202.

Seal,R.P. and Amara,S.G. (1999). Excitatory amino acid transporters: a family in flux. Annu. Rev. Pharmacol. Toxicol. *39*, 431-456.

Seal,R.P., Leighton,B.H., and Amara,S.G. (2000). A model for the topology of excitatory amino acid transporters determined by the extracellular accessibility of substituted cysteines. Neuron *25*, 695-706.

Seal,R.P., Shigeri,Y., Eliasof,S., Leighton,B.H., and Amara,S.G. (2001). Sulfhydryl modification of V449C in the glutamate transporter EAAT1 abolishes substrate transport but not the substrate-gated anion conductance. Proc. Natl. Acad. Sci. U. S. A *98*, 15324-15329.

Shi,S.H., Hayashi,Y., Petralia,R.S., Zaman,S.H., Wenthold,R.J., Svoboda,K., and Malinow,R. (1999). Rapid spine delivery and redistribution of AMPA receptors after synaptic NMDA receptor activation. Science *284*, 1811-1816.

Simon,J., Kidd,E.J., Smith,F.M., Chessell,I.P., Murrell-Lagnado,R., Humphrey,P.P., and Barnard,E.A. (1997). Localization and functional expression of splice variants of the P2X2 receptor. Mol. Pharmacol. *52*, 237-248.

Slotboom,D.J., Konings,W.N., and Lolkema,J.S. (1999). Structural features of the glutamate transporter family. Microbiol. Mol. Biol. Rev. *63*, 293-307.

Slotboom,D.J., Konings,W.N., and Lolkema,J.S. (2001a). Cysteine-scanning mutagenesis reveals a highly amphipathic, pore-lining membrane-spanning helix in the glutamate transporter GltT. J. Biol. Chem. *276*, 10775-10781.

Slotboom,D.J., Konings,W.N., and Lolkema,J.S. (2001b). The structure of glutamate transporters shows channel-like features. FEBS Lett. *492*, 183-186.

Smith,F.M., Humphrey,P.P., and Murrell-Lagnado,R.D. (1999). Identification of amino acids within the P2X2 receptor C-terminus that regulate desensitization. J. Physiol *520 Pt 1*, 91-99.

Spooner,P.J., Friesen,R.H., Knol,J., Poolman,B., and Watts,A. (2000). Rotational mobility and orientational stability of a transport protein in lipid membranes. Biophys. J. *79*, 756-766.

Storck,T., Schulte,S., Hofmann,K., and Stoffel,W. (1992). Structure, expression, and functional analysis of a Na(+)-dependent glutamate/aspartate transporter from rat brain. Proc. Natl. Acad. Sci. U. S. A *89*, 10955-10959.

Surprenant,A., Rassendren,F., Kawashima,E., North,R.A., and Buell,G. (1996). The cytolytic P2Z receptor for extracellular ATP identified as a P2X receptor (P2X7). Science *272*, 735-738.

Tanaka,K., Watase,K., Manabe,T., Yamada,K., Watanabe,M., Takahashi,K., Iwama,H., Nishikawa,T., Ichihara,N., Kikuchi,T., Okuyama,S., Kawashima,N., Hori,S., Takimoto,M., and Wada,K. (1997). Epilepsy and exacerbation of brain injury in mice lacking the glutamate transporter GLT-1. Science *276*, 1699-1702.

Taylor, M. E. and Drickamer, K. Introduction to Glycobiology. 2003. Oxford University Press.
Ref Type: Generic

Torp,R., Danbolt,N.C., Babaie,E., Bjoras,M., Seeberg,E., Storm-Mathisen,J., and Ottersen,O.P. (1994). Differential expression of two glial glutamate transporters in the rat brain: an in situ hybridization study. Eur. J. Neurosci. *6*, 936-942.

Torres,G.E., Egan,T.M., and Voigt,M.M. (1998a). N-Linked glycosylation is essential for the functional expression of the recombinant P2X2 receptor. Biochemistry *37*, 14845-14851.

Torres,G.E., Egan,T.M., and Voigt,M.M. (1998b). Topological analysis of the ATP-gated ionotropic [correction of ionotrophic] P2X2 receptor subunit. FEBS Lett. *425*, 19-23.

Vallee,R.B. (1986). Purification of brain microtubules and microtubule-associated protein 1 using taxol. Methods Enzymol. *134*, 104-115.

van Rossum,D., Kuhse,J., and Betz,H. (1999b). Dynamic interaction between soluble tubulin and C-terminal domains of N-methyl-D-aspartate receptor subunits. J. Neurochem. *72*, 962-973.

van Rossum,D., Kuhse,J., and Betz,H. (1999a). Dynamic interaction between soluble tubulin and C-terminal domains of N-methyl-D-aspartate receptor subunits. J. Neurochem. *72*, 962-973.

Veenhoff,L.M., Heuberger,E.H., and Poolman,B. (2002). Quaternary structure and function of transport proteins. Trends Biochem. Sci. *27*, 242-249.

Virginio,C., Church,D., North,R.A., and Surprenant,A. (1997). Effects of divalent cations, protons and calmidazolium at the rat P2X7 receptor. Neuropharmacology *36*, 1285-1294.

Virginio,C., MacKenzie,A., North,R.A., and Surprenant,A. (1999). Kinetics of cell lysis, dye uptake and permeability changes in cells expressing the rat P2X7 receptor. J. Physiol *519 Pt 2*, 335-346.

Wadiche,J.I., Amara,S.G., and Kavanaugh,M.P. (1995). Ion fluxes associated with excitatory amino acid transport. Neuron *15*, 721-728.

Wang,H., Bedford,F.K., Brandon,N.J., Moss,S.J., and Olsen,R.W. (1999). GABA(A)-receptor-associated protein links GABA(A) receptors and the cytoskeleton. Nature *397*, 69-72.

Wang,H. and Olsen,R.W. (2000). Binding of the GABA(A) receptor-associated protein (GABARAP) to microtubules and microfilaments suggests involvement of the cytoskeleton in GABARAPGABA(A) receptor interaction. J. Neurochem. *75*, 644-655.

Welbourne,T.C. and Matthews,J.C. (1999). Glutamate transport and renal function. Am. J. Physiol *277*, F501-F505.

Wilson,R. and Brophy,P.J. (1989). Role for the oligodendrocyte cytoskeleton in myelination. J. Neurosci. Res. *22*, 439-448.

Yang,A.S. and Honig,B. (2000). An integrated approach to the analysis and modeling of protein sequences and structures. II. On the relationship between sequence and structural similarity for proteins that are not obviously related in sequence. J. Mol. Biol. *301*, 679-689.

Yernool,D., Boudker,O., Folta-Stogniew,E., and Gouaux,E. (2003). Trimeric Subunit Stoichiometry of the Glutamate Transporters from Bacillus caldotenax and Bacillus stearothermophilus. Biochemistry *42*, 12981-12988.

Yin,C.C., Aldema-Ramos,M.L., Borges-Walmsley,M.I., Taylor,R.W., Walmsley,A.R., Levy,S.B., and Bullough,P.A. (2000). The quarternary molecular architecture of TetA, a secondary tetracycline transporter from Escherichia coli. Mol. Microbiol. *38*, 482-492.

Zerangue,N. and Kavanaugh,M.P. (1996). Flux coupling in a neuronal glutamate transporter. Nature *383*, 634-637.

Zhao,Z., Lim,L., and Manser,E. (2001). Blot overlays with 32P-labeled fusion proteins. Methods *24*, 194-200.

Zhou,Z. and Hume,R.I. (1998). Two mechanisms for inward rectification of current flow through the purinoceptor P2X2 class of ATP-gated channels. J. Physiol *507 ( Pt 2)*, 353-364.

# VI/ Appendix

## VI-1. Abbreviations

| | |
|---|---|
| AD | Alzheimer's disease |
| ALS | Amyotrophic lateral sclerosis |
| APS | Ammonium persulfate |
| BN | Blue native |
| BSA | Bovine serum albumine |
| BzATP | 2',3'-(benzoyl-4-benzoyl)-ATP |
| CBP | Calmoduline binding peptide |
| CNS | Central nervous system |
| 2D | two-dimensional |
| DDM | Dodecylmaltoside |
| DMA | Dimethyl adipimidate•2 HCl |
| DMS | Dimethyl suberimidate•2 HCl |
| DNA | Deoxyribonucleic acid |
| DTSSP | 3,3'-Dithiobis(sulfosuccinimidylpropionate) |
| DTT | Dithiothreitol |
| EAAT | Excitatory amino acid transporter |
| ec | Escherichia coli |
| ECL | enhanced chemiluminescence |
| EDTA | Ethylene Diamine Tetraacetic Acid |
| EGFP | Enhanced Green Fluorescent Protein |
| EndoH | Endoglycosidase H |
| ER | Endoplasmic reticulum |
| FRET | Fluorescence resonance energy transfer |
| GFP | Green fluorescent protein |
| Glu | Glutamate |
| GST | Glutathione S-transferase |
| GTP | Guanosine 5'-triphosphate |
| h | human |
| HEK293 | Human embryonic kidney cell 293 |
| His | Histidine |
| HRP | Horseradish peroxydase |
| 5-HT | Serotonin |
| IP | Immunoprecipitation |
| IPTG | Isopropyl ß-D-thiogalactopyranoside |
| KB | kilobases |
| kDa | kiloDalton |
| LB | Luria Bertoni |
| LGICs | Ligand-gated ion channels |
| MALDI | Matrix-assisted laser desorption ionisation |
| MBP | Myelin basic protein |
| MW | Molecular weight marker |
| N | Asparagine |
| NTA | Nitrilotriacetic acid |

| | |
|---|---|
| dNTPs | deoxyribonucleosides triphosphate |
| NTR | Non translated region |
| PAGE | Polyacrylamide gel electrophoresis |
| PC12 | Pheochromocytoma cell |
| PCR | Polymerase chain reaction |
| PDI | Protein disulfide isomerase |
| PKA | Protein kinase A |
| PKC | Protein kinase C |
| PNGase F | Peptide N-glycosidase F |
| PVDF | Polyvinylidene difluoride |
| r | rat |
| RNA | Ribonucleic acid |
| rpm | rounds per minutes |
| S | Sulfur |
| SDS | Sodium dodecyl sulfate |
| SH | Sulfhydryl |
| SRP | Signal-recognition particle |
| TAP | Tandem affinity purification |
| TBST | Tris-buffer Saline-Tween |
| TCA | Tri-Chloro-acetic acid |
| TE-buffer | Tris-EDTA-buffer |
| TEV | Tobacco etch virus |
| TM | Transmembrane |
| TOF | Time of Flight |
| v | volume |
| w | weight |
| WT | Wild type |

# VI-2. Constructs and primers

## 2.1 DNA constructs

| Name | Contruct | Cloning | Primers |
|---|---|---|---|
| Rat $P2X_2$Cterm | 1029 in PGEX 2T | 5´BamHI | 943:AAAGGATCCATGAACAAAAACAAGCTCTACAGCCATAAGAA |
| | | 3´EcoRI | 944 :AAAGAATTCTTATCAAAGTTGGGCCAAACCTTTGGG |
| Rat $P2X_5$Cterm | 1030 in PGEX 2T | 5´BamHI | 951 :AAAGGATCCATGAGGAAGAGTGAGTTTTACCGAGACAAGAAGTTT |
| | | 3´EcoRI | 952 :AAAGAATTCTTACTACGTCTTCACTGGATGCAAGATCTGTGA |
| Rat $P2X_7$Cterm | 1032 in PGEX 2T | 5´BamHI | 1037:AAAGGATCCCAGACGGACTTCTTGGAACTGTCTAGGCTC |
| | | 3´EcoRI | 1068:AAAGAATTCTTATCAGTAGGGATACTTGAAGCCACTGTACTGCC |
| Tubulin | 1062 in PNKS 4 | 5´Aat II | 1128:AAAAAGACGTCGAAGTAGCCACCATGAGGGAAATCGTGCACATCC AGG |
| | | 3´EcoRI | 1129:AAAAAGAATTCTGCTCATTATGCCTCTTCTTCTGCCTCCTCTCCGAA ATCC |
| His-Tubulin | 1063 in PNKS 4 | Mutagenesis | 1171:GAAGTAGCCACCATGCATCATCATCATCATCATAGGGAAATCGTGC AC |
| | | | 1172:GTGCACGATTTCCCTATGATGATGATGATGATGCATGGTGGCTACT TC |
| Calmodulin | 1052 in PNKS 4 | 5´Nco I | 1105:TTAAAAGCTCGCACCATGGCTGATCAGCTGACTGAA |
| | | 3´Xba I | 1106:TTTTCTAGAGGTCTTCATTTTGCAGTCATCATCTGTACGAATTCTTC ATAGTTG |
| His-Calmodulin | 1077 in PNKS 4 | Mutagenesis | 1143:CGAAGTAGCCACCATGCATCATCATCATCATCATGCTGATCAGCTG ACTG |
| | | | 1144:CAGTCAGCTGATCAGCATGATGATGATGATGATGCATGGTGGCTA CTTCG |
| GST-$P2X_2^{406-472}$ | 1064 in PGEX 2T | 5´BamHI | 1130:AAAGGATCCCCATCAGGTGAAGGACCAACTTTGG |
| | | 3´EcoRI | 944 |
| GST-$P2X_2^{356-412}$ | 1065 in PGEX 2T | 5´BamHI | 943 |
| | | 3´EcoRI | 1140:AAAGAATTCTTATCATGGTCCTTCACCTGATGGAGGG |
| GST-$P2X_2^{356-381}$ | 1132 in PGEX 2T | 5´BamHI | 1183:CATCCCTCAAGTAGATGGCCTTAGAAGCTTGCCCTTGTCTTGGG |
| | | 3´EcoRI | 1184:CCCAAGACAAGGGCAAGCTTCTAAGGCCATCTACTTGAGGGATG |
| GST-$P2X_2^{371-412}$ | 1147 in PGEX 2T | 5´BamHI | 1205:AAAGGATCCACTCCAAAGCATCCCTCAAGTAGATGGCCTG |
| | | 3´EcoRI | 1206:AAAGAATTCTTATCATGGTCCTTCACCTGATGGAGGGCTGGGTG |
| GST-$P2X_2^{371-472}$ | 1152 in PGEX 2T | 5´BamHI | 944 |
| | | 3´EcoRI | 1205:AAAGGATCCACTCCAAAGCATCCCTCAAGTAGATGGCCTG |
| GST-$P2X_2^{371-390}$ | 1181 in PGEX 2T | 5´BamHI | 1205 |
| | | 3´EcoRI | 1263:AAAGAATTCTTATCAGATCTGGCCCAAGACAAGGGCAAGGGTC |
| GST-$P2X_2^{391-412}$ | 1180 in PGEX 2T | 5´BamHI | 1206 |
| | | 3´EcoRI | 1262:AAAGGATCCCCTCCCCCACCTAGTCACTACTCCCAG |
| Rapsyn | 1116 in PNKS2 | 5´AatII | 1166:AAAAAGACGTCGGCTTGGGGAGGATGGGGCAGGAC |
| | | 3´EcoRI | 1167:AAAAAGAATTCTGCTTATCATACAAATCCAGGCTTCATGGAGGAGC GG |
| His-$P2X_{2a}$ | 0849 in PNKS2 | 5´AatII | |
| | | 3´EcoRI | |
| His-$P2X_1$-GFP+AatII | 1179 in PNKS2 | 3´EcoRI | 1260: CACTATAGAATAAAAGCTTGGACGTCTGCAGGTCGACTCTAGAGG |
| | | 3´EcoRI | 1261: CCTCTAGAGTCGACCTGCAGACGTCCAAGCTTTTATTCTATAGTG |
| His-$P2X_{2a}$-GFP | 1218 in PNKS2 | AatII | Ligation in 1179=862 ($P2X_1$-GFP)+AatII |
| | | AccI/NarI | |
| His-$P2X_{2a}$+BsrGI | 1194 in PNKS2 | 5´AatII | 1278:GTTCATGAACAAAAACAAGCTGTACAGCCATAAGAAGTTCG |
| | | 3´EcoRI | 1279:CGAACTTCTTATGGCTGTACAGCTTGTTTTTGTTCATGAAC |
| His-$P2X_{2b}$ | 1195 in PNKS2 | 5´AatII | Digestion of 1194 with BsrGI and NdeI; Ligation with the primers 1298-1299 |
| | | 3´EcoRI | 1298GTACAGCCATAAGAAGTTCGACAAGGTGGTCGACACACTTGGCCAG CA: |
| | | | 1299:TATGCTGGCCAAGTGTGTCGACCACCTTGTCGAACTTCTTATGGCT |
| His-$P2X_{2a}$-GFP+BsrGI | 1680 in PNKS2 | 5´AatII | 1278:GTTCATGAACAAAAACAAGCTGTACAGCCATAAGAAGTTCG |
| | | 3´EcoRI | 1279:CGAACTTCTTATGGCTGTACAGCTTGTTTTTGTTCATGAAC |
| His-$P2X_{2a}$-GFPΔBsrGI | 1681 in PNKS2 | 5´AatII | 1880:GCATGGACGAGCTGTATAAGTCCGGACTCAG |
| | | 3´EcoRI | 1881:CTGAGTCCGGACTTATACAGCTCGTCCATGC |
| His-$P2X_{2b}$-GFP | 1682 in PNKS2 | 5´AatII | Digestion of 1681 with BsrGI and NdeI |
| | | 3´EcoRI | Ligation with the primers 1298-1299 |
| TetA(B) | 1722 in PNKS4 | 5´AatII | 1934:AAAAAAGACGTCGAAGTAGCCACCATGAATAGTTCGACAAAGATC GCATTGG |
| | | 3' XbaI | 1935: AAAAAATCTAGATGGCTTCAAGCACTTGTCTCCTGTTTACTCCCCT |
| TetA(B)-His | 1723 in PNKS4 | Mutagenesis | 1936:CAGGAGACAAGTGCTCACCATCACCATCACCATTGAAGCCATCTAG ACTAG |

| | | | |
|---|---|---|---|
| TetA(B)-His | 1723 in PNKS4 | Mutagenesis | 1937:CTAGTCTAGATGGCTTCAATGGTGATGGTGATGGTGAGCACTTGT CTCCTG |

## 2.2 Primer used for sequencing

| Plasmid/construct | Region | Primers |
|---|---|---|
| pGEX-2T | 5′ NTR | 1246: GGGCTGGCAAGCCACGTTTGGTG |
| | 3′ NTR | 1247: CCGGGAGCTGCATGTGTCAGAGG |
| pNKS | 5′ NTR | 1103: CACATACGATTTAGGTGACACTATAG |
| | 3′ NTR | 900: TATTCCGTTTTTGTTTTGGGAC |
| Tubulin in PNKS4 (1062) | 1012-1032 bp | 1147: CTACCTCCTTCATGGACATCC reverse primer |
| | 330-347 bp | 1148: GGTCAGTCTGGGGCAGGC |
| GFP | 5′ GFP | 1314: CTCGACCAGGATGGGCAC intern GFP – reverse primer |

# VII/ Summary

Reliable communication in the central nervous system requires the precise control of the duration and the intensity of neurotransmitter action at specific molecular targets. After their release at the synapse, neurotransmitters activate pre- and/or postsynaptic receptors. To terminate synaptic transmission, neurotransmitters are in turn inactivated by either enzymatic degradation or active uptake into neuronal and/or glial cells by neurotransmitter transporters. In the present study, two types of membrane proteins involved in transcellular signal transduction were investigated, the P2X receptors, which are ATP-gated ion channels and the glutamate transporters of the EAAT family.

The first part of this study is concerned with the targeting and anchoring of P2X receptors at specific locations. P2X receptors play a role of fast excitatory neurotransmission to extracellular ATP in both the peripheral and central nervous system. For several ligand-gated ion channel, like glycine receptors or nicotinic acetylcholine receptors, it is known that specific binding proteins exist, which are involved in receptor trafficking and anchoring of the receptors at appropriate sites on the synapse. Within the P2X family, amino acid homology is scattered over the protein sequence excepted of the cytoplasmic C-terminal tails, which do not share significant sequence similarity, indicating that they might provide peculiar properties to the respective receptor isoforms. Using GST fusion proteins containing the C terminal end of the $P2X_{2A}$, $P2X_5$ and $P2X_7$ subunits as baits, ßIII tubulin was identified by MALDI-TOF mass spectrometry as a direct interacting partner of $P2X_{2A}$. ßIII tubulin did not interact with $P2X_5$ nor with $P2X_7$. The tubulin binding motif of $P2X_{2A}$ could be confined to a 42 amino acid long region ranging from amino acid 371 to 412 of the complete $P2X_{2A}$ subunit. This domain, which includes a total of six serine residues and twelve proline residues, interestingly overlaps to a significant extent with a 69 amino acid long sequence, which is lacking in $P2X_{2B}$, a splice variant of $P2X_{2A}$. $P2X_{2B}$ receptors are known to desensitize

significantly faster than $P2X_{2A}$ receptors. The interaction of the $P2X_{2A}$ receptor with ßIII tubulin may contribute to receptor desensitization as well as tethering of the $P2X_{2A}$ receptor at specialized regions of the cell.

In a second part of this work, the oligomeric state of two distantly related glutamate transporters, the human glial glutamate transporter hEAAT2, and the glutamate transporter ecgltP of *E.coli* was determined. Excitatory amino acid transporters (EAATs) buffer and remove synaptically released L-glutamate and maintain its concentration below neurotoxic levels. Mammalian glutamate transporter subunits are known to form homomultimers, but controversial numbers of subunits per transporter complex have been reported, ranging from 2-5. Both hEAAT2 and ecgltP proteins expressed at high levels in *Xenopus laevis* oocytes, from which they were purified in a [$^{35}$S]methionine-labeled form under non-denaturing conditions by metal affinity chromatography. Blue native PAGE analysis revealed that both the hEAAT2 and ecgltP transporters exist exclusively as homogenous populations of homotrimers in *Xenopus* oocytes. The trimeric structure was corroborated by chemical cross-linking. Also, ecgltP purified as a recombinant protein from its natural host *E.coli* migrated as a trimeric protein on blue native PAGE gels. The conservation of the quaternary structure from prokaryotes to mammals assigns an important functional role to the trimeric structure. Glutamate transporters are known to exhibit a dual mode of operation by functioning both as glutamate $Na^+/K^+/H^+$ co-transporters and as anion channels. It is intriguing to speculate that the EAAT monomer is responsible for the secondary active transport of glutamate, whereas a barrel-like arrangement of the three subunits forms a central anion pore mediating anion conductivity.

# VIII/ Deutsche Zusammenfassung

Zuverlässige Kommunikation in Zentralnervensystem benötigt die präzise Kontrolle der Dauer und der Intensität der Wirkung eines Neurotransmitters an seiner spezifischen molekularen Zielstruktur. Nach ihrer Freisetzung in den synaptischen Spalt aktivieren Neurotransmitter prä- und postsynaptische Rezeptoren. Um die synaptische Erregungs-übertragung zu beenden, werden die Neurotransmitter entweder durch enzymatischen Abbau inaktiviert oder durch aktive Rückaufnahme in die präsynaptische Nervenendigung und/oder Aufnahme in Glial-Zellen aus dem subsynaptischen Spalt entfernt. In der vorliegenden Studie wurden zwei Membranprotein-Typen, die beide bei der transzellulären Signaltansduktion beteiligt sind, untersucht, (i) als P2X-Rezeptoren bezeichnete ATP-gesteuerte Ionenkanäle und (ii) Glutamattransporter aus der EAAT-Familie.

Der erste Teil dieser Studie befasst sich mit der biochemischen Suche nach Proteinen, die mit P2X-Rezeptoren interagieren. P2X-Rezeptoren sind Liganden-gesteuerte Ionenkanäle, die von extrazellulärem ATP aktiviert werden und die eine wichtige Rolle bei verschiedenen Prozessen spielen wie beispielsweise der schnellen aktivierenden synaptischen Erregungsübertragung zwischen Neuronen, von Neuronen auf glatte Muskelzellen und der Lyse Antigen-präsentierender Zellen. Die sieben Untereinheiten-Isoformen, die die P2X-Rezeptorfamilie begründen, teilen eine gemeinsame Membran-Topologie mit zwei Membran-durchspannenden Regionen, die beide zur Ausbildung der inneren Wand des Kationenkanals beitragen. Zwischen den P2X-Isoformen homologe Bereiche erstrecken sich über die gesamten Polypeptidketten mit Ausnahme der cytoplasmatisch lokalisierten C-terminalen Enden, die praktisch keine Sequenzähnlichkeiten besitzen. Die fehlenden Sequenzähnlichkeit legt den Gedanken nahe, dass die cytoplasmatischen C-Termini den verschiedenen P2X-Rezeptoren Subtyp-spezifische Eigenschaften verleihen könnten.

Für mehrere Ligand-gesteuerte Ionenkanäle wie Glycin-Rezeptoren und nikotinische Acetylcholin-Rezeptoren wurden spezifische Bindungsproteine identifiziert, die dem „intrazellulären Trafficking" sowie der Verankerung an der Synapse dienen. Zu den Proteinen, die sich in postsynaptischen Membranverdickungen (PSD, post synaptic density) anreichern und eine Verbindung zum Cytoskelet herstellen, gehören Gephyrin, Rapsyn und GABARAP. Um zu untersuchen, ob ähnliche spezifische Bindeproteine auch für P2X-Rezeptoren vorkommen, wurden GST-Fusionsproteine, die die intrazellulären C-terminalen Domänen von $P2X_2$-, $P2X_5$- und $P2X_7$-Untereinheiten beinhalten, in *E.coli* exprimiert und über eine Glutathion-Sepharose-Matrix aufgereinigt. Diese drei GST-Fusionsproteine wurden als Köder eingesetzt, um interagierende Proteine aus Detergenzextrakt von Rattengehirnen zu „fischen" und anschließend durch SDS-PAGE und Coomassie-Färbung darzustellen. Auf diese Weise gefundene Proteine wurden weiter durch MALDI-TOF-Massenspektrometrie analysiert. Als Interaktionspartner der $P2X_2$-Untereinheit wurden ßIII-Tubulin und MBP (Myelin Basic Protein) identifiziert. Diese Interaktionen wurden durch Immunoblot-Analysen bestätigt. Während MBP mit allen drei GST-Fusionsproteinen ko-isoliert wurde, war die Interaktion von ßIII-Tubulin $P2X_2$-spezifisch. Durch einen „Overlay-Assay" konnte gezeigt werden, dass der cytoplasmatische C-Terminus der $P2X_2$-Untereinheit und ßIII-Tubulin direkt miteinander interagieren.

Um das Tubulin-Bindungsmotiv auf der $P2X_2$-Untereinheit genauer zu lokalisieren, wurden eine Reihe weiterer GST-$P2X_2$-Fusionsproteine hergestellt, die unterschiedliche Bereiche des cytoplasmatischen Endes der $P2X_2$-Untereinheit einschlossen. Durch den Bindungsassay mit Rattengehirnextrakt in Verbindung mit SDS-PAGE und Immunoblotting konnte das Tubulin-Bindungsmotif auf eine 42 Aminosäure lange Region der $P2X_2$-Untereinheit eingeschränkt werden, die sich von Aminosäure 371 bis 412 der intakten $P2X_2$-Untereinheit erstreckt. Diese Domäne, die insgesamt sechs Serinreste sowie zwölf Prolinreste enthält, überlappt interessanterweise weitgehend mit einer 69 Aminosäuren langen Sequenz,

die der $P2X_{2B}$-Untereinheit - einer Splice-Variante der $P2X_2$-Untereinheit - fehlt. $P2X_{2B}$-Rezeptoren sind bekannt dafür, dass sie schneller als $P2X_2$ Rezeptoren desensibilisieren. Die Interaktion zwischen $P2X_2$-Rezeptoren und ßIII-Tubulin könnte sowohl für die Rezeptor-Desensibilisierung als auch für die subzelluläre Lokalisierung von $P2X_2$-Rezeptoren von Bedeutung sein.

In einem zweiten Teil dieser Arbeit wurde die Quartärstruktur zweier entfernt verwandter Glutamattransporter, dem humanem Glutamattransporter hEAAT2 und dem E. coli-Glutamattransporter ecgltP bestimmt. Die Aminosäure L-Glutamat wird als wichtigster exzitatorischer Neurotransmitter im Zentralnervensystem angesehen und ist bei vielen zentralen Gehirnfunktionen wie Erkennen, Gedächtnis und Lernen beteiligt. In hohen Konzentrationen ist Glutamat jedoch neurotoxisch. Plasmamembranständige Transporter für exzitatorische Aminosäuren (EAATs, excitatory amino acid transporters) puffern die subsynaptische Glutamatkonzentration ab und halten sie unter dem neurotoxischen Spiegel, indem sie L-Glutamat aus dem synaptischen Spalt wieder entfernen. Sowohl an der Plasmamembran als auch in Membranen synaptischer Vesikel ist die Neurotransmitter-Aufnahme direkt an transmembranäre Ionengradienten gekoppelt, die die Energie für die Aufnahme liefern.

Von Säugetier-Glutamattransporter-Untereinheiten ist bekannt, dass sie Homomultimere ausbilden. Die genaue Anzahl an Untereinheiten pro Transporter ist jedoch umstritten und schwankt zwischen zwei und fünf. In der vorliegenden Arbeit wurden der humane EAAT2-Transporter hEAAT2 und der E. coli-Glutamattransporter ecgltP durch cRNA-Injektion in *Xenopus*-Oocyten exprimiert, und, nach metabolischer Markierung mit [$^{35}$S]Methionin, durch $Ni^{2+}$-NTA-Chromatografie unter nicht-denaturierenden Bedingungen gereinigt. Analyse der nicht-denaturierten und partiell denaturierten Proteinproben durch blaue native Polyacrylamid-Gelelektrophorese ergab, dass der hEAAT2-Transporter als homogene Population von Homotrimeren in *Xenopus*-Oozyten vorliegt. Die trimere

Struktur wurde durch chemische Vernetzung mit den beiden Cross-linkern DMA (Dimethyl-adipimidat) und DMS (Dimethyl-suberimidat) bestätigt.

Durch Glycosidasen-Behandlung und Expression von N-Glycan-Minus-Mutanten konnte gezeigt werden, dass jede EAAT2-Untereinheit nur eine Kohlenhydrat-Seitenkette trägt, die – in zeitlichem Abstand zur Synthese - im homotrimeren Proteinkomplex Endoglycosidase-H-resistente Zucker erwirbt. Glykosylierung war allerdings weder für die Stabilität des Proteines noch für die Assemblierung zu Homotrimeren von Bedeutung, da eine nicht-glykosylierbare EAAT2-Mutante ebenfalls gut exprimiert wurde und effizient zu Homotrimeren assemblierte.

Analoge Experimente mit dem bakteriellen Glutamattransporter ergaben, dass ecgltP als N-Glykan-freies bakterielles Protein bemerkenswert gut in *Xenopus*-Oozyten synthetisiert wird und ebenfalls effizient zu einem Homotrimer assembliert. Auch für diesen (in Oocyten allerdings nicht funktionellen) Transporter konnte die homotrimere Struktur durch chemische Quervernetzung in Verbindung mit SDS-PAGE und Autoradiografie abgesichert werden. Zusätzlich wurde ein ecgltP-Concatamer exprimiert, dass aus zwei hintereinandergeschalteten ecgltP-Monomeren besteht. Die beiden Monomere waren durch eine 18 Aminosäuren lange Linkersequenz kovalent miteinander verbunden. Die oligomeren Strukturen, die dieses dimere ecgltP-Concatamer eingingen, sind vollkommen mit der homotrimeren Struktur des Wildtyp-ecgltP-Transporters vereinbar. Bemerkenswerter Weise wurde ein nicht unerheblicher Teil der concatameren Dimere zeitabhängig proteolytisch in Monomere gespalten. Nach der sich um 1-2 kDa unterscheidenden Masse der proteolytisch gebildeten Monomere zu urteilen, muss die Spaltung kurz vor bzw. hinter dem Linker eingetreten sein. Diese durch Proteolyse entstandenen Monomere assemblierten zu Homotrimeren, die sich auf den blauen nativen PAGE-Gelen wie Homotrimere verhielten, die aus exprimierten Monomeren assemblierten. Es handelt sich (neben einem $P2X_1$-Concatamer) hierbei um das zweite Beispiel eines in unserer Arbeitsgruppe analysierten Membranprotein-Concatamers, das in Oocyten

zu Monomeren prozessiert wird. Die Expression von Concatameren ist in der Ionenkanalanalyse ein beliebtes Verfahren, um aus funktionellen Messungen Rückschlüsse über die Stöchiometrie und die Anordnung von Untereinheiten in multimeren Proteinkomplexen zu bestimmen. Da die Prozessierung von Concatameren zu kleineren Proteinen, die sich praktisch nicht von exprimierten Monomeren unterscheiden, offenbar kein Einzelfalls ist, scheinen funktionelle Daten solange fragwürdig, bis das Entstehen von Proteolyseprodukten durch biochemische Analysen mit Sicherheit ausgeshclossen ist.

In einer letzten Serie von Experimenten bin ich der Frage nachgegangen, welche Domänen bei der ecgltP-Trimerisierung beteiligt sind. Zu diesem Zweck habe ich verschiedene ecgltP-Deletionmutanten in *Xenopus*-Oocyten exprimiert und, nach nativer Reinigung durch $Ni^{2+}$-NA-Chromatografie, durch blaue native PAGE analysiert. Deletion von bis zu 169 C-terminalen Aminosäuren störte die Trimerisierung nicht. Umfassendere Deletionen von bis zu 207 Aminosäuren verhinderte dagegen die Trimerisierung ebenso wie Deletion der ersten N-terminalen 83 Aminosäuren. Diese Daten lassen den Schluss zu, dass mindestens eine N- und eine C-terminale Proteindomäne an der Assemblierung zu Trimeren beteiligt sind.

Die evolutionäre Konservierung der trimeren Struktur der Glutamattransporter von *E. coli* bis zum Menschen ist ein starker Hinweis darauf, dass der Quartärstruktur eine wichtige funktionelle Rolle zukommt. In diesem Zusammenhang ist interessant, dass Glutamat-transporter sowohl als Transporter als auch als Anionenkanäle fungieren, indem sie neben dem an den Glutamattransport gekoppelten elektrogenen Ionenflux auch eine Anionen-Leitfähigkeit vermitteln, der vom Glutamattransport thermodynamisch abgekoppelt ist. Es ist vorgeschlagen worden, dass die Anionen-Leitfähigkeit der Dämpfung der neuronalen Erregbarkeit dient. Möglicherweise steht die Anionenkanal-Funktion in direkten Zusammenhang mit der trimeren Struktur, die dazu dienen könnte, durch ringförmige Anordnung bestimmter Transmembrandomänen

jeder der drei Untereinheiten eine Ionenkanal-ähnliche zentrale Ionenpore zu schaffen.

# IX/ References

## Publications

**Gendreau S**, Schirmer J, Schmalzing G.
Identification of a tubulin binding motif on the $P2X_2$ receptor
*J Chromatogr B Analyt Technol Biomed Life Sci.*
2003 Mar 25;786(1-2):311-8

**Gendreau S**, Voswinkel S, Torres-Salazar D, Lang N, Heidtmann H, Schmalzing G, Hidalgo P, and Fahlke C
A trimeric quaternary structure is conserved in bacterial and human glutamate transporters
*J Biol Chem.*
2004 Sep 17;279(38):39505-12

## Lectures

**European Contest for Young Scientists on Protein Purification: From Gene to Functional Protein.**
"Identification of a tubulin binding motif on the $P2X_2$ receptor"
Paris, France; 10-11 Juni 2002

**Lectures serial of the DFG research group FOR 450/1.**
"Analysis of the oligomeric structure of bacterial and mammalian glutamate transporters by blue native page"
Aachen, Germany; 7$^{th}$ of February 2003

**44$^{th}$ springmeeting of the DGPT** (Deutsche Gesellschaft für experimentelle und klinische Pharmakologie und Toxikologie).
Mainz, Germany; 17$^{th}$-20$^{th}$ of March 2003

**45$^{th}$ springmeeting of the DGPT** (Deutsche Gesellschaft für experimentelle und klinische Pharmakologie und Toxikologie).
Mainz, Germany; 09$^{th}$-11$^{th}$ of March 2004

## Posters

**43$^{th}$ springmeeting of the DGPT** (Deutsche Gesellschaft für experimentelle und klinische Pharmakologie und Toxikologie).
Mainz, Germany; 12$^{th}$-14$^{th}$ of March 2002

# X/ Curriculum Vitae

| | |
|---|---|
| 25.03.1976 | Born in Ivry/seine, France |

## School

| | |
|---|---|
| Sept. 1982 to July 1991 | Elementary school (France) |
| Sept. 1991 to July 1994 | High school (Lyon, France) |
| Certificate: June 1994 | Final secondary-school examinations<br>Topics: Mathematics and Physics |

## Studies

University Paul Sabatier, Toulouse (France)

| | |
|---|---|
| Oct. 1994 to June 1996 | First year of medical studies |
| Oct. 1996 to June 1997 | General Biology |
| Oct. 1997 to June 1998 | Biology, main subject: Biochemistry |
| Oct. 1998 to June 1999 | Biology, main subject: Structural biochemistry |
| Certificate: Sept. 2000 | Master's Degree, main subject: Haemostasis and blood vessels biology and pharmacology<br>University Paris 7 (France) |

## Thesis

| | |
|---|---|
| Oct. 2000 to May 2004 | Thesis in the group of Prof. Dr. G. Schmalzing at the Department of Molecular Pharmacology of the Institute for Pharmacology and Toxicology in Aachen (Germany) |

Title: Modulation of protein functions by homo- and heterophilic protein interactions as studied with P2X receptors and glutamate transporters

# XI/ Acknowledgements

Firstly, I should like to thank Prof. Dr. Günther Schmalzing, who was my supervisor during these four very intense years. Thank you, Günther, for integrating me in your group and for motivating me to bring this work to a good end. I wish you, your family and your group all the best for the coming years.

Secondly, I wish to thank my examinators, Prof. Lambrecht, Prof. Fendler and Prof. Steinhilber because they accepted to attend my exam; I also wish to thank them for posing sharp but friendly questions afterwards. Special thanks go to Prof Lambrecht for kindly accepting to be my PhD supervisor.

It is now the time to convey my thanks to my colleagues (Cristina, Niklas, Heike, Wiebke, Klaus-Dieter, Karin, Svenja, Ralf, Christian, Silvia, Marion (Peters), Paul, Barbara, Jörg, Katrin, Gabriele, Herr Breidbach). It was nice to work with you and it was nice to talk to you (yes, I know I talk too much!). You made these four years seem short and pleasant. I am happy to call many of you my friends and I wish you lots of luck with your PhD studies (never give up!). I also wish you all the best in your lifes.

Very special thanks go to the man who has taken up the task to share his life with me. A big, huge thanks to you for these last three years, Matthias. Thank you for your patience and for being at my side and giving me strength during the hard moments. I love you each day more.

Last but not least, I wish to thank my parents, my brother, Angelika, Hartwig and all my friends (Carsten, Birgit, Martin, Sven, Jürgen) who have come to celebrate with me and made this day an unforgettable moment of my life.